



Review article

Synthesis, pharmacological evaluation and structure-activity relationship of recently discovered enzyme antagonist azoles



Atukuri Dorababu *

Department of Studies in Chemistry, SRMPP Govt. First Grade College, Huvinahadagali, 583219, Karnataka, India

ARTICLE INFO

Keywords:

Natural product chemistry
Organic chemistry
Enzyme inhibitors
Carbonic anhydrase
COX
Pyrazole
Thiazole

ABSTRACT

Global people are suffering from the legion of diseases. Cytotoxic property of the chemical compound would not solely influence effective drug properties and reduce unnecessary side effects. Proteins/enzymes responsible for microbe proliferation or survival are specifically targeted and inhibited successfully making the cells to undergo apoptosis. Furthermore, isoforms of essential enzymes have distinct physiological functions; thereby inhibition of essential enzyme isoforms is an apt way to the clinical approach of disease neutralization. Drugs are designed so as to play significant roles such as signaling pathways in the oncogenic process including cell proliferation, invasion, and angiogenesis. The present review comprises collective information of the recent synthesis of various organic drug compounds in brief, which could inhibit particular enzyme. The review also covers the correlation of the structure of a drug molecule designed and its inhibitory activity. Also, the most significant enzyme inhibitors are highlighted and structural moieties/core units responsible for remarkable inhibitory values are emphasized.

1. Introduction

Enzyme inhibitors are drug molecules capable of reducing the enzymatic activity by binding to the enzyme. Inhibition of an enzyme is crucial for pathogen's survival that could make a pathogen weak and destroy it subsequently. In addition to this, the enzyme inhibitors are also used to maintain metabolic balance in case of inhibition of metabolic enzymes when they are overexpressed. Besides this, some drug molecules bind to enzymes and enhance enzymatic activity. The mechanism of enzyme inhibition involves the reversible or irreversible binding of the drug molecule to an enzyme thereby ceasing substrate to enter enzyme's active site. The non-covalent type of interactions prevail in between reversible inhibitors and enzyme while covalent bonding is observed for irreversible inhibitor-enzyme complex; wherein modification of key amino acid residues required for enzymatic activity is usually noticed. In spite of the cruciality of enzyme inhibitors, these have been designed and synthesized continuously and it has been a potential area of research in biochemistry and pharmacology. The apt enzyme inhibitors should possess characteristics such as high specificity and potency. In the case of reversible inhibitors, some of the inhibitors have a remarkably similar structure with that of substrates. For instance, inhibitors of DHFR and protease inhibitors mimic the structures of the substrate. One more strategic design involves the design of enzyme inhibitors as transition

state mimics possessing higher binding interaction than substrate-based designs.

The irreversible enzyme inhibitors most often possess reactive functional groups such as nitrogen mustards, aldehydes, haloalkanes, alkenes, Michael acceptors, phenyl sulfonates and fluorophosphonates. Hence the researchers have utilized the above mentioned information in the design and development of drug compounds as enzyme inhibitors. This derivative work includes synthesis of many series of compounds possessing enzyme inhibitory properties [5,6]. Since diverse chemical pharmacores prevail that could inhibit various enzymes, the enzyme inhibitors are described in different classes depending upon the designed structural entity [7,8]. The type of enzyme being inhibited is also accounted for in the classification. In each class of enzyme inhibitors, pharmacology, in particular, enzyme inhibition properties are described. Additionally, the structure and activity relationship (SAR) of potent enzyme inhibitors is discussed. The structural motifs attributed to noteworthy inhibitory results have been identified and highlighted in order to encourage further research and develop more efficient enzyme inhibitors.

1.1. [1,4] Dioxino [2,3-f] quinazoline derivatives

c-Met and VEGFR-2 are the tyrosine kinases that are responsible for the signaling pathways in the oncogenic process including regulation of

* Corresponding author.

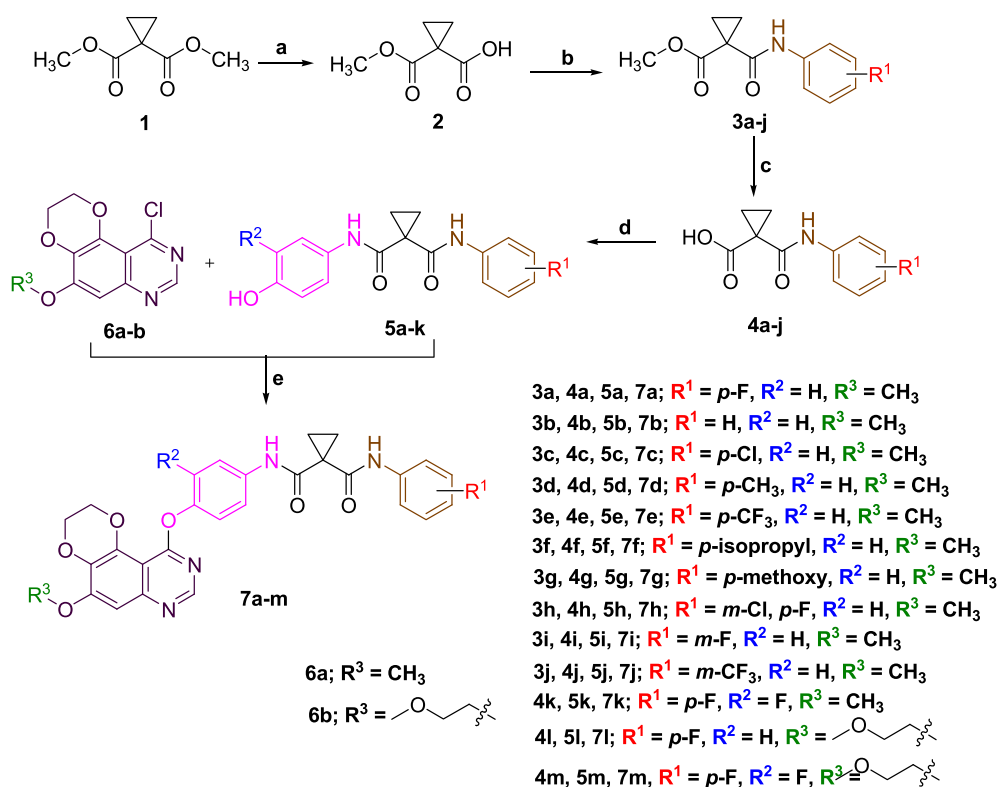
E-mail address: dora1687@gmail.com.

cell proliferation, invasion, and angiogenesis. Hence, the design strategy involves the preparation of the enzyme inhibitors that could inhibit c-Met and VEGFR-2 effectively. Dioxino [2,3-*f*] quinazoline derivatives have been designed as dual c-Met and VEGFR-2 inhibitors taking the consideration of pharmacological importance of cyclopropane-1,1-dicarboxamide moiety of cabozantinib or foretinib and the dihydro [1,4] dioxino [2,3-*f*] quinazoline core structure towards enzyme inhibition [1].

Synthetic route involves hydrolysis of one of the ester group of compound **1** by LiOH to get carboxylic acid derivative **2**, followed by amidation at the carboxylic acid end with aniline/substituted anilines leading to β -amido ester **3a-j** and the sequence of reactions was repeated wherein second ester functionality was cleaved resulting into β -amino ester **4a-j** followed by amidation with various 3-substituted-4-hydroxyanilines rendering diamide derivative **5a-k**. Finally, compound **6a-b** undergoes nucleophilic substitution with **5a-k** to yield [1,4] dioxino [2,3-*f*] quinazoline derivatives **7a-m** (Scheme 1).

The lead compounds **7a-7m** were tested for enzyme inhibitory activity against VEGFR-2 kinase wherein good inhibitory potencies were exhibited by **7a** (IC_{50} = 18.9 nM), **7k** (IC_{50} = 3.5 nM), **7l** (IC_{50} = 8.8 nM)

and **7m** (IC_{50} = 4.8 nM). The most potent inhibitors **7k** and **7m** (Figure 1) possessed comparable activities with that of reference compound cabozantinib (IC_{50} = 3.6 nM) in which derivative **7k** has almost identical inhibitory potential with that of the reference compound. The other derivatives have shown the IC_{50} values in the range of 139–834 nM. Compounds **7e** and **7f** were totally inactive at the evaluated drug concentration. Based on the remarkable VEGFR-2 kinase inhibitory activity; compounds **7a**, **7k**, **7l**, and **7m** were chosen to investigate c-Met enzyme inhibitory activity. Surprisingly the selected derivatives are also active towards c-Met and IC_{50} values were found to be 18.5 nM, 7.3 nM, 9.9 nM and 5.8 nM for compounds **7a**, **7k**, **7l**, and **7m** respectively. The derivative **7m** stood atop amongst c-Met inhibitors and has higher potency compared to cabozantinib (IC_{50} = 6.8 nM). The structure-activity relationship inferred that the substituent attached to the phenyl ring of cyclopropane-1,1-dicarboxamide moiety has a great impact on inhibitory activity wherein the derivatives with electron-withdrawing atom fluoro at *p*-position were notable inhibitors. While the presence of electron-withdrawing moieties at *p*-position has paved to reduced activities. All the four potent compounds have exhibited dual inhibitory activity. However when it comes to selectivity, compound **7k** having methyl motif



Scheme 1. Synthesis of dual c-Met and VEGFR-2 inhibitors [1]; **Reagents and conditions:** (a) LiOH, MeOH/H₂O, rt, 1h; (b) EDC, HOBT, DCM, aniline or substituted aniline; (c) LiOH, MeOH/H₂O, rt; (d) EDC, DMA, substituted or unsubstituted 4-aminophenol; (e) K₂CO₃, isopropanol.

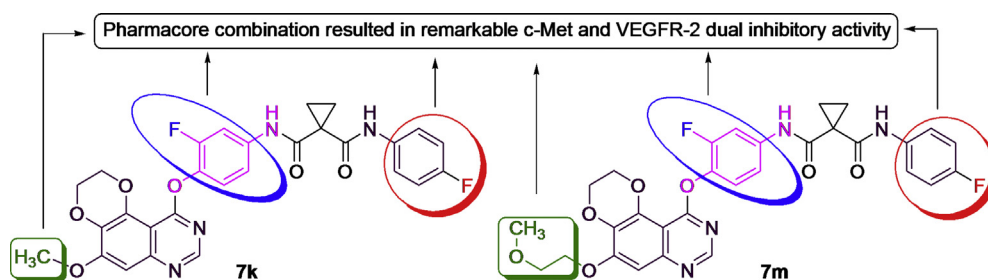


Figure 1. Structures of most potent dual c-Met and VEGFR-2 inhibitors.

at quinazoline 7-oxygen atom has selectivity towards VEGFR-2 while compound **7m** possessing methoxyethyl moiety at quinazoline 7-oxygen atom inclines towards c-Met.

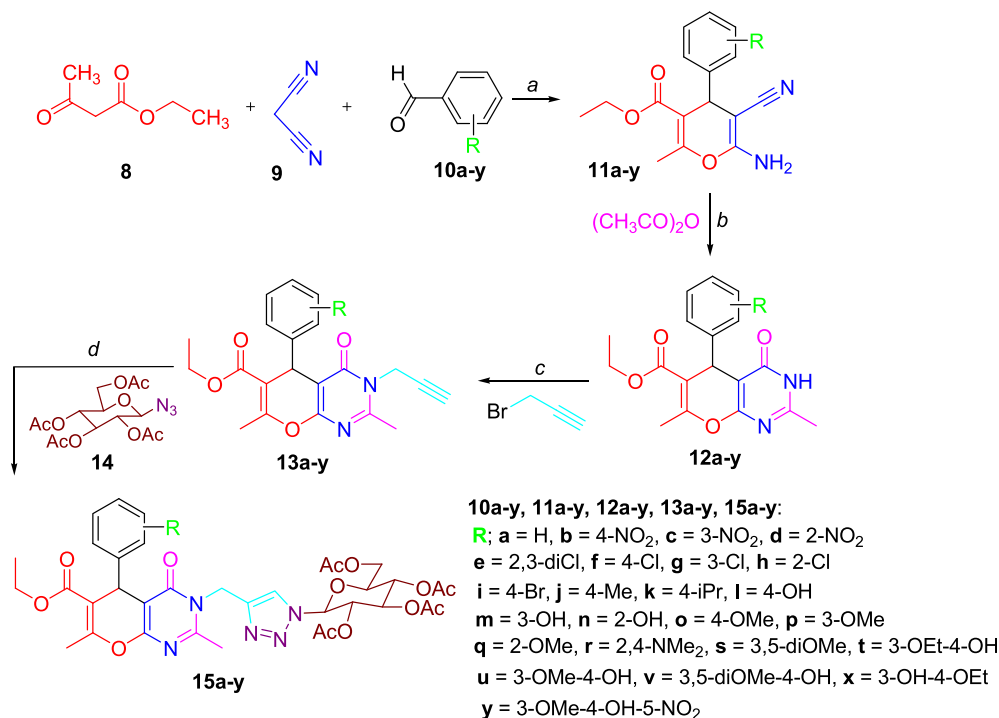
1.2. 1,2,3-1H-Triazoles-linked 4H-pyrano [2,3-d] pyrimidine

The important classes of enzymes, namely, protein tyrosine phosphatases and protein tyrosine kinases are crucial for signal transduction of cellular processes such as immune response, metabolism, growth and gene transcription. Likewise, the other two protein kinase phosphatases (PtpA and PtpB) are reported to be secreted by MTB in infected human macrophages which take prime responsibility for the cause of mycobacterium tuberculosis. Further, these enzymes can be utilized as clinical targets for the design and development of potential drug molecules. Taken together with the medicinal properties of pyrano[2,3-d]pyrimidine moiety towards anti-tubercular activity and decent MTB PtpB inhibitory activity of 1,2,3-1H-triazole, a structural framework is designed anticipating better MTB PtpB inhibitory activity [2].

The synthetic route goes in this way; firstly three-component cyclization reaction of ester **8**, malononitrile **9** and various aromatic aldehydes **10a-y** has produced cyclic amino nitrile **11a-y** wherein the

adjacent amino and nitrile groups are utilized for intramolecular cyclization with acetic anhydride to form 4[H]-pyranopyrimidines **12a-y**. Propargyl motif of propargyl bromide is appended to NH group of intermediate **12a-y** by nucleophilic substitution yielding **13a-y** which is subsequently tethered with D-glucose via triazole formation paving to lead compounds **15a-y** (Scheme 2).

The synthesized derivatives are allowed to inhibit the MTB PtpB enzyme. Except for inactive compounds **15i-k**, other derivatives have exhibited weak to remarkable inhibitory activity. The compounds **15g**, **15t**, and **15u** yielded moderate activity with IC₅₀ values of $9.52 \pm 1.13 \mu\text{M}$, $7.94 \pm 0.23 \mu\text{M}$ and $7.51 \pm 0.33 \mu\text{M}$ respectively. Further, remarkable inhibitory activity is observed for the compounds **15v** ($2.22 \pm 0.23 \mu\text{M}$), **15x** ($3.53 \pm 0.19 \mu\text{M}$) and **15y** ($1.56 \pm 0.21 \mu\text{M}$) (Figure 2) wherein most significant inhibitory activity is bestowed for compound **15y** possessing -OMe, -OH, and -NO₂ at 3-, 4- and 5-positions of phenyl ring respectively. SAR studies revealed that electron-donating -OH group at p-position of phenyl ring has the strongest impact on inhibitory activity excluding compound **15l** which exhibited weak activity. A combination of the -OH and alkoxy moieties has resulted in noteworthy potencies (**15v** and **15x**). Besides, the presence of the 5-nitro group along with -OMe and -OH groups at 3- and 4-positions elicited the highest activity.



Scheme 2. Synthetic route for preparation of 1,2,3-1H-triazoles derivatized 4H-pyrano [2,3-d] pyrimidine analogs [2]; **Reagents and conditions:** (a) Ammonium solution 25%, 25 °C, 3 h, or Cu@MOF-5 (10 mol%), 96% EtOH, 50 °C, 1 h; (b) Acetic anhydride, Conc. H₂SO₄ (cat.), 15 min, in refluxing, then 25 °C, 24 h; (c) Propargyl bromide, anhydrous potassium carbonate, dry acetone, in refluxing, 4–5 h; (d) Cu@MOF-5 (cat.), 79–80 °C, abs. EtOH, 4–5 h.

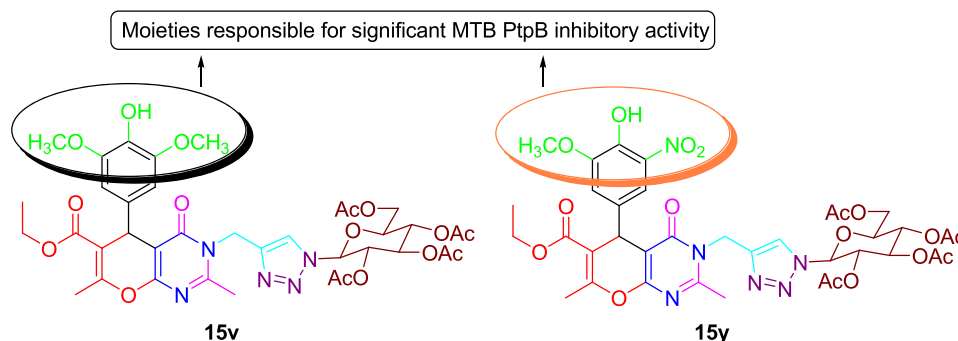


Figure 2. Illustration of structures of remarkable MTB PtpB inhibitors.

1.3. 1,2,4-Triazole-5-one derivatives

Inhibition of tumoral carbonic anhydrases (CA) could lead to slow-down of metastasis and reduced cancer symptoms. However, most of the discovered CA inhibitors have also inhibited isoforms of CA and thereby reduced efficiencies are observed. In order to enhance the efficiency of the CA inhibitors, the pharmacologically significant phenolic motif and 1,2,4-triazole ring are brought together in a framework of 1,2,4-triazole-5-one derivatives [3].

Two series of 1,2,4-triazole derivatives have been designed wherein synthesis of the first series of compounds **18a-e** commences from 1,2,4-triazole-*N*-amine **16**. In the first step, triazole **16** is alkylated at *N*₄ to give 4-heptyl-1,2,4-triazole **17** which on condensation with various 4-halosallylaldehyde yielded hydrazone analogs **18a-e**. In the second series, 4-heptyl-1,2,4-triazole **17** is deaminated to corresponding 1,2,4-triazole **19** (Scheme 3).

The deaminated derivative **19** is treated with ethyl bromoacetate to afford *N*-substituted-1,2,4-triazole derivative **20** followed by cleavage at ester linkage with hydrazine yielded semicarbazide analog **21**. Ultimately the semicarbazide **21** is condensed with various 4-substituted salicylaldehyde to form compounds **22a-e**.

The designed derivatives are tested for bovine carbonic anhydrase II potentials using reference compound sulfanilamide. Among the two series of inhibitors, hydrazone analogs **18a-e** have shown significant inhibitory activity. Amongst them, 4-bromophenol analog **18c** (Figure 3) has exhibited the most potent activity ($67.07 \pm 0.69\%$) with IC_{50} value of $60.80 \mu\text{M}$. However, its activity is moderate compared to sulfanilamide ($93.00 \pm 0.24\%$) with IC_{50} value of $3 \mu\text{M}$. The other derivatives have percentage inhibitions in the range of $18.41 \pm 0.01\%$ to $64.97 \pm 0.05\%$. Moderate electron-withdrawing -Br atom at the *p*-position of the phenolic ring in addition to semicarbazide linker flanked by 4-alkylated 1,2,4-triazole and 4-bromophenol have enhanced its inhibitory property to a greater extent.

1.4. 1,2,4-Triazole-based benzothiazole/benzoxazole derivatives

The activated macrophages produce pro-inflammatory cytokines such as interleukins and TNF- α which mediate the inflammation. P^{38} MAP, one of the isoforms of pro-inflammatory kinases is also included under the class of kinases, inhibition of which would be an efficient approach for reducing inflammation and chronic inflammatory diseases. In this

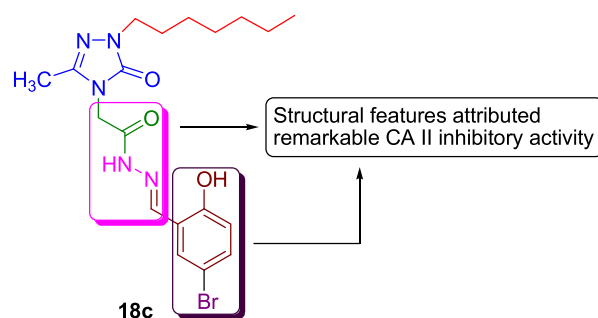


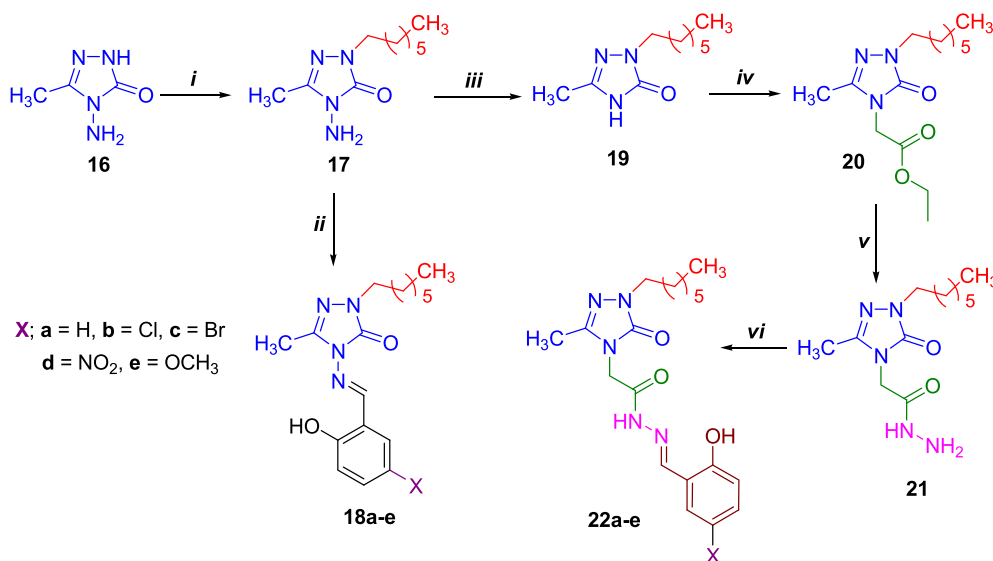
Figure 3. Structure of 1,2,4-triazole-5-one derivative with significant CA II inhibitory activity.

conjuncture anti-inflammatory and $p^{38\alpha}$ MAB kinase inhibitory activities of heteroaryl scaffolds, benzothiazole and benzoxazole are utilized for the synthesis of 1,2,4-triazole-based benzothiazole/benzoxazole derivatives as $p^{38\alpha}$ MAB kinase inhibitors [4].

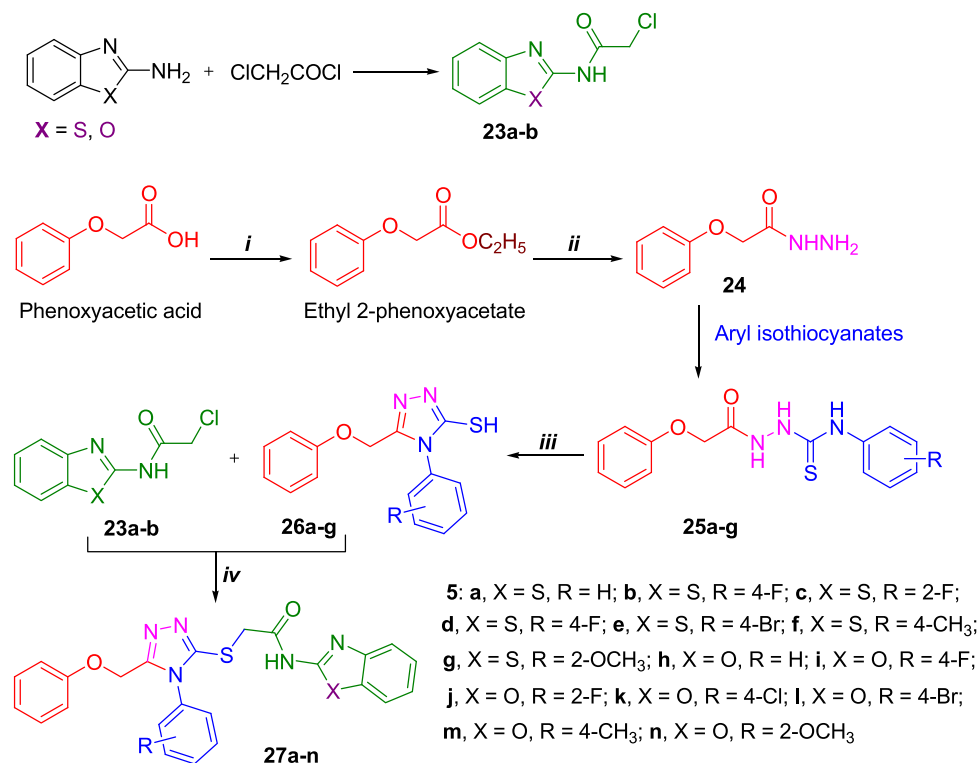
Preparation of the final compounds **27a-n** entails synthesis of benzothiazole/benzoxazole derivatives **23a-b** and reserved for further use in Scheme 4. The scheme starts from esterification of phenoxy acetic acid to get ethyl 2-phenoxy acetate which is then treated with hydrazine affording semicarbazide **24**. The reaction of compound **24** with various aryl isothiocyanates gave thiourea derivatives **25a-g** and cyclization of these thiourea derivatives yielded triazole 2-thiols **26a-g**. Initially, prepared compound **23a-b** is appended to SH of triazole 2-thiol leading to 1,2,4-triazole-based benzothiazole/benzoxazole derivatives (Scheme 4).

The title compounds have been screened for $p^{38\alpha}$ MAB kinase inhibitory activity using reference compound SB203580. Alongside percent inhibition of the protein is also carried out. The tested derivatives have found to inhibit in the range of 47.97–85.36% and the corresponding derivatives have $p^{38\alpha}$ MAB kinase inhibitory activity in the range of 0.031–1.273 %. Out of the evaluated compounds, noteworthy results were shown by the compounds **27b**, **27d**, **27i**, and **27k** (Table 1). These derivatives have potentials comparable to the SB203580; particularly compounds **27b** and **27i** (Figure 4) have greater inhibitory values than that of the reference compound.

SAR studies infer that in general electron-withdrawing groups have a higher impact on inhibitory activity. Again position of the electron-withdrawing group and its electronegativity are responsible for the



Scheme 3. Synthesis of compounds **18a-e** [3]; **Reagents and conditions:** *i*. absolute ethanol, NaOEt/1-bromoheptane, reflux; *ii*. 4-X-salicylaldehyde, 160–165 °C, oil bath heating; *iii*. H_3PO_2 solution, NaNO_2 , room temperature; *iv*. absolute ethanol, NaOEt/ethyl bromoacetate, reflux; *v*. butanol, $\text{NH}_2\text{NH}_2 \cdot \text{H}_2\text{O}$, reflux; *vi*. ethanol, 4-X-salicylaldehyde, reflux.



Scheme 4. Synthesis of 1,2,4-triazole-based benzothiazole/benzoxazole derivatives (**27a-n**) [4]; **Reagents and conditions:** i) Conc. H₂SO₄, ethanol; ii) NH₂NH₂·H₂O, Abs. ethanol; iii) 8% w/v NaOH; iv) Anhyd. K₂CO₃, acetone.

Table 1. % Inhibition values of denaturation and p38 α MAB kinase inhibitory activity of the title compounds.

Compound	% inhibition of denaturation	p38 α MAB kinase inhibitory activity
		IC ₅₀ (μ M) \pm SEM
27b	85.36	0.031 \pm 0.14
27d	81.48	0.075 \pm 0.11
27i	82.89	0.038 \pm 0.12
27k	79.19	0.082 \pm 0.09
Diclofenac sodium	82.54	-
SB203580	-	0.042 \pm 0.27

strongest inhibition. The compounds **27b** and **27i** possessed fluoro group at *p*-position of the benzene ring directly attached to triazole have inhibited to a larger extent. In particular, combination of 4-fluoro group and benzothiazole (**27b**) has the perfect molecular structure for greatest inhibition. Decreased electronegativity of the group attached at benzene 4-position led to abated inhibitory values wherein **27d** and **27k** yielded decreased inhibitions. The derivatives with electron-donating groups have exhibited the least inhibitory activities.

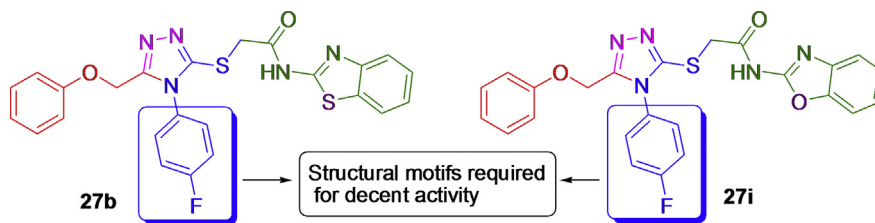


Figure 4. Structures of 1,2,4-triazole derivatized benzothiazoles/benzoxazoles possessing noteworthy p38 α MAB kinase inhibitory activities.

1.5. 1,2,4-Trisubstituted imidazolinones

Hypoxia induces human carbonic anhydrase *hCA IX* expression in solid tumors viz., glioma, breast cancer, and colon cancer. Inhibition of *hCA IX* could be an attractive drug target approach; as such an act strongly suppresses the growth of both primary tumor phases as well as metastasis. Combining the CA inhibitory activity of benzenesulfonamide derivatives with the p38 α MAPK inhibitory activity possessed by the imidazole resulted in 1,2,4-trisubstituted imidazolinones [5].

Initially amido acid functionality of benzamide acid derivatives **28a**, **b** is cyclized in presence of *p*-substituted benzaldehydes to oxazolone ring derivatives **29a-d** (Scheme 5); further, these derivatives are utilized as intermediates for the design of the target molecules. Among the four intermediates, first two intermediate compounds **29a** and **29b** are ring inserted with *p*-amino benzene sulfonamide analogs to form tri-substituted imidazolinone scaffolds **30a-l** (Scheme 6).

The other two intermediate compounds **29c** and **29d** are also allowed to get ring inserted with *p*-aminobenzene sulfonamide producing compounds **31a** and **31b**. Target compounds **33a-f** are obtained on the treatment of derivatives **31a** and **31b** with compounds **32a-c** (Scheme 7).

All the synthesized molecules are evaluated for their p38 α MAPK inhibitory activity using sorafenib. Most of the derivatives have exhibited

decent inhibition in comparison to reference. Out of them, the most potent inhibitory activity ($IC_{50} = 0.056 \mu\text{M}$) is bestowed by the compound **30h**; about 28 fold highly potent compared to sorafenib ($IC_{50} = 1.58 \mu\text{M}$). Slightly lower inhibitory activity yet stronger activity amongst the evaluated molecules is shown by the derivatives **30c**, **30g**, **31a**, and **33e** with identical activity ($IC_{50} = 0.14 \mu\text{M}$). These derivatives have 11-fold higher inhibitory potency than that of sorafenib. Compound **33c** ($IC_{50} = 0.134 \mu\text{M}$) could also be included in the significant p38 α MAPK inhibitors list. Correlation of structure and activity revealed that most significant p38 α MAPK inhibitor **30h** possesses 3,4-dimethoxybenzene and 4-(*N*-acetyl benzenesulfonamide motifs on its imidazolinone ring.

The designed derivatives are tested for CA inhibitory activity towards hCA isoforms, I, II, IV, and IX using acetazolamide (AAZ) and inhibitory values are represented as K_i values. Surprising inhibitory activity is observed towards the four isoforms of CA wherein compound **31a** (Figure 5) rendered most potent inhibitory activity towards all four CA isoenzymes CA I ($K_i = 95.0 \text{ nM}$), II ($K_i = 0.83 \text{ nM}$), IV ($K_i = 6.9 \text{ nM}$) and IX ($K_i = 12.4 \text{ nM}$). Dual inhibition is also observed in the case of compound **31a**. Removal of the 3-methoxy moiety, removal of methyl 4-methoxybenzylidene group and deacetylation of sulfonamide of p38 α MAPK inhibitor have converted into the dual p38 α MAPK/CA inhibitory. This result indicated that primary benzenesulfonamide, 4-hydroxybenzylidene, and 4-methoxyphenyl moieties are most crucial for its dual inhibitory properties.

1.6. 1*H*-Pyrazolo [3,4-*b*] pyridine derivatives

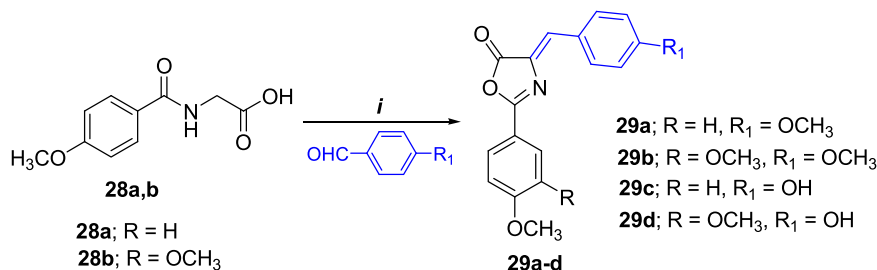
Acetylcholinesterase (AChE) inhibition is the most attractive approach for the design of anti-AD drugs. 1*H*-Pyrazolo [3,4-*b*] pyridine

derivatives have been reported to exhibit cyclin-dependent kinases, GSK 3 inhibition properties, and other prominent pharmacological activities. Considering this, novel 1*H*-pyrazolo [3,4-*b*] pyridine derivatives are designed as AChE inhibitors [6].

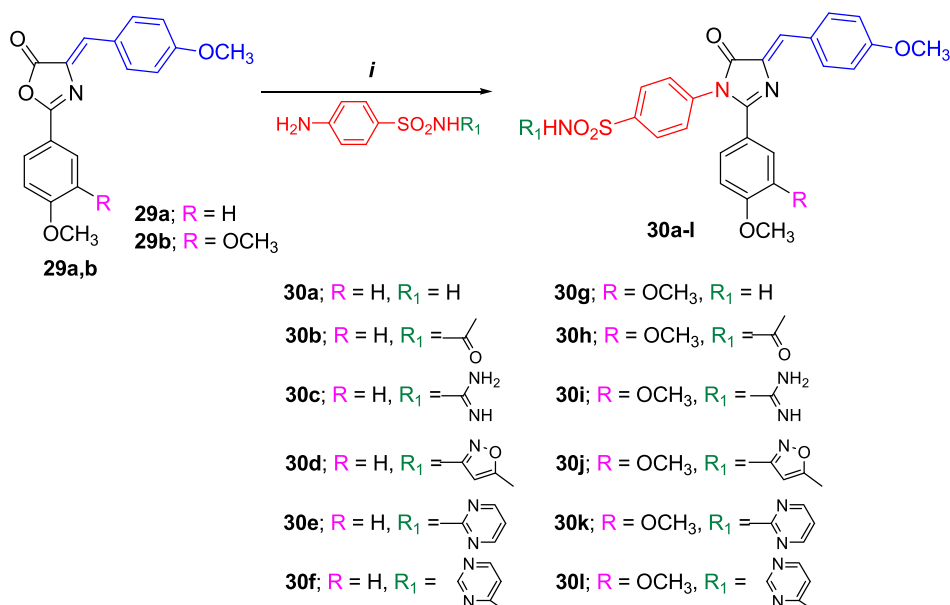
2-Chloro-3-cyano-pyridine **34** is cyclized to pyrazolopyridine-3-amine **35** using hydrazine which is subsequently treated with chloroacetylchloride gave useful scaffold **36** for target compound design. *p*-Substituted aniline is treated with diester **37** to form a substituted product **38a, b** and on cyclization yielded 4-chloroquinoline **39a, b** which is allowed to undergo nucleophilic substitution reaction with piperazine affording 4-piperazinoquinolines **40a, b**. The intermediate compounds **40a, b** are converted into target compounds **41a, b** using the initially synthesized compound **36** (Scheme 8).

Hydroxyl-triazolopyrimidine derivative **43** is chlorinated to get chloro analog **44** which on substitution reaction with piperazine has produced piperazine derivatized triazolopyrimidine **45**. The final compound **46** is synthesized from compound **45** using compound **36** (Scheme 9). 4,7-Chloroquinoline **47** on nucleophilic substitution with piperazine formed piperazine analog **48** and followed by second nucleophilic substitution with compound **36** has resulted in final compound **49** (Scheme 9). Similarly, the target compound **51** is synthesized from compound **34** with two successive nucleophilic substitutions using piperazine and compound **36** and first and second nucleophiles (Scheme 9). Finally, treatment of compound **36** with morpholine/*N*-methyl piperazine/piperidine resulted in target compounds **52–54** (Scheme 10).

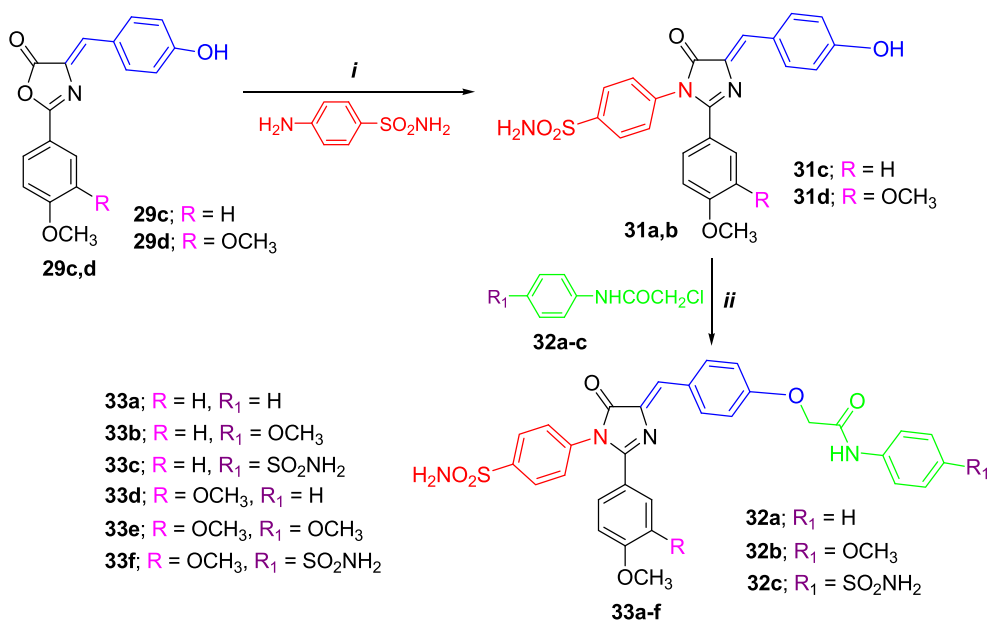
The designed molecules are screened for AChE inhibitory activity using donepezil as a reference compound. Most of the derivatives have decent inhibitory activity, out of which compound **42** ($IC_{50} = 0.045 \pm 0.010 \mu\text{M}$), **46** ($IC_{50} = 0.022 \pm 0.010 \mu\text{M}$) have inhibitory activity as



Scheme 5. Synthesis of intermediate compounds **29a-d**; Reagents and conditions; *i*) acetic anhydride, fused sodium acetate (100 °C).



Scheme 6. Synthetic route for the preparation of final compounds **30a-l** [5]; Reagents and conditions; *i*) glacial acetic acid, fused sodium acetate, water bath (100 °C).



Scheme 7. Synthesis of target compounds **31a, b** and **33a-f** [5]; **Reagents and reaction conditions:** *i*) glacial acetic acid, fused sodium acetate, water bath, (100 °C); *ii*) K₂CO₃, DMF, rt stir (30 min), **5a-c** (100 °C).

good as the donepezil (IC₅₀ = 0.049 ± 0.05 μM). Significant inhibitory activity is shown by 7-chloro-quinoline analog **49** (IC₅₀ = 0.012 ± 0.006 μM). To the surprise, simple molecules possessing pyrazolo-pyridine moiety tethered to 6-membered alicyclic heterocycles *via* amide linkage bestowed the most potent AChE inhibitory values. Compound **52** (IC₅₀ = 0.0048 ± 0.001 μM) with pyrazolo-pyridine moiety linked to piperidine is found to have 10-fold higher inhibitory potency compared to donepezil. Alongside, the morpholine analog **54** (IC₅₀ = 0.0049 ± 0.001 μM) has almost similar IC₅₀ value with that of **52**. Structure and activity correlation inferred that inactiveness of compounds **41a** and **41b** might be because of the presence of the ester functionality at quinolone 3-position. However, modification of **41a, b** involving removal of ester group and simultaneous introduction of -Cl at quinolone 7-position paved to the best inhibition properties of **49**. A high negative inductive effect of 2-cyanopyridine could be the reason for the least inhibition property of compound **51**.

1.7. 2,4,5-Trisubstituted-1,2,4-triazole-3-one

Tyrosinase, a copper-containing metalloenzyme plays a prominent role in the biosynthetic pathway of melanin pigment. Melanin is an important pigment reported to be found in various animal parts such as eyes, hair, and skin; it has been reported to protect human skin against UV radiation. However, a higher amount of melanin production and hyperpigmentation are responsible for dermatological disorders like melasma, chloasma, freckles, etc. Thereby the drugs that inhibit tyrosinase could reduce the problems associated with its hyperactivity. 1,2,4-

Triazole compounds have been reported as excellent tyrosinase inhibitors and are being used in cosmetics and pharmaceutical industry. This tyrosinase inhibitory history of 1,2,4-triazoles has inspired to engineer novel 2,4,5-trisubstituted-1,2,4-triazole-3-one scaffolds [7].

The design of the target compounds comprises, heptylation of compound **16** to form compound **17** which is deaminated to afford 1,2,4-triazole derivative **19**. Nucleophilic substitution of compound **19** with various substituted benzyl bromides resulted in *N*-benzyl triazolone scaffolds **55a-d** (Scheme 11).

In the tyrosinase inhibitory activity performed on target compounds with kojic acid as a reference compound, compared to kojic acid (97.2 ± 0.2%) at 1M concentration, compounds **55a** and **55b** have exhibited maximum tyrosinase inhibition percent of 52.9 ± 0.1% at 30 mM and 56.5 ± 0.9% at 6 mM concentration respectively. The corresponding IC₅₀ values are 25 mM and 5 mM respectively for compounds **55a** and **55b** respectively wherein compound **55a** is 3.6 fold higher potent compared to kojic acid (18 mM). As the maximum solubility of compound **55a** is 6 mM, it cannot inhibit tyrosinase beyond 56.5%. The structure-activity relationship shows that the 4-bromobenzyl motif has rendered maximum tyrosinase inhibitory potency. While the exchange of the substituent with higher electronegative groups at benzyl 4-position of **55a** has decreased the inhibitory properties to a larger extent.

1.8. Aryl carboximidamides and 3-aryl-1,2,4-oxadiazoles

COX-1 and COX-2 are the cyclooxygenase isoenzymes that could catalyze the synthesis of prostaglandins, thromboxane, and

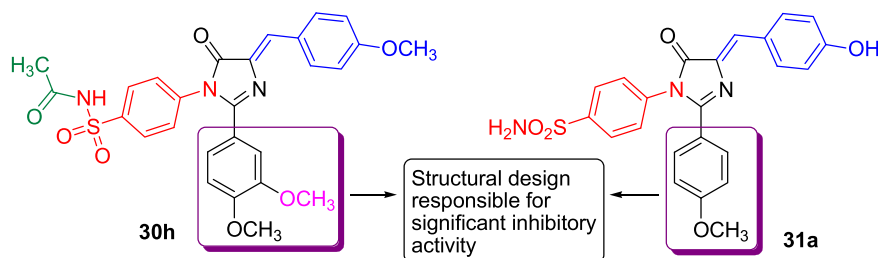
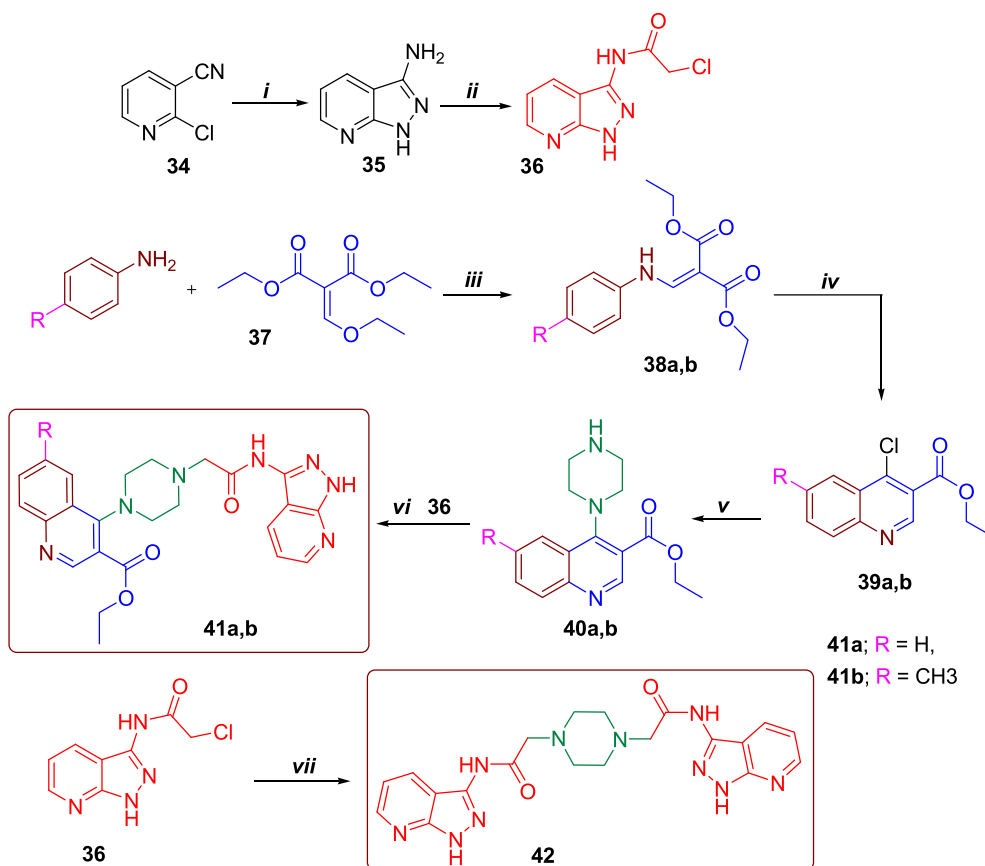
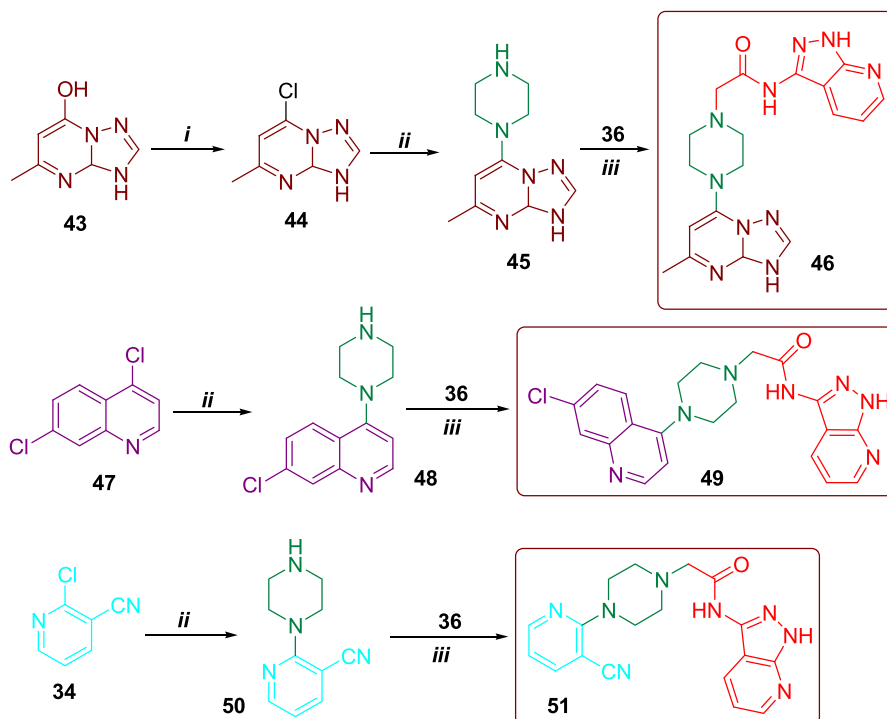


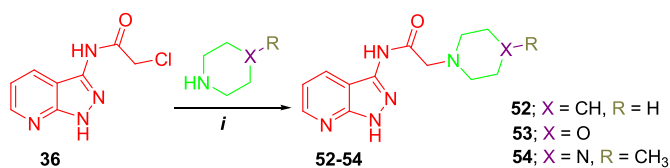
Figure 5. Structure of significant p38αMAPK inhibitor **30h** and p38αMAPK inhibitor/CA dual inhibitor **31a**.



Scheme 8. Synthesis of target compounds 41a, b and 42 [6]; **Reagents and conditions:** (i) Hydrazine hydrate, EtOH, 60 °C; (ii) glacial AcOH, NaOAc, chloroacetyl chloride, RT; (iii) Benzene, 83 °C; (iv) POCl₃, 110 °C; (v) piperazine, MeOH, reflux; (vi) TEA, THF, reflux; (vii) piperazine, TEA, THF, 60 °C.



Scheme 9. Synthetic route for preparation of final compounds 49 and 51 [6]; **Reagents and conditions:** i) POCl₃, 110 °C; ii) piperazine, MeOH, reflux; iii) TEA, THF, reflux.



Scheme 10. Synthesis of pyrazolo-pyridine derivatives 52–54 [6]; **Reagents and conditions:** Piperazine analogs, THF, 65 °C.

levuloglandins. Inhibition of COX enzymes would provide relief from inflammatory, pyretic, thrombotic, neurodegenerative disorders. In the literature, amidoxime and 1,2,4-oxadiazole-possessing scaffolds have antihyperglycemic activity, anti-inflammatory properties, and other pharmacological effects. Thus, such pharmacologically significant moiety is made use in the design of aryl carboximidamides and 3-aryl-1,2,4-oxadiazoles as COX inhibitors [8].

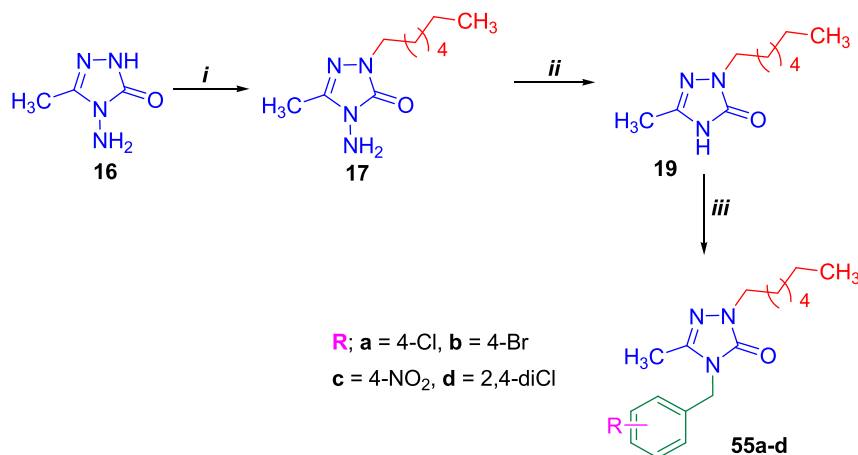
Naproxen 56 is appended to *N'*-hydroxy benzamidine 57 affording aryl carboximidamides 58a-f as one synthetic route. While the carboxylic acid and *N'*-hydroxyamidine functionalities of reactants 56 and 57 respectively are used for cyclization to render oxadiazole derivatives 59a-f (Scheme 12).

The COX-2 enzyme inhibitory activity is determined using celecoxib as a reference compound. All the aryl carboximidamides 58a-f exhibited higher inhibitory potency compared to a reference compound ($IC_{50} = 42.60$ nM). Among these evaluated derivatives, 58a, 58b, 58c, and 58f are the derivatives having noteworthy inhibitory potencies (Table 2);

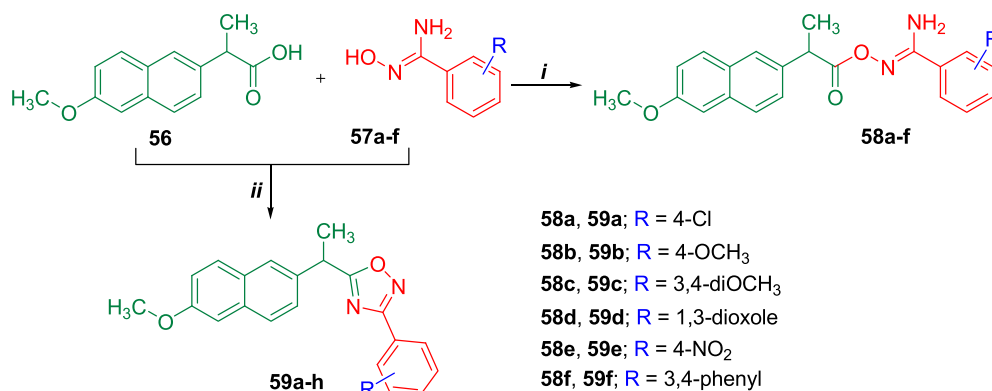
Table 2. COX-2 and 15-LOX inhibitory values of potent final compounds.

Compound	COX-2 IC_{50} (nM)	15-LOX
58a	7.15	1.77
58b	7.48	4.91
58c	6.40	2.07
58f	8.13	3.34
celecoxib	42.60	8.05

wherein compound 58c is approximately 6.6-fold higher potent than reference compound. Accordingly, the same derivatives have also rendered good 15-LOX inhibitory properties and the compound 58a (Figure 6) has bestowed with the strongest inhibitory activity. The structural significance of the potent inhibitor 58c includes the presence of the electron-donating -OCH₃ groups at 3,4-positions of benzamidine motif which bestowed that particular compound with the greatest inhibitory value. The replacement of the electron-donating groups with electron-withdrawing moieties has reduced the inhibitory activity gradually. In the case of LOX inhibitory activity, compound 58a is the most potent molecule possessing chloro group at 4-position of benzamidine moiety. However, the most prominent LOX inhibitor has a negative inductive group -Cl at benzamidine *p*-position. While the compound 58c stands next to the compound 58a probably due to the presence of two methoxy moieties (possessing negative inductive effect) at 3- and 4-positions of benzamidine motif. But an increase in electronegativity to a



Scheme 11. Synthetic route for design of 2,4-trisubstituted-1,2,4-triazole-3-one scaffolds [7]; **Reagents and conditions:** i) absolute ethanol, NaOEt/1-bromoheptane, reflux; ii) H₃PO₂ solution, NaNO₂, room temperature; iii) NaOEt/substituted benzyl bromides.



Scheme 12. Schematic representation of the design of the target compounds 58a-f and 59a-f [8]; **Reagent and reaction conditions:** i) CDI, Acetonitrile, r.t. 3 h; ii) CDI, Acetonitrile, r.t. 3 h, then reflux 24 h.

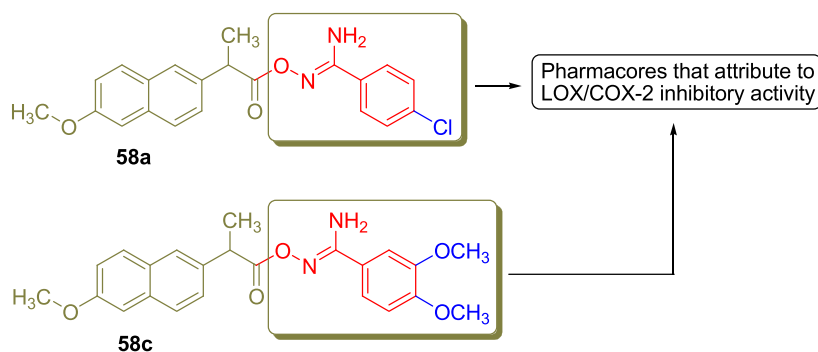


Figure 6. Illustration of the structure of most potent LOX inhibitor (58a) and COX-2 inhibitor (58c).

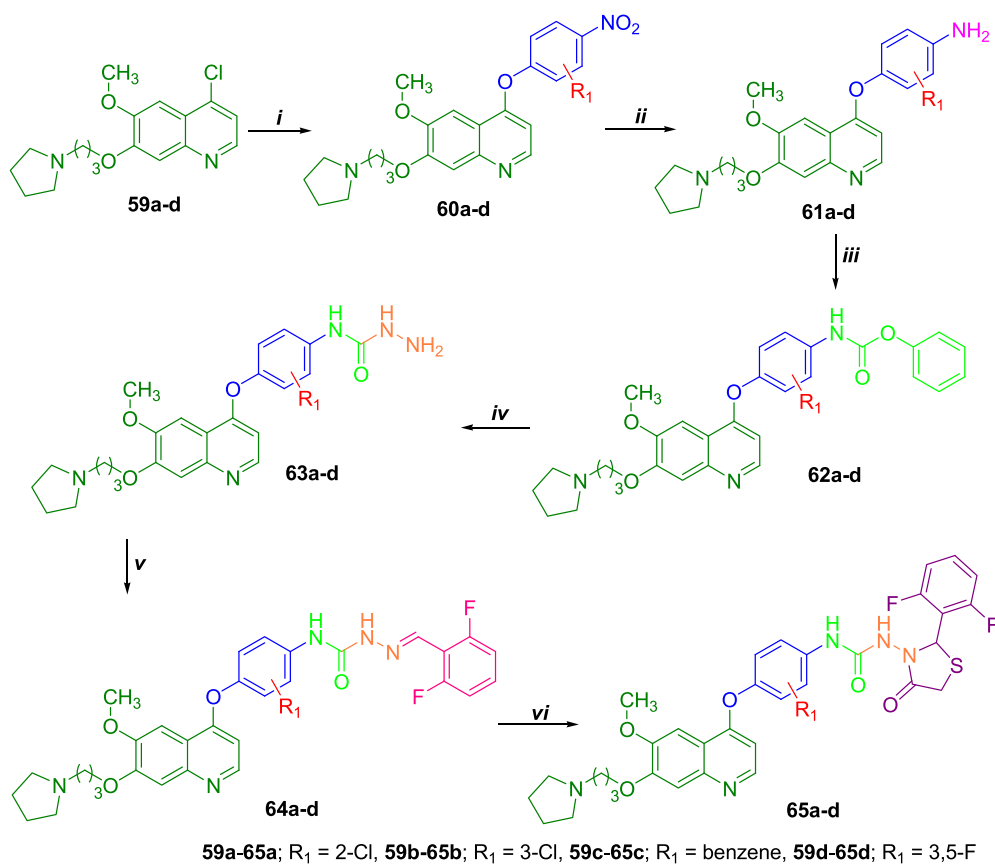
larger extent in the case of compound **58e** has resulted in weak inhibitory activity. When compared the aryl carboximidamides derivatives have displayed stronger inhibitory activity than that of oxadiazoles scaffolds towards both COX-2 and 15-LOX enzymes.

1.9. *N*₁-(4-((7-(3-(4-Ethyl piperazine-1-yl)propoxy)-6-methoxyquinolin-4-yl)oxy)-3,5-difluoro phenyl)-*N*₃-(2-(2,6-difluorophenyl)-4-oxothiazolidin-3-yl)urea

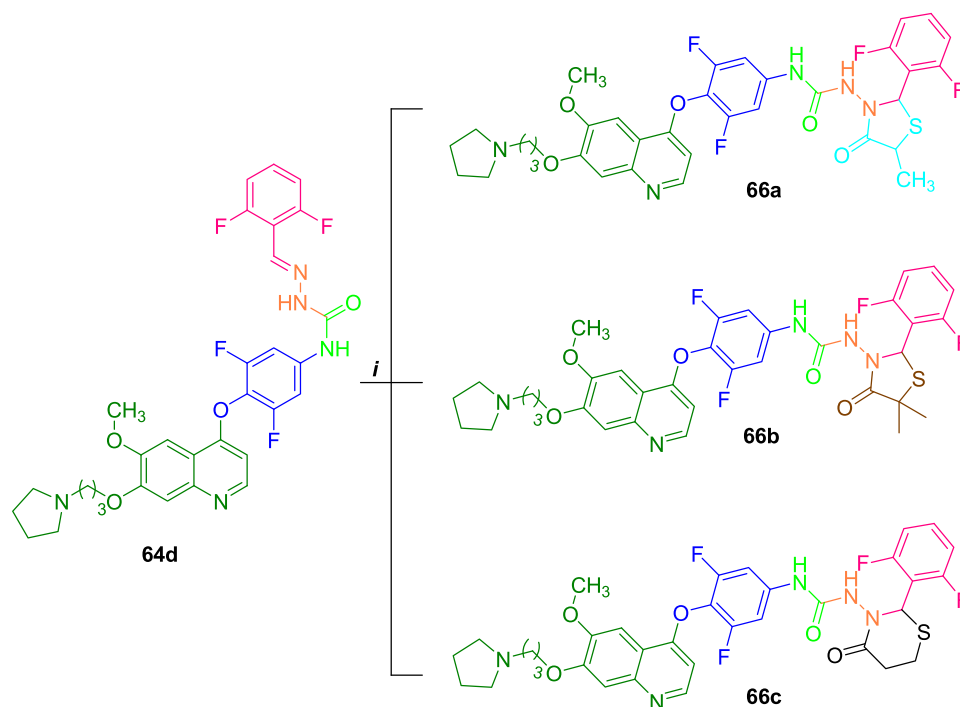
Tyrosine kinases are expressed in both normal and malignant cells; wherein c-Met, Ron, c-Kit, AXL, and IGF-1R could be quoted as few tyrosine kinases whose inhibition properties have been determined. Therefore, the drugs with tyrosine kinase inhibition properties would be attractive chemotherapeutic agents. To develop newer and efficient

chemotherapeutics, urea derivatives are designed as multi-tyrosine kinase inhibitors [9].

4-Chloroquinoline derivatives **59a-d** are allowed to undergo nucleophilic substitution with substituted 4-nitrophenol or 4-nitro-1-naphthol to give ethereal derivatives of quinoline **60a-d** in which nitro group is reduced to form corresponding amine scaffolds **61a-d**. The carbamate derivatives **62a-d** have resulted upon the treatment of compounds **61a-d** with phenyl carbonchloridate. The carbamates **62a-d** are hydrolyzed with hydrazine yielding semicarbazide analogs **63a-d** which are on condensation with 2,6-difluoro benzaldehyde afforded benzylidene-semicarbazide hybrids **64a-d** followed by cyclization with mercaptoacetic acid gave title compounds **65a-d** (Scheme 13). In continuation, the intermediate compound **64d** is utilized for the design of cyclized products. The use of 2-methyl mercaptoacetic acid, 3-mercaptopropionic acid



Scheme 13. Design and synthesis of multi-tyrosine kinase inhibitors [9]; *i*) substituted 4-nitrophenol or 4-nitro-1-naphthol, PhCl, reflux; *ii*) Fe, Conc. HCl, 95% EtOH-H₂O, reflux; *iii*) phenyl carbonchloridate, CH₂Cl₂, pyridine, rt; *iv*) 80% NH₂NH₂-H₂O, xylene, 70 °C; *v*) 2,6-difluorobenzaldehyde, *i*-PrOH, HOAc, reflux; *vi*) SiCl₄, mercaptoacetic acid, CH₂Cl₂, reflux.



Scheme 14. Synthetic route for the preparation of the compounds **66a-c** [9]; **Reagents and conditions:** i) SiCl_4 , 2-methylmercaptoacetic acid, 3-mercapto propionic acid or 2, 2-dimethyl-mercapto acetic acid, CH_2Cl_2 , reflux.

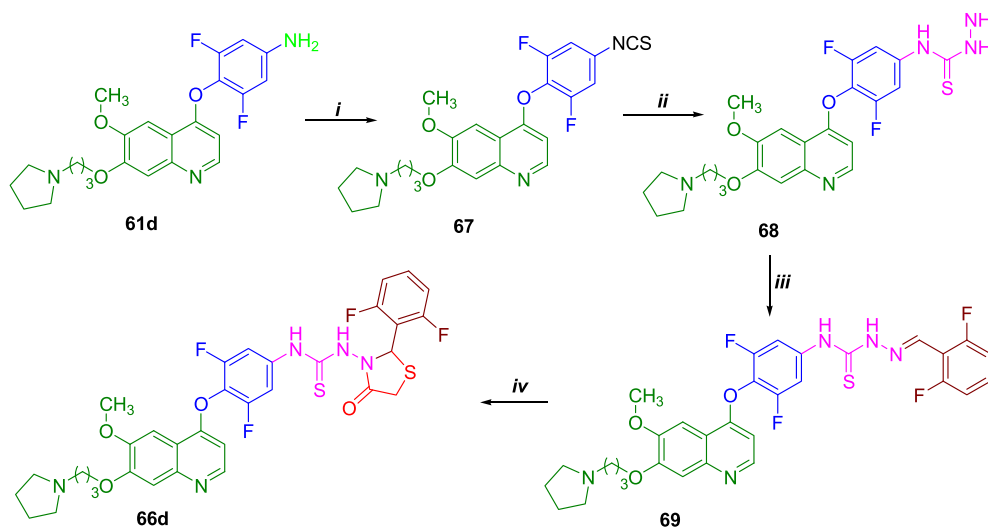
and 2, 2-dimethyl mercaptoacetic acid for cyclization of **64d** produced **66a**, **66b**, and **66c** respectively (Scheme 14).

Compound **61d** is reused as intermediate wherein the amine functionality is converted to isothiocyanate yielding compound **67** which is reacted with hydrazine to produce corresponding thiosemicarbazide **68**. The compound **68** is allowed to undergo a condensation reaction with 2,6-difluoro benzaldehyde, followed by cyclization with mercaptoacetic acid to yield compound **66d** (Scheme 15).

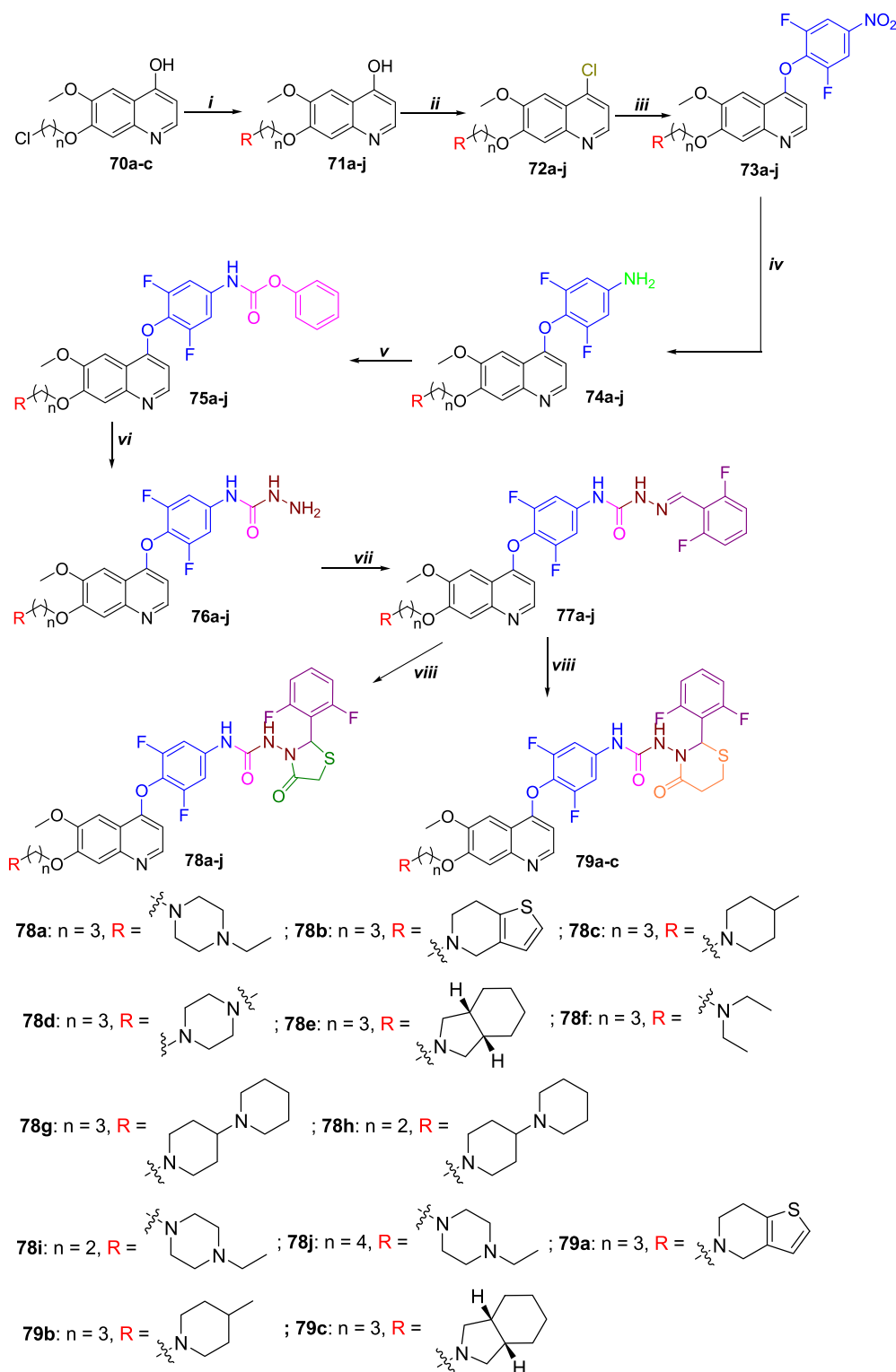
4-Hydroxyquinoline derivatives **70a-c** are allowed to undergo nucleophilic substitution with various secondary amines produced **71a-j** which upon chlorination gave 4-chloroquinoline analogs **72a-j**. Second nucleophilic substitution of compounds **72a-j** with 2,6-difluoro-4-nitrophenol formed 4-aryloxy quinoline derivatives **73a-j** which yielded

corresponding amines **74a-j** on reduction. Carbamates **75a-j** have been resulted by the treatment of **74a-j** with phenyl carbonchloridate and subsequent hydrolysis with hydrazine hydrate yielded **76a-j**. Condensation products **77a-j** are resulted by the reaction of compounds **76a-j** with 2,6-difluorobenzaldehyde. The intermediate compounds **77a-j** are cyclized with mercaptoacetic acid and 3-mercapto propionic acid to form final compounds **78a-j** and **79a-c** respectively (Scheme 16).

Considering cabozantinib as a reference compound, the designed derivatives are screened for c-Met kinase inhibitory activity against the cancer cell lines A549, HT-29, and MDA-MB-231. In the case of compounds **65a-d**, identical percent inhibition towards c-Met is exhibited by compound **65d** (Table 3) having 3,5-difluorobenzene moiety to that of reference. The compound **66c** with thiazinone ring has shown better



Scheme 15. Synthesis of the thiourea derivative **66d** [9]; **Reagents and conditions:** i) CCl_4 , NaHCO_3 , H_2O , rt; ii) 80% $\text{NH}_2\text{NH}_2 \cdot \text{H}_2\text{O}$, CH_2Cl_2 , rt; iii) 2,6-difluoro-benzaldehyde, *i*-PrOH, HOAc, reflux; iv) SiCl_4 , mercaptoacetic acid, CH_2Cl_2 , reflux.



Scheme 16. Synthesis of compounds **78a-j** and **79a-c**; **Reagents and conditions** [9]: **i**) amine, CH_3CN , reflux; **ii**) POCl_3 , reflux; **iii**) **2, 6-difluoro-4-nitrophenol**, PhCl , reflux; **iv**) Fe , Conc. HCl , 95% $\text{EtOH-H}_2\text{O}$, reflux; **v**) phenyl carbonochloridate, CH_2Cl_2 , pyridine, rt; **vi**) 80% $\text{NH}_2\text{NH}_2\text{-H}_2\text{O}$, xylene, 70 °C; **vii**) 2,6-difluorobenzaldehyde, $i\text{-PrOH}$, HOAc , reflux; **viii**) SiCl_4 , mercaptoacetic acid or 3-mercaptopropionic acid, CH_2Cl_2 , reflux.

inhibition properties. Meanwhile, compound **78a** possessing *N*-ethyl piperazine motif & thiazolone ring and compound **78f** with diethylamine & thiazolone motifs have elicited excellent inhibitory properties towards all cancer cell lines.

Structure-activity relationship reveals that the significant *c*-Met inhibitory activity of compound **65d** is attributed to the 3,5-difluoro-4-

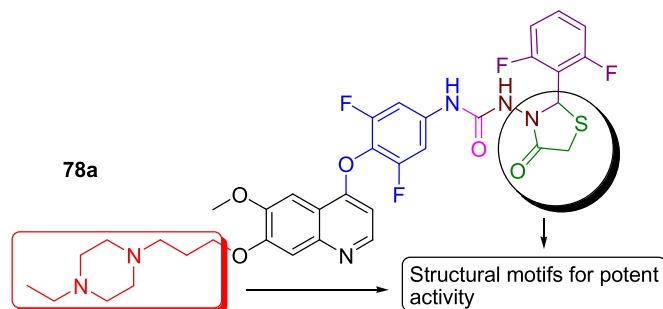
oxyaniline moiety. The particular compound has exhibited activity higher than previously reported 3-F analog which infers that second -F atom has boosted the inhibitory activity. Change in the halogen atom and its position resulted in diminished activity than that of compound **65d**. In the **66a-d** series of compounds, thiazinone ringed molecules displayed the most prominent activity. Other molecules of this series with methyl

Table 3. c-Met inhibitory properties of most potent compounds.

Compd.	c-Met Inhibition (%)	IC ₅₀ (μM)		
		A549	HT-29	MDA-MB-231
65d	79.06	0.56 ± 0.048	0.23 ± 0.022	8.35 ± 0.86
66c	68.95	0.40 ± 0.058	0.27 ± 0.019	9.65 ± 0.78
78a	83.82	0.35 ± 0.029	0.073 ± 0.0086	3.10 ± 0.47
78f	78.57	0.45 ± 0.051	0.091 ± 0.0096	3.79 ± 0.51
Cabozantinib	80.76	9.52 ± 0.91	11.5 ± 1.1	13.4 ± 1.2

thiazolone (66a) and dimethylthiazolone (66b) ring shown reduced inhibitory activity. In other series of derivatives 78a-j, N-propyl pyrrolidine ring at 7-position of quinoline moiety is substituted by various cyclic secondary amines in a combination of different alkyl chains. The maximum inhibitory properties have been elicited by the compound 78a (Figure 7) with N-ethyl-N-propyl piperazine motif. Likewise, compound 78f possessing N, N'-diethylamine exhibited decent inhibitory effects whose potential is next to the potency of 78a. When it comes to structural modification, varying of secondary amines and alkyl chains for remaining derivatives shown weak activity. Even with identical moiety N-ethyl-N-propyl piperazine in the compounds 78i and 78j, they failed to exhibit good inhibitory activity as they have ethyl and butyl chains respectively. Also abated inhibitory effects are observed with N-methyl piperazine motif in case of compound 78d with propyl chain. In the series 78a-j, semicarbazide functionality is transformed to thiosemicarbazide to check the c-Met inhibitory properties. Unfortunately, no single compound has enough inhibitory effect which could be comparable to compound 78a. Out of all the final compounds, designed compound 78a is found to be more apt as a c-Met inhibitor wherein it is 27-fold and 157-fold higher potent towards A549 and HT-29 respectively compared to the reference compound. While approximately 4.3-fold stronger inhibitory activity is observed for the MDA-MB-231 cell line. In the same way compound 78f has 21-fold, 126-fold and 3.5-fold greater potencies towards A549, HT-29, and MDA-MB-231 cell lines respectively compared to cabozantinib.

Considering the most potent activity of compound 78a, it is chosen for inhibitory screening towards other tyrosine kinases such as c-Met, Ron, c-Kit, KDR, HER-2, ALK, c-Src, IGF-1R, EGFR, and AXL. Except for a few kinases such as HER-2, ALK, and IGF-1R, the compound 78a met with good expectations (Table 4). Amongst them, the compound 78a has

**Figure 7.** Structure of potent multi-tyrosine kinase inhibitor.**Table 4.** Multi-tyrosine kinase profile of compound 78a.

Kinase	IC ₅₀ (μM)	Kinase	IC ₅₀ (μM)
c-Met	0.015	ALK	>10
Ron	0.0029	c-Src	0.24
c-Kit	0.064	IGF-1R	2.1
KDR	0.85	EGFR	0.52
HER-2	>10	AXL	0.053

elicited the most potent activity towards the kinase Ron. Thereby it can be a perfect multi-tyrosine kinase inhibitor.

2. 5,6-Dichloro-2-methyl-1H-benzimidazole derivatives

Urease is a redox metalloenzyme present in most of the plants and animals; wherein it causes diseases such as pyelonephritis, urolithiasis, duodenal ulcer, chronic gastritis, etc. Hence to counteract these negative effects of urease, pharmaceutical drugs with urease inhibitory effects are most essential and thereby such inhibitors are designed and synthesized. Compounds such as imidazoles, hydroxamic acid, phosphoramidites, humic acid and 1,4-benzoquinone can be included as some of the important urease inhibitors. Further, urease inhibitory potency of 5,6-dichlorobenzimidazole scaffolds, benzyl derivatized benzimidazoles and 4,5-dichlorobenzimidazole analogs possessing cyclopropyl ring at C₂ position has triggered to design and investigate novel 2-methyl benzimidazole derivatives [10].

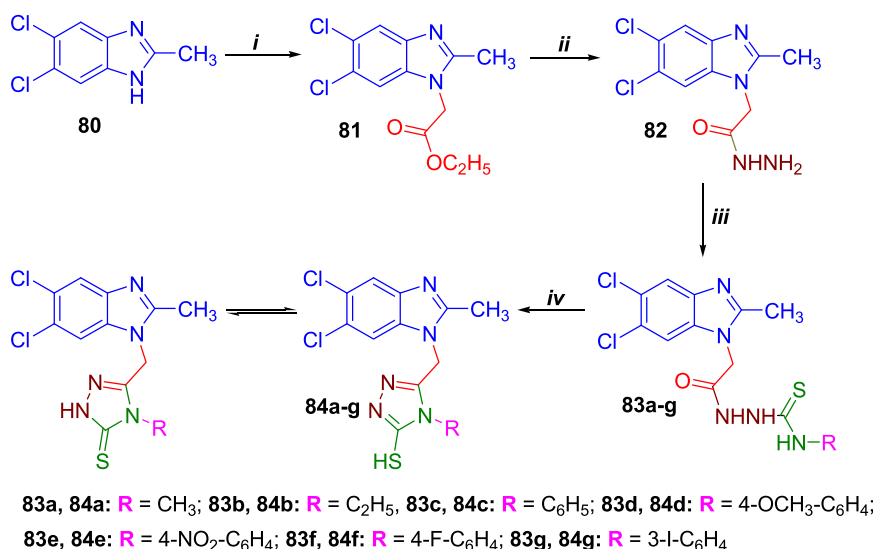
5,6-Chloro-2-methyl benzimidazole 80 is nucleophilically treated with bromoethylacetate forming N-substituted benzimidazole 81 in which ester group is transformed to semicarbazide 82 and on subsequent reaction with substituted thiocyanates afforded thiosemicarbazide derivatives 83a-g. Finally, the cyclization reaction of the derivatives 83a-g with NaOH/NaHCO₃ yielded N₁-methylene triazole benzimidazoles 84a-g (Scheme 17).

All the synthesized benzimidazole derivatives are tested for their anti-urease activity in the presence of the standard urease inhibitor thiourea and found to be good urease inhibitors (IC₅₀ = 0.0294 ± 0.0015 to 0.1494 ± 0.0041 μM). Unsubstituted benzimidazole 80, N-ester substituted compound 81, its semicarbazide derivative 82 and compounds 84a, 84b have weak inhibitory activity compared to subsequent analogs. Other derivatives have shown significant effects. The most potent urease inhibitory property is displayed by the compounds 83e (IC₅₀ = 0.0354 ± 0.0017 μM) and 84e (IC₅₀ = 0.0294 ± 0.0015 μM). Compound 84g can also be included in potential urease inhibitors list with IC₅₀ value of 0.0357 ± 0.0015 μM.

Correlation between evaluated structures and their inhibitory values show that compounds 80, 81, and 82 do not yield any fruitful results as they lack the pharmacological significant functionality. Attachment of substituted thiosemicarbazide functionality has resulted in enhanced inhibitory activity in the case of compounds 83a-j. Particularly compound 83e (Figure 8) possessing 4-nitrobenzene connected to thiosemicarbazide moiety has bestowed with the greatest activity. Alkyl and simple phenyl as well 4-OCH₃, 4-F and 3-I phenyl analogs exhibited little reduced activity. The corresponding cyclized molecules triazole-thiol derivatized benzimidazoles 84a-j could reach up to the mark except for N-alkyl triazolethiol-benzimidazoles 84a and 84b. Out of the potent molecules of this series, compound 84e has turned out as a noteworthy molecule. Again electron-withdrawing 4-nitrobenzene motif has rendered significant urease inhibitory activity.

2.1. 5-Arylisothiazol-3(2H)-one-1,1-(di)oxides

Overexpression of carbonic anhydrases such as hCA IX and XII have shown in certain cancer types. A cyclic secondary sulphonamide, 1,2-benzisothiazol-3-(2H)-one-1,1-dioxide has been described as a selective hCA IX inhibitor. Inspired by the CA inhibitory activity of N-substituted



Scheme 17. Synthetic route for the preparation of the final compounds 84a-g [10]; **Reagents and conditions:** i) bromoethylacetate, K₂CO₃, acetone; ii) NH₂NH₂•H₂O, EtOH, reflux; iii) R-CNS, EtOH, reflux; iv) 2N NaOH/1M NaHCO₃.

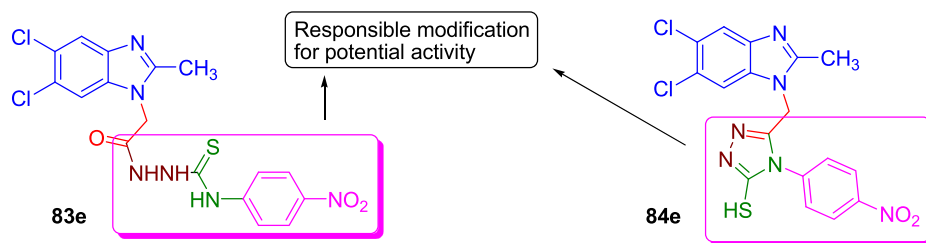


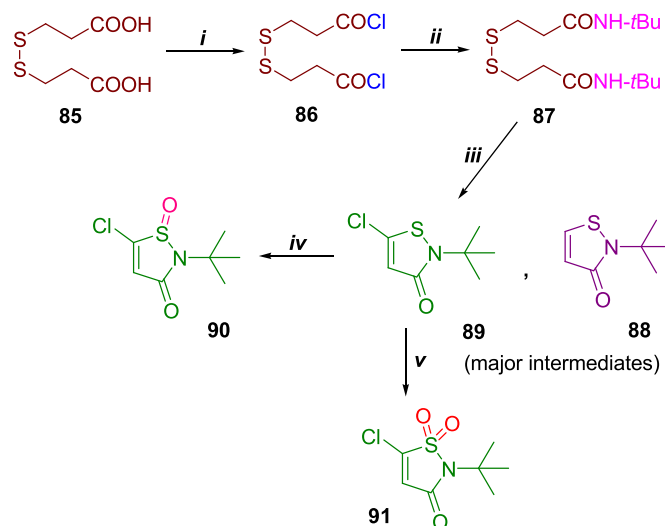
Figure 8. Structures of the remarkable urease inhibitors.

saccharin derivatives, a series of *N-tert*-butylisothiazolones are reported to have CA inhibitory activities [11].

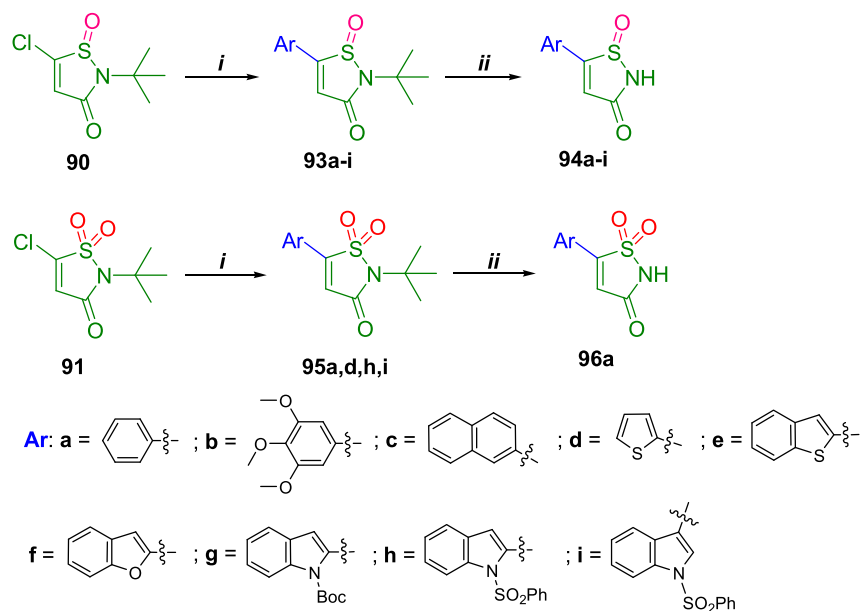
Bis(3-Thiopropionic acid) **85** is chlorinated with thionyl chloride to give carbonyl chloride analog **86** which on treatment with *t*-butyl amine to yield corresponding amide **87**. *t*Butylamide of thiopropionic acid **87** is cyclized mediated by thionyl chloride and afforded isothiazole derivatives wherein compounds **88** and **89** are major isothiazoles formed. 5-Chloro-*N-tert*-butylisothiazole **89** is further oxidized with *m*-CPBA in equivalents 1.4 and 3 eq producing isothiazole monoxide **90** and isothiazole dioxide **91** respectively (Scheme 18). Compounds **90** and **91** are utilized for the further design of 5-arylisothiazole derivatives. Compound **90** is allowed to undergo Suzuki coupling with various aryl boronic acids to yield coupled products **93a-i** which on dealkylation rendered compounds **94a-i**. The similar reaction conditions are maintained for compound **90** to synthesize compound **96a** (Scheme 19).

The newly designed derivatives are allowed to inhibit isoenzymes *h*CA I, *h*CA II, *h*CA IX and *h*CA XII of CA using reference compound AAZ. No single compound has possessed significant inhibitory activity towards *h*CA I, *h*CA II isoenzymes. A poor activity is shown by the compound **90** and **95i** towards *h*CA I and *h*CA II enzymes respectively. However, few derivatives are successful in exhibiting remarkable inhibitory activity towards *h*CA IX and *h*CA XII. Compared to reference ($K_i = 12$ nM) compound **93i** ($K_i = 8.8$ nM) is significant *h*CA IX inhibitor. Besides these, derivatives **93a** and **95i** have been reported to possess excellent *h*CA IX inhibitory properties with K_i values of 4.5 nM and 4.3 nM respectively. The inhibitory properties of compounds **93a** and **95i** are approximately threefold higher potent than the reference compound. While the CA inhibition towards XII, some derivatives have displayed decent activity. In that, compound **93a** ($K_i = 4.3$ nM) has exhibited slightly higher activity than the reference compound. The excellent

inhibitory activity is elicited by the compound **93i** (Figure 9) with K_i value of 0.76 nM whose inhibitory activity is 7.6 times stronger than that of AAZ. Other significant inhibitors include compounds **95a** and **95i** (Figure 9) having K_i values of 0.97 nM and 0.94 nM respectively; corresponding K_i values are 5.8 fold stronger compared to AAZ.



Scheme 18. Synthetic pathway for the preparation of the compounds **90** and **91** [11]; **Reagents and conditions:** i) SOCl₂, dry CH₂Cl₂, rt (10 min), 80 °C (2.5–3h); ii) *t*Bu-NH₂, dry CH₂Cl₂, 80 °C (12h); iii) SO₂Cl₂, ClCH₂CH₂Cl, rt (24h); iv) *m*-CPBA (1.4 eq), CH₂Cl₂; v) *m*-CPBA (3.0 eq).



Scheme 19. Synthetic route for preparation of target 5-arylisothiazole oxide scaffolds; **Reagents and conditions:** *i*) Ar-B(OH)₂ (2.0 eq), K₂CO₃ solid, 80 °C/GPA: Pd(PPh₃)₄, THF or GPA: PdCl₂(dppf), CH₂Cl₂, DME, sealed tube; *ii*) TFA, MW, sealed tube.

Whatever the structure and its modification of the inhibitor, no significant inhibition is observed toward both *hCA* I and *hCA* II enzymes. Among the isothiazole monoxides, the derivative **93i** possessing (*N*-sulfonylphenyl)-benzimidazole connected *via* 3-position shown stronger inhibitory effects than the standard compound. The identical motif attachment to the isothiazole ring *via* 2-position (compound **93h**) has shown fivefold diminished activity. Other heterocycles containing isothiazoles with heteroatoms such as S (**93e**) or O (**93f**) displayed abated inhibitory activity. Also, the substitution of the phenylsulfonyl moiety with *-Boc* (**93g**) has not resulted in a good inhibitory property. Surprisingly, simple phenyl substituted isothiazole scaffold **93a** has turned to be the most potent IX inhibitor. Further oxidation of compound at sulfur led to the formation of derivative **95i** in which the inhibitory activity ($K_i = 4.3$ nM) is doubled compared to that of compound **93i**. When it comes to structure-activity relationship towards *hCA* XII, simple phenyl substituted analog **93a** ($K_i = 4.3$ nM) is successful in inhibition of *hCA* XII and its activity is comparable to reference compound ($K_i = 5.7$ nM). Compound **93i** with decent *hCA* IX inhibitory activity has got its inhibitory activity extended to the *hCA* XII enzyme also. A little reduced activity is rendered by the dioxide analog **95i** of compound **93i** which reveals that little significance has prevailed with monoxide and dioxide isothiazole derivatives. However, a difference in inhibitory activity is seen in between simple phenyl isothiazole monoxide **93a** and its dioxide analog **95a**. It indicates that the dioxide fragment is crucial for potential *hCA* XII inhibitory activity. Finally, *N*-debutylated isothiazole scaffolds are not found to be good *hCA* inhibitors.

2.2. Anti-fungal azoles

Fungal infections have become most common in animals and plants in which *Candida albicans* is a most general fungal pathogen. To address these serious issues, azoles are the chemical agents that have been engineered. Lanosterol-14 α -demethylase, a prominent enzyme of fungus (a major fungal plasma membrane component) is essential for the synthesis of ergosterol. Lanosterol-14 α -demethylase has been targeted for the design of the potent anti-fungal agents. Considering this, reported antifungal agents are assessed for their lanosterol-14 α -demethylase inhibitory activity [12]. Here the enzyme inhibitory activity is correlated with the molecular descriptors; wherein the principal component analysis method is employed. Using this method, lanosterol-14 α -demethylase inhibitory activity (IC₅₀ values) of the various anti-fungal agents is judged with proper justification.

In this method, the anti-fungal activity of each azole anti-fungal agent is analyzed by three major factors/components; wherein the first principal component demonstrates the molecular complexity of the anti-fungal agents. The second principal component indicates hydrogen bond interactions, topological polar surface area, and lipophilicity. Finally, the third principal component explains the undefined atom stereocenter in addition to lipophilicity. The first, second and third components are accounted for in the proportion of 51.79:25.50:11.38 respectively. The assessment of the various anti-fungal agents indicated that Itraconazole (Figure 10) is found to have better comprehensive value and lowest IC₅₀ value among the other anti-fungal agents (Table 5). The

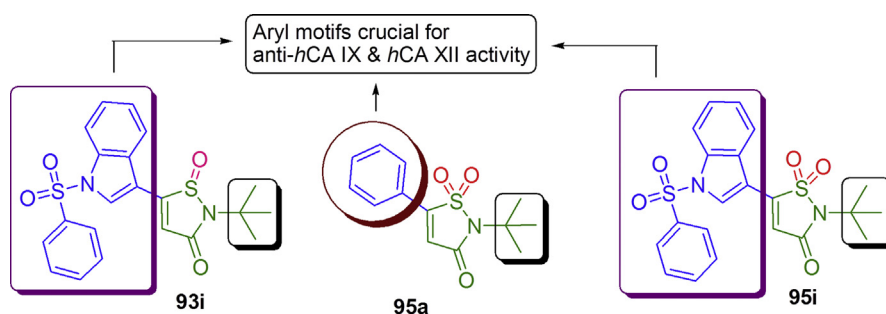


Figure 9. Structures of 5-arylisothiazoles as most significant CA IX and XII inhibitors.

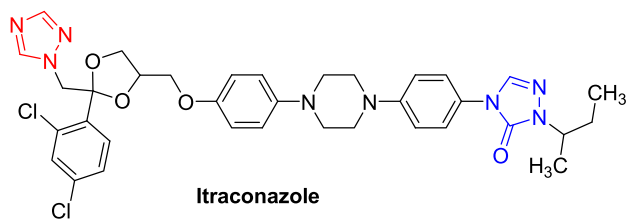


Figure 10. Structure of potent lanosterol-14 α -demethylase inhibitor.

itraconazole is followed by the fluconazole and ketoconazole in the potent comprehension values list. The results inferred that IC_{50} is not only the factor to look for the design of a potent drug molecule but it is the comprehensive factor, the balance of the three principal components. Although the Flusilazole, Imazalil, Miconazole, and Penconazole have decent IC_{50} values but ranked 14, 15, 16 and 17 respectively that reveals that a great significance lies with the first principal component.

2.3. 1,2-Benzisothiazol-3(2H)-one-1,1-dioxide derivatives

The COX inhibition properties of saccharin and pyrazole derivative celecoxib have been demonstrated. Similarly, pyrazolyl benzene sulfonamides connected to thiazolidinones and pyrazoles exhibited higher COX-2 selectivity. Here in 1,2-benzisothiazol-3(2H)-one-1,1-dioxide derivatives have been designed and synthesized as COX-1/COX-2 inhibitors [13].

The sodium salt of saccharin **97**, benzylated at *N*-position formed *N*-benzylated saccharin **98**, which on hydrolysis using hydrazine given hydrazide analog **99**. Subsequently, compound **99** is utilized as intermediate for the design of target compounds. In one way, compound **99** is allowed to undergo intramolecular cyclization to produce oxadiazole thiol **100**, followed by ethyl/benzyl substitution on thiol functionality gave oxadiazole thiol derivatives **101a-b**. Again, intermediate **99** is utilized in one more way, wherein thiosemicarbazide derivative **102** is synthesized from compound **99** using CS_2 ; intra-molecular cyclization of which resulted in triazole-thiol **103**. The condensation of compound **103**

with various 4-substituted benzaldehydes paved to triazole imines **104a-d** (Scheme 20).

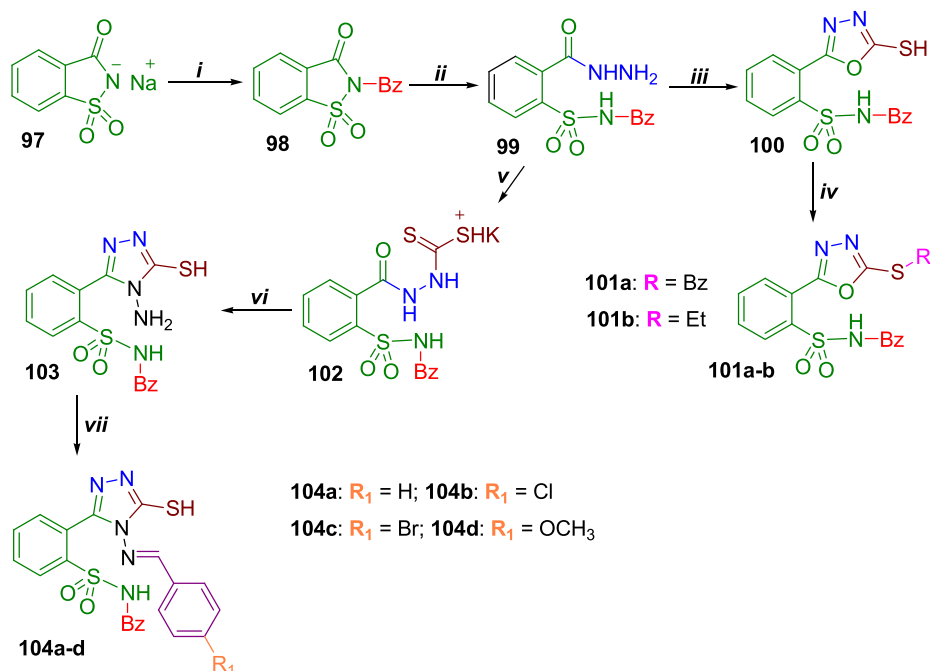
N-Isopropylation of saccharin produced compound **105** followed by hydrolysis with hydrazine has given hydrazide derivative **106**. Hydrazide functionality is utilized for intramolecular cyclization with benzoylacetate and benzoyl acetone to render the final compounds **107** and **108** respectively (Scheme 21). Diethyl malonate is attached to saccharin forming *N*-substituted saccharin **109**. Diester functionality is transformed into dihydrazide analog **110**, in which the hydrazide fragments are cyclized to pyrazole modified saccharin **111** as a first part. The second part involves condensation of the dihydrazide analog with 4-substituted benzaldehydes to form diimine derivatives of saccharin **112a-c** (Scheme 22).

The designed compounds have been allowed to inhibit COX-1/COX-2 enzymes in the presence of the standard COX inhibitor celecoxib. Almost every single compound synthesized has exhibited higher potential ($IC_{50} = 1.98$ – 12.23 μ M) in comparison with celecoxib ($IC_{50} = 14.8$ μ M). However, amongst the competing inhibitors, the isothiazole imines **112a** (Figure 11) and **112b** exhibited the most potent COX-1 inhibitory activity with IC_{50} values 1.98 μ M and 2.78 μ M respectively. However, not a quite good inhibitory activity is displayed by the evaluated molecules towards the enzyme COX-2 wherein the inhibitory activity is in the range of $IC_{50} = 0.05$ – 0.71 μ M. Compound **107** has shown some significance ($IC_{50} = 0.09$ μ M) yet half the activity exhibited by reference. The derivatives **108** ($IC_{50} = 0.06$ μ M) and **111** ($IC_{50} = 0.05$ μ M) are successful in rendering strongest inhibitory activity which are almost similar to that of standard compound ($IC_{50} = 0.05$ μ M).

The compound **103** possessing benzylated sulfonamide and triazole-thiol moieties exhibited decent activity ($IC_{50} = 2.98$ μ M). Further structural modification comprising condensation products **104a-d** displayed diminished inhibitory effects. However, unexpectedly gradual increased inhibitory activity is observed for the compounds **104a-d** with an increase in bulkiness with respect to benzene 4-position. The activity is desperately reduced in the case of pyrazole derivatives **107**, **108** and **111**. It indicates that pyrazole derivatives are not apt candidates for COX-1 inhibitory activity. Benzylidene-hydrazide derivative of saccharin **112a** is found to be the most potent COX-1 inhibitor. But the inhibitory properties are reported to be reduced a little for compound **112b** with –F

Table 5. Principal component analysis of azoles as anti-fungal inhibitors.

Anti-fungal drug	Principal Component Score				Rank	IC_{50} (μ M)
	Component 1	Component 2	Component 3	Comprehensive		
Itraconazole	11.0063	1.4266	3.1907	6.4271	1	0.039
Fluconazole	7.3476	3.8262	0.1646	4.7998	2	0.051
Ketoconazole	8.1369	0.9626	1.7690	4.6609	3	0.064
Bitertanol	6.7464	1.3138	2.9667	3.8957	4	0.330
Triadimenol	6.2233	1.3138	2.9667	3.8957	5	0.330
Propiconazole	6.3124	0.5664	3.1313	3.7700	6	0.150
Triadimefon	6.2432	0.9526	1.9976	3.7036	7	0.130
Tebuconazole	6.3006	0.6124	2.3679	3.6887	8	0.350
Hexaconazole	6.2842	0.6124	2.3679	2.3679	9	0.066
Cyproconazole	5.8822	1.0154	2.8845	3.6336	10	0.100
Myclobutanil	6.2899	0.5310	2.0388	3.6249	11	0.140
Epoxiconazole	5.9337	0.6880	3.0079	3.5908	12	0.220
Prochloraz	6.3856	-0.3572	1.8924	3.4314	13	0.098
Flusilazole	5.8708	0.3585	1.5222	3.3051	14	0.085
Imazalil	5.8969	-0.4431	2.4090	3.2151	15	0.082
Miconazole	6.0850	-1.1988	3.0261	3.1901	16	0.072
Penconazole	5.4482	-0.7162	2.6559	2.9412	17	0.076
Bifonazole	4.8339	-1.4026	2.8204	2.4668	18	0.300
Clotrimazole	4.8796	-1.5034	2.0570	2.3779	19	0.091

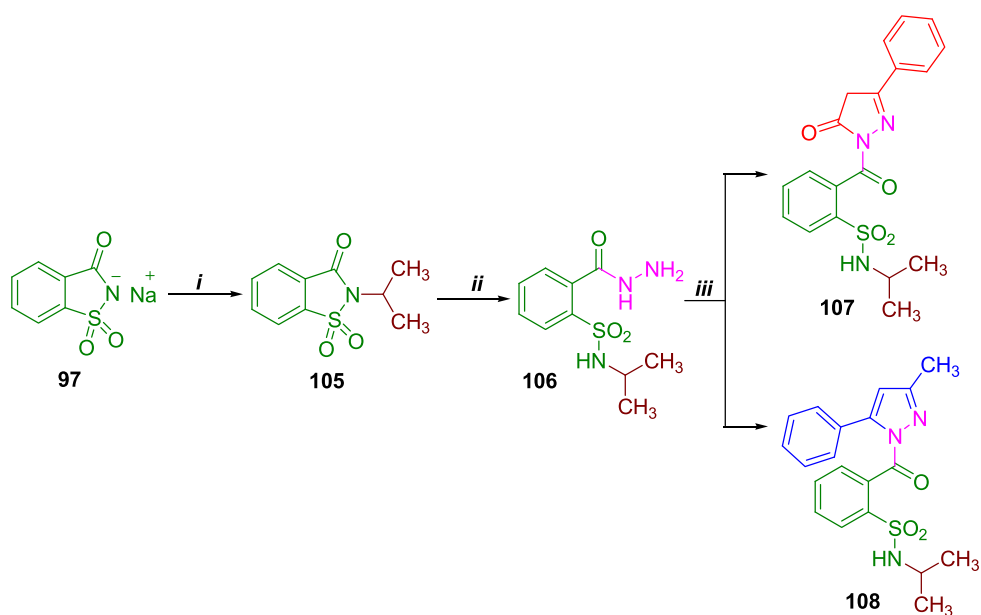


Scheme 20. Illustration of synthetic route for preparation of compounds **101a-b** [13]; **Reagents and conditions:** *i*) benzyl bromide, DMF, reflux (2h); *ii*) NH_2NH_2 , rt (15 min); *iii*) CS_2 , KOH, EtOH, reflux (6h); *iv*) benzyl bromide and or ethyl iodide, EtOH, KOH, rt (2h); *v*) EtOH, CS_2 , KOH, rt (14h); *vi*) NH_2NH_2 , reflux (1h); *vii*) Ar-CHO, AcOH, reflux (20min).

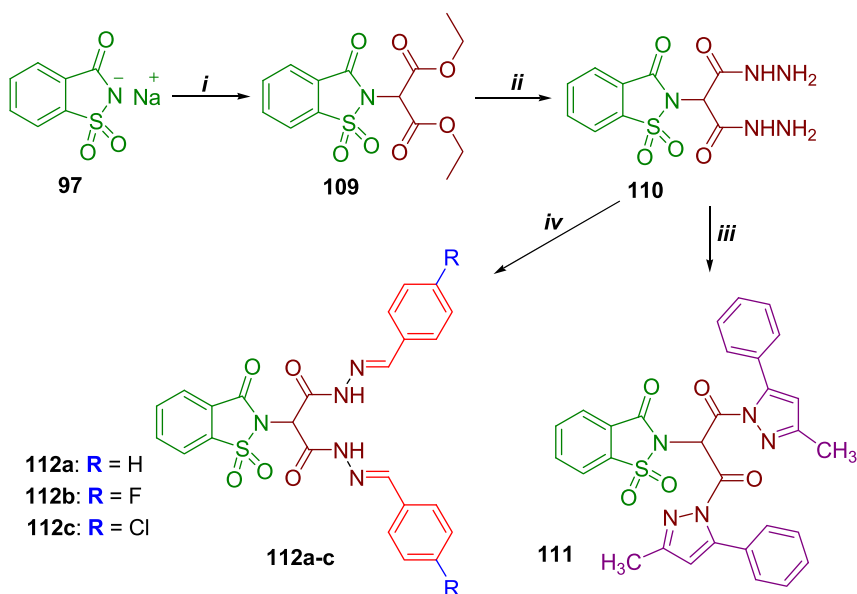
substitution at benzylidene 4-position. Again the activity lowered greatly for **112c** with -Cl substitution inferring that inhibitory activity reduced with elevated bulkiness at benzylidene 4-position. In the case of COX-2 inhibition properties, only the pyrazole analogs **107**, **108**, and **111** have shown good COX-2 inhibitory effects. Comparatively compound **107** possessing pyrazolone ring in combination with *N*-isopropyl sulfonamide fragment rendered half the inhibitory activity to that of pyrazole analog **108**. But the compound **111** having two pyrazole rings and an intact saccharin ring has bestowed strongest COX-2 inhibitory activity. These facts indicate that COX-2 selectivity is observed for the pyrazolone ring compounds and benzylidene-hydrazide analogs are selective COX-1 inhibitors.

2.4. Benzene sulfonamides linked quinazoline scaffolds

Carbonic anhydrases *hCA* IV, IX and XII have been reported for their involvement in rheumatoid arthritis. The transmembrane isoforms *hCA* IX/XII are demonstrated to have overexpressed in many hypoxic tumors. The quinazolinone pharmacore has been utilized for the design of the CA inhibitors. 4-(Quinazolin-4-ylamino) benzene sulfonamides and 4-(quinazolin-4-yloxy) benzenesulfonamide exerted decent cytosolic *hCA* I & II and the transmembrane *hCA* IX & XII inhibitory properties. Based on the above rationale, a new series of 2-substituted-mercapto-3-substituted-4(3*H*)-quinazolinones appending benzenesulfonamide moiety to it [14] is designed.



Scheme 21. Representation of design of compounds **107** and **108** [13]; **Reagents and conditions:** *i*) Isopropyl iodide, DMF, reflux, (2h); *ii*) NH_2NH_2 , rt (2h); *iii*) benzoylacetone and/or benzoyl acetone, EtOH, AcOH, reflux (12h).



Scheme 22. Synthesis of the final compounds **111** and **112a-c** [13]; **Reagents and conditions:** *i*) diethyl 2-bromomalonate, DMF, reflux (2h); *ii*) NH_2NH_2 , rt (20min); *iii*) benzoyl acetone, EtOH, AcOH, reflux (12h); *iv*) Ar-CHO, EtOH, AcOH, reflux (2h).

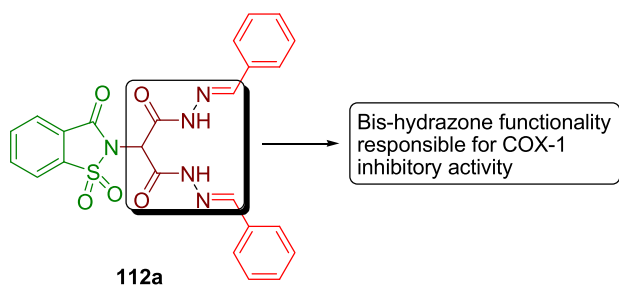
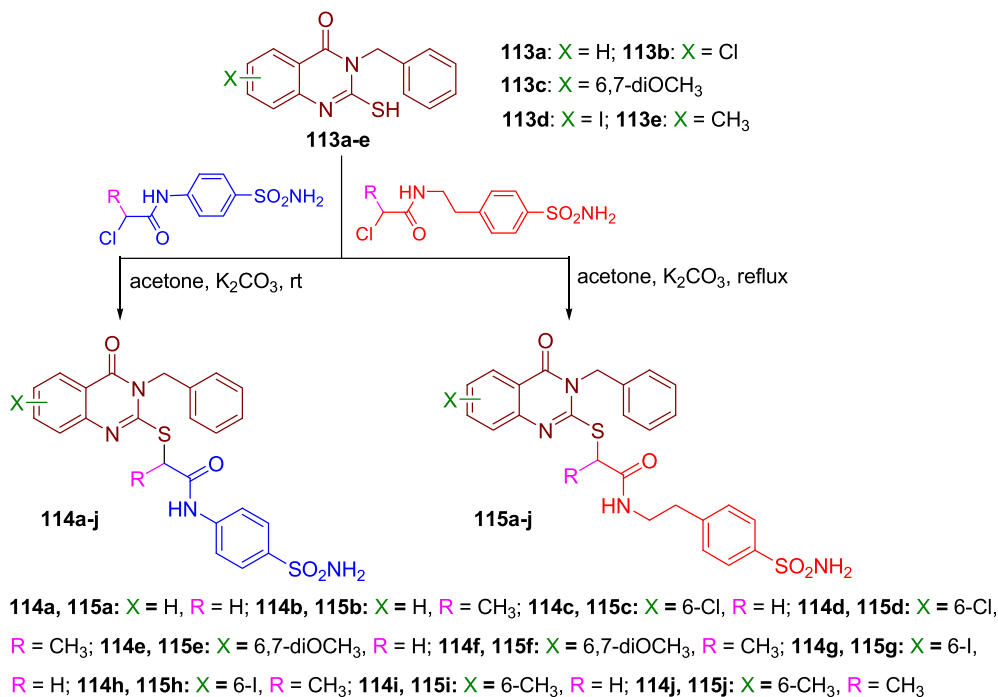
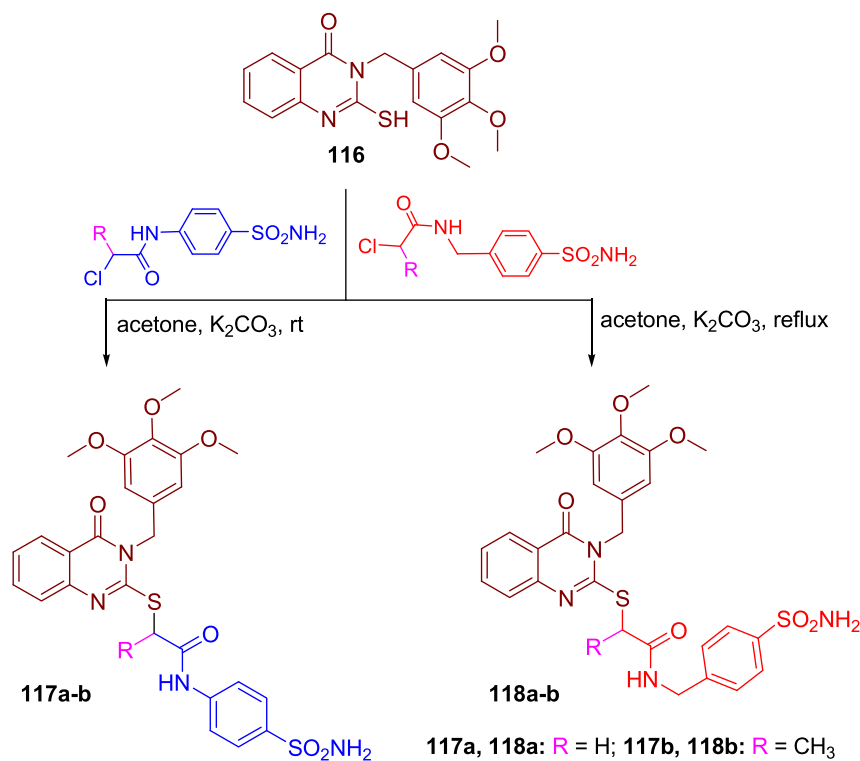


Figure 11. Structure of compound **112a** possessing COX-1 inhibitory.

The synthesis of compounds **114a-j** and **115a-j** comprises treatment of N_3 -benzyl-quinazolinone thiol scaffolds **113a-e** with sulfonamide derivatives possessing chloroanilide functionality at 4-position to get corresponding derivatives **114a-i**. In the second part, compounds **113a-e** have been allowed to undergo nucleophilic substitution with sulfonamide derivatives tethered to chloroanilide functionality via ethylene chain producing compounds **115a-j** (Scheme 23). Secondly, quinazolinone-2-thiol connected with 3,4,5-trimethoxybenzyl moiety at N_3 -position **116** is reacted with 4-chloroanilide substituted benzene-sulfonamides to produce compounds **117a-b**; while its nucleophilic substitution with sulfonamide derivatives linked to chloroanilide functionality via methylene chain resulted in compounds **118a-b** (Scheme 24). C_6 , N_3 -Substituted quinazolinone-2-thiol derivatives **119a-g**



Scheme 23. Preparation of target compounds **114a-j** and **115a-j** [14].



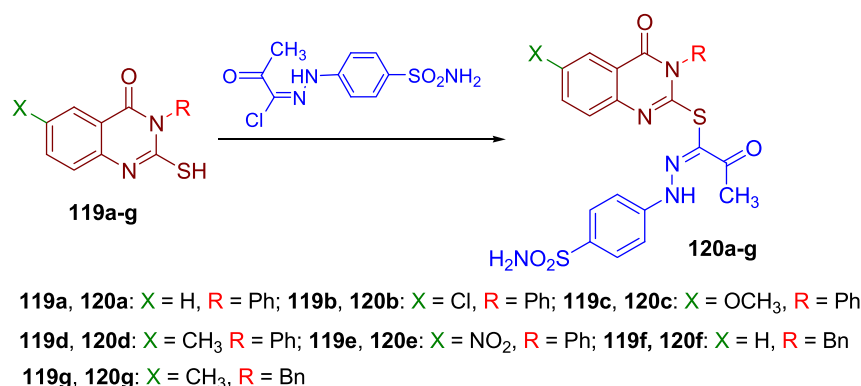
Scheme 24. Synthetic route for the preparation of the compounds **117a-b** and **118a-b** [14].

appended to imine-hydrazone benzenesulfonamide rendered derivatives **120a-g** (Scheme 25).

In the pharmacological activity towards CA, the compound **114f** has elicited the most potent *hCA* I inhibitory activity ($K_i = 39.4$ nM) sixfold higher potency than the reference compound **AAZ** ($K_i = 250.0$ nM). While the compounds **115a** ($K_i = 78.2$ nM), **120a** ($K_i = 86.6$ nM), and **120c** ($K_i = 83.9$ nM) have almost similar inhibitory activities which are significantly greater than **AAZ**. The remarkable *hCA* II inhibitory effect ($K_i = 3.30$ nM) is displayed by the compound **114f**. Only a few of the evaluated compounds could inhibit *hCA* II effectively. To mention, compounds **115i** ($K_i = 6.90$ nM) and **115j** ($K_i = 5.20$ nM) exhibited noteworthy inhibitory properties. Similar activity is shown by the derivative **120c** ($K_i = 6.20$ nM). The excellent inhibitory activity ($K_i = 0.73$ nM) is bestowed by the compound **120a** which possessed 16.5-fold stronger inhibitory effect in comparison with **AAZ** ($K_i = 12.0$ nM). The most of screened molecules have exhibited almost similar *hCA* IX inhibitory values compared to **AAZ** ($K_i = 25.0$ nM). Out of those compounds, **120a** ($K_i = 1.80$ nM) and **120c** ($K_i = 1.60$ nM) (Figure 12) are reported to possess the strongest inhibitory potentials with 14- and 15-

fold better inhibitory potentials respectively than that of reference. Not so good *hCA* XII inhibitory effects are exerted by the synthesized derivatives. However, a few compounds could reach the inhibitory activity of the standard compound **AAZ** ($K_i = 5.70$ nM). Amongst them, compounds **114e** ($K_i = 7.60$ nM) and **115g** ($K_i = 5.20$ nM) stood top of the *hCA* XII inhibitors.

The compound **114f** possessing 6,7-dimethoxy quinazolinone-2-thiol and propanilide benzenesulfonamide moiety has the greatest *hCA* I inhibitory activity. However, removal or substitution of $-OCH_3$ groups by other groups has significantly reduced the activity. Amongst the few potent *hCA* II inhibitors, **120a** has turned out to be strongest inhibitory molecule. Structurally it possesses benzene sulfonamide hydrazone of ketone thiol at 2-position and benzene at *N*₃-position of simple quinazolinone motif. In this series, substitution at 6-position of quinazolinone ring shown abated activity except for 6-methoxy substituted compound **120c** which exhibited satisfactory inhibitory value. Except for compounds **114a** & **114b**, all the molecules of **114a-j** and **115a-j** have displayed satisfactory inhibitory properties ($K_i = 5.0$ – 65.2 nM). While deteriorated activities are observed for compounds **117a-b** and **118a-b**



Scheme 25. Schematic representation of compounds **119a-g** and **120a-g** [14].

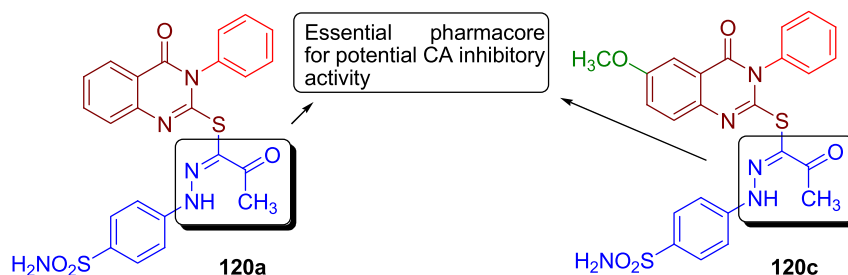


Figure 12. Structures of potent CA inhibitors.

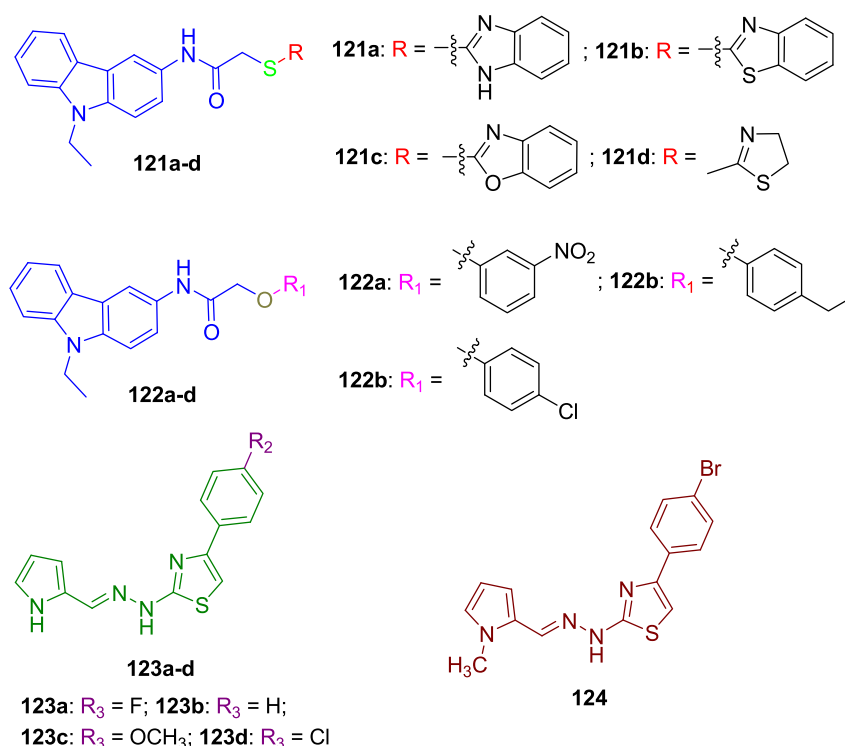
which might be attributed to sterically hindered 3,4,5-trimethoxybenzyl moiety connected at quinazolinone N_3 -position. Excluding for a few compounds, all the tested derivatives possessed decent *hCA* IX inhibitory properties irrespective of their structural variation. However, compound **120a** and **120c** appended with phenyl ring at N_3 -position and benzenesulfonamide hydrazone of ketone thiol rendered finest inhibitory activity. In case of inhibitory activity towards *hCA* XII, no more than a few derivatives displayed good inhibitory potencies; particularly **115g** has shown strong impact which is attributed to the 6-iodoquinazolinone tethered to benzenesulfonamide via *N*-ethylthioacetamide fragment. Decreased/increased fragment chain length or change in the substitution at 6-/or 7-positions of quinazolinone resulted in lowered activities. An overall observation of the structure and its activity reveals that **114a-b**, **117a-b**, and **118a-b** have shown inactivity towards all isoforms of CA. While the compounds **120a** and **120c** have good inhibitory potential towards all isoforms of the enzyme which infer that hydrazone of keto-thiol is crucial for CA inhibitory activity.

2.5. Carbazole and hydrazone derivatives

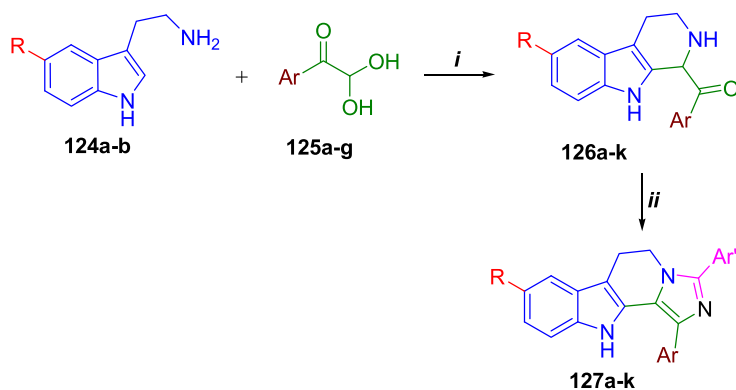
Tyrosinase enzyme is involved in the hyperpigmentation of the skin; melasma, flecks, lentigo, nevus, ephelis, and melanoma of pregnancy are few skin disorders to be mentioned. To address these issues, tyrosinase

inhibitors are being designed and synthesized. Carbazole-substituted chalcone urea derivatives are demonstrated as decent tyrosinase inhibitors. Also, hydrazone-bridged thiazole-pyrazole scaffolds have shown to possess inhibition properties towards tyrosinase. In this context, tyrosinase inhibition properties of the previously synthesized [15, 16, 17] carbazole and hydrazone-bridged thiazole-pyrazole derivatives are described [18].

The synthesized derivatives are screened for their mushroom tyrosinase inhibitory activity using kojic acid as standard inhibitor (Scheme 26). Out of the twelve derivatives prepared, compound **121a** ($K_i = 1.64 \pm 0.03 \mu\text{M}$) has exhibited most potent tyrosinase inhibitory activity with 2.8-fold higher potency compared to kojic acid ($K_i = 4.43 \pm 0.20 \mu\text{M}$). Almost similar inhibitory effect ($K_i = 4.34 \pm 0.04 \mu\text{M}$) is exerted by the derivative **121c** compared to that of the reference compound. Compound **121d** ($K_i = 3.46 \pm 0.07 \mu\text{M}$) could also exhibit significant inhibitory activity. The potential activity is observed in the case of carbazole analogs; particularly compound **121a** possessing *N*-ethyl carbazole appended to benzimidazole via thiopropanamide linker exhibited most potent inhibitory activity. The substitution of benzimidazole with benzothiazole resulted in compound **121b** with reduced inhibitory activity. While benzoxazole derivative **121c** has some improvement but yet diminished activity compared to compound **121a**. Further improved activity is exhibited by thiazole derivatized carbazole **121d**. Another series of



Scheme 26. Illustration of the structures of carbazole and hydrazone-bridged thiazole-pyrazole derivatives [18].



- 127a:** R = H, Ar = Ph, Ar' = 4-CH₃-Ph; **127b:** R = H, Ar = Ph, Ar' = 4-F-Ph;
127c: R = H, Ar = Ph, Ar' = 4-Cl-Ph; **127d:** R = H, Ar = 4-CH₃-Ph, Ar' = 3-CH₃-Ph;
127e: R = H, Ar = 4-CH₃-Ph, Ar' = 4-CH₃-Ph; **127f:** R = H, Ar = 4-CH₃-Ph, Ar' = 4-Cl-Ph;
127g: R = OCH₃, Ar = 4-OCH₃-Ph, Ar' = 4-Cl-Ph; **127h:** R = H, Ar = 4-OCH₃-Ph, Ar' = Ph;
127i: R = H, Ar = 4-OCH₃-Ph, Ar' = 3-CH₃-Ph; **127j:** R = H, Ar = 4-OCH₃-Ph, Ar' = 4-F-Ph;
127k: R = OCH₃, Ar = 4-OCH₃-Ph, Ar' = Ph; **127l:** R = H, Ar = 4-OCH₃-Ph, Ar' = 3-CH₃-Ph;
127m: R = OCH₃, Ar = 4-OCH₃-Ph, Ar' = 4-F-Ph; **127n:** R = OCH₃, Ar = 4-OCH₃-Ph, Ar' = thiophene-2-yl;
127o: R = H, Ar = 4-Cl-Ph, Ar' = Ph; **127p:** R = H, Ar = 4-Cl-Ph, Ar' = 3-CH₃Ph;
127q: R = H, Ar = 4-Cl-Ph, Ar' = thiophene-2-yl; **127r:** R = H, Ar = 4-Cl-Ph, Ar' = 4-OCH₃Ph;
127s: R = OCH₃, Ar = 4-Cl-Ph, Ar' = thiophene-2-yl; **127t:** R = H, Ar = 4-Br-Ph, Ar' = 4-OCH₃Ph;
127u: R = H, Ar = 4-Cl-Ph, Ar' = 4-Cl-Ph; **127v:** R = OCH₃, Ar = 4-Cl-Ph, Ar' = Ph;
127w: R = OCH₃, Ar = 4-Br-Ph, Ar' = 4-F-Ph;

Scheme 27. Synthesis of carbazole-imidazole derivatives **127a-w** [19]; **Conditions and reagents:** i) TFA (70%), CHCl₃, 50 °C (1h); Ar'CHO, NH₄OAc, 80 °C (8h).

carbazoles **122a-c** synthesized wherein the 4-substituted aromatic rings are connected through propanamide oxide have shown moderate inhibitory activity. It indicates that thiopropanamide fragment bestowed the strongest inhibitory effects. The series of molecules entailing pyrrole ring connected to thiazole by hydrazone-bridge **123a-d** have also failed to satisfactory results. In these derivatives, compound **123d** possessing 4-chlorophenyl ring attached to thiazole at 3-position shown inhibitory activity almost similar to that of the reference compound.

2.6. Carbazole-imidazole derivatives

α -Glucosidase, a digestive enzyme functions in the cleavage of the α -1,4-glycosidic bonds of polysaccharides with subsequent conversion into glucose. Control of blood glucose levels in type 2 diabetes patients is very necessary; in this regard monitor of α -glucosidase function is the foremost objective. Hence, α -glucosidase is an apt target for the design and discovery of therapeutic drugs. Based on the α -glucosidase inhibitory activity of carbazole analogs and pharmacological importance of imidazole, novel fused carbazole-imidazole derivatives are designed as potent anti- α -glucosidase agents [19].

Synthesis of the final compounds has commenced from indole derivatives. 3-Ethylamino-5-substituted indole derivatives **124a-b** are cyclized with aryl ketodiol **125a-j** to afford carbazole derivatives **126a-k** which upon further cyclization at 2,3-positions of carbazole using substituted aromatic aldehydes and ammonium acetate gave fused imidazole-carbazole scaffolds **127a-k** (Scheme 27).

All the designed molecules are evaluated for their α -glucosidase inhibitory activity using acarbose as a standard inhibitor. All the tested derivatives have exhibited better inhibitory activity ($IC_{50} = 74 \pm 0.7$ – $298.3 \pm 0.9 \mu M$) compared to acarbose ($IC_{50} = 750 \pm 1.5 \mu M$). Amongst the tested compounds, few derivatives namely compounds,

127c, **127f**, **127k**, **127n**, and **127r** have displayed significant inhibitory activity (Table 6). Furthermore, the carbazole-imidazole scaffolds such as **127o** (Figure 13), **127t**, **127v**, and **127w** rendered promising inhibitory effects. Particularly compound **127v** resulted in a striking activity. In the structure-activity correlation studies, the potent inhibitory activity of all the four compounds **127o**, **127t**, **127v**, and **127w** is attributed to the 4-Cl/4-Br-phenyl ring appended to 2-position of carbazole-imidazole derivatives. In these compounds, the derivative **127v** with simple phenyl ring at the 4-position of carbazole-imidazole moiety has shown remarkable inhibitory activity. However, replacement of phenyl ring with 4-electron donating/electron-withdrawing substituted phenyl rings led to diminished activity and the greater extent of reduction in the inhibitory activity is observed for 4-F substituted phenyl analog **127w**.

2.7. Coumarin-1,3,4-oxadiazole hybrids

Overexpression of carbonic anhydrases is associated with the proliferation, angiogenesis, and metastasis in a variety of cancers. CA inhibition would be an efficient approach for the treatment of cancer. Coumarin can form favorable interactions with active sites of the proteins and enzymes; thereby possessing a wide variety of pharmacological activities including cancer. CA IX and XII inhibitory activities of the 7-hydroxycoumarin and *N*-acyl benzene sulfonamide dihydro-1,3,4-oxadiazole hybrids has prompted to design a novel series of CA inhibitors wherein coumarin motif is connected to 1,3,4-oxadiazole ring [20].

7-Hydroxy-4-methyl coumarin **128** is prepared from resorcinol and ethyl acetoacetate which is transformed into corresponding coumarin ester **129** upon treatment with ethyl bromoacetate. The ester **129** is hydrolyzed with hydrazine to form semihydrazide **130** which is subsequently cyclized with CS₂ yielding oxadiazole-2-thiol coumarin scaffold

Table 6. α -Glucosidase inhibitory potentials of the potent carbazole-imidazole derivatives.

Compd	α -glucosidase activity
	IC ₅₀ (μ M)
127c	123.0 \pm 1.0
127f	120.0 \pm 0.6
127k	129.0 \pm 1.0
127n	136.3 \pm 1.3
127r	144.3 \pm 1.0
127o	81.0 \pm 0.8
127t	84.3 \pm 0.5
127v	74.0 \pm 0.7
127w	93.5 \pm 0.5

131. Various arylalkyl halides/alkyl halides substitution of compound **131** has resulted in final compounds **132a-t** (Scheme 28).

Using **AAZ** as a reference compound, *hCA* inhibitory activity of the synthesized compounds is evaluated. In the inhibitory activity towards *hCA* I & II, no single derivative exhibited decent activity. All the evaluated derivatives have possessed moderate inhibitory activity (IC₅₀ > 100 μ M). Also, the designed derivatives failed to reach the inhibitory boundary of **AAZ** (IC₅₀ = 0.025 μ M) in the case of *hCA* IX. However compound **132n** (IC₅₀ = 2.34 μ M) managed to exhibit some significance yet 100-fold lower activity compared to **AAZ**. Surprisingly, the derivatives **1327a-h** displayed prominent inhibitory potentials towards *hCA* XII (Table 7). Amongst these, compound **132b** elicited excellent activity with 25-times lower activity compared to **AAZ**.

As per the observation of the drug molecule aimed to inhibit the *hCA* enzymes, most of the compounds were inactive towards *hCA* I & II; similar effects are observed here in case of 1,3,4-oxadiazole coumarin analogs **132a-t**. The compound **132b** (Figure 14) possessing coumarin appended with methylene oxadiazole thiol and in turn benzoyl moiety attached to thiol functionality of oxadiazole has bestowed with remarkable inhibitory activity. Corresponding benzyl analog **132a** has shown little diminished activity. Also, insertion of methylene fragment in case of compound **132c** lowered inhibitory activity is observed. Only two 4-substituted benzyl derivatives namely compound 4-ethoxycarbonyl benzyl derivative **132f** and **132h** possessing 4-nitrobenzyl motif have displayed significant activity; another 4-substituted benzyl has not met the requirements. These facts reveal that substitution at 4-position of benzyl ring could not be considered as a useful structural modification. Alongside, alkyl chain modified derivatives namely; isobutyl analog **132d**, chlorobutylene derivative **132e**, and ethylacetate modified compound **132g** resulted in good inhibitory activity. When it comes to modification of phenacyl analog **132c** at 4-position; no single compound has turned out to be a potent CA inhibitor. It indicated that irrespective of the nature of the group, substitution at 4-position of phenacyl moiety would end up with negative results.

2.8. C- β -D-Glucopyranosyl azole derivatives

Type-2 diabetes caused as a result of abnormal insulin secretion or insulin resistance is the most common clinical issue to be addressed. Elevated glucose production is responsible for high glucose levels in the body. Conversion of liver glycogen to glucose through liver glycogenolysis is catalyzed by glycogen phosphorylase enzyme (GPase). Thereby inhibition of the GPase might be a validated approach to treat type-2 diabetes. Based on previously designed GPase inhibitors, novel C- β -D-glucopyranosyl azole derivatives are prepared in order to enhance the effectiveness of GPase inhibitors [21].

Glucosyl bromomethyl ketone **133** is cyclized with arylthioamides to give corresponding thiazole derivatives **134a-c** which upon debenzoylation resulted in final compounds **135a-c**. The compound **133** is again utilized for cyclization with various carboxamidines to yield imidazole analogs **136a-c** and subsequent removal of benzoyl groups has produced **137a-c** (Scheme 29). In another series of derivatives, formamide salt **138** is treated with α -bromoacyl naphthalene to undergo cyclization process affording imidazole derivative **139** and finally yielded compound **140** on debenzoylation (Scheme 30).

The glucosyl derivatives prepared are evaluated for their GPase inhibitory activity using 1,4-dideoxy-1,4-imino-D-arabinitol (DAB). Although the inhibitory activity is not up to the mark compared to previously designed derivatives, two compounds have succeeded to display significant activity. In that compound **137b** (IC₅₀ = 4.58 μ M) (Figure 15) has exhibited moderate GPase inhibitory activity. The most potent inhibitory activity is elicited by the compound **140** (IC₅₀ = 1.97 μ M) amongst the other derivatives. Inhibitory potentials displayed by both the potent inhibitors **137b** and **140** are comparatively lower than that of DAB (IC₅₀ \leq 1.0 μ M). Except for 2-(2-naphthyl) thiazole derivative **135b** (IC₅₀ = 26.2 μ M); no thiazole glucosyl derivative has shown expected inhibitory activity. Similarly, imidazole analogs have shown weak inhibitory activity excluding compound **137b** which entails 1-naphthyl moiety and glucosyl motif at 2- and 4-positions of imidazole. Appending of naphthyl moiety at 1-position of imidazole (**137c**) diminished upto 15-fold compared to 2-naphthyl derivative **137b**.

2.9. Diaryl-1,5-diazoles

Overexpression of COX-2 and 5-LOX enzymes responsible for inflammation leads to elevation of downstream prostaglandin PGE₂ and LTB₄ levels respectively. PGE₂ could increase the metastasis of tumor cells; while the COX-2 promotes tumor cell survival. COX-2 and 5-LOX pathways are two principal pathways of metabolism of arachidonic acid. Inhibition of COX-2/5-LOX would become the best anti-tumor agents. Diarylpyrazole scaffolds have been reported to possess dual COX-2/5-LOX inhibitory properties. This prompted to design molecules by incorporating diaryl-1,5-diazoles and morpholine motifs [22].

Here 3,4-disubstituted acetophenones **141a-k** are transformed to diketesters **142a-k** upon reaction with dimethyl oxalate. 1,3-

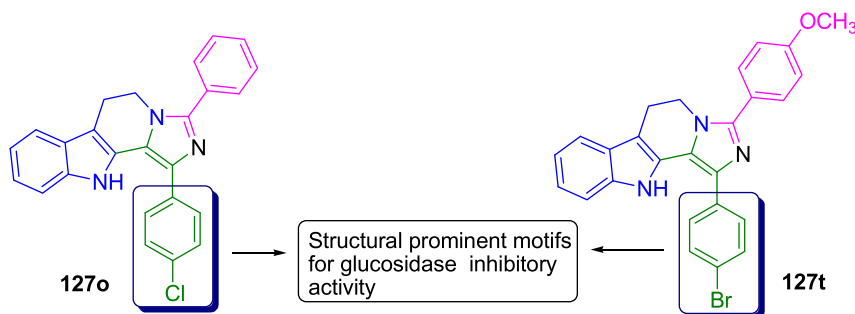
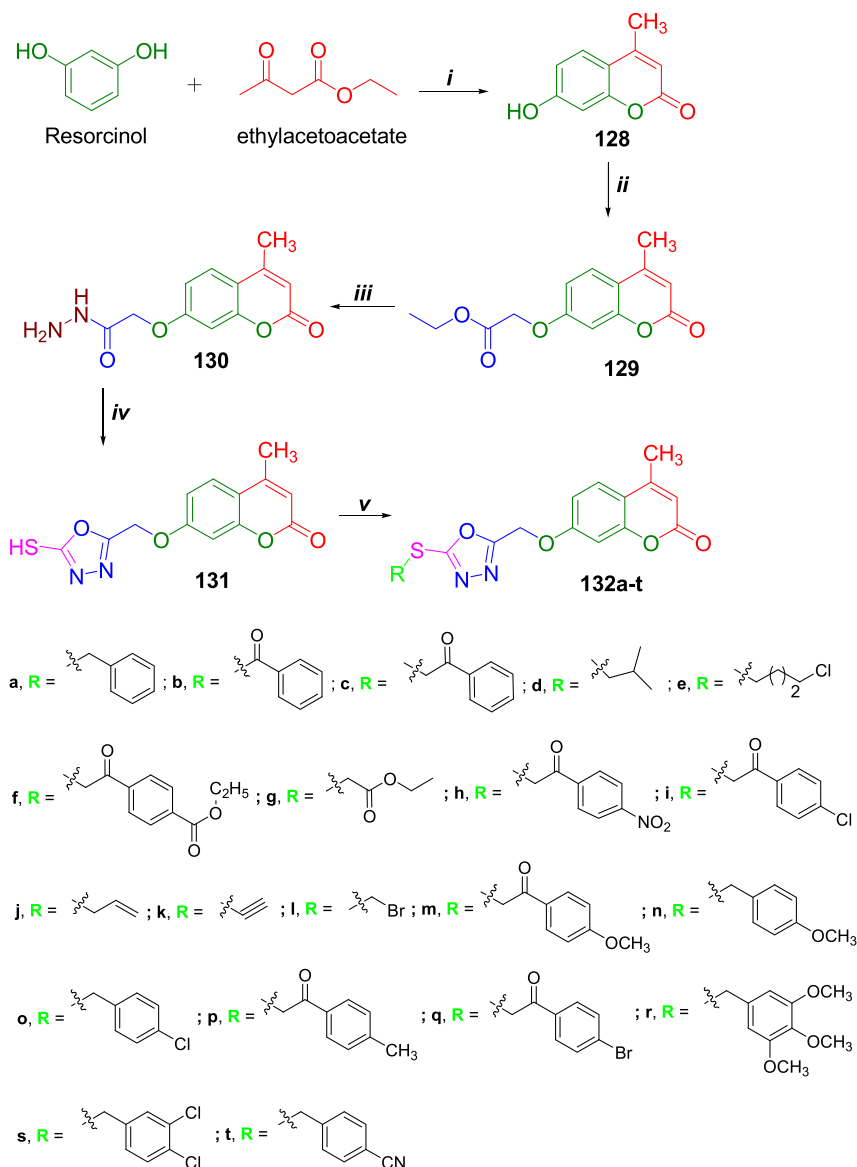


Figure 13. Representation of carbazole-imidazole derivatives as potent α -glucosidase inhibitors.



Scheme 28. Synthesis of the target molecules **132a-t** [20]; **Reagents and conditions:** *i*) Conc. H_2SO_4 , 0–10 °C (2–3h); *ii*) ethyl bromoacetate, K_2CO_3 , acetone, reflux (6h); *iii*) $\text{NH}_2\text{NH}_2\cdot\text{H}_2\text{O}$, THF, reflux (4h); *iv*) CS_2 , NaOH, EtOH, reflux (12h); *v*) R-X, K_2CO_3 , acetone, reflux (3–5h).

Diketoester functionality of compounds **142a-k** is allowed to undergo intermolecular cyclization with 4-hydrazonyl benzenesulfonamide to obtain pyrazole sulfonamide derivatives **143a-k**; corresponding pyrazole carboxylic analogs **144a-k** are yielded by ester hydrolysis of **143a-k**.

Table 7. Potent hCA XII inhibitory values of the coumarin derivatives.

Compd	hCA activity
	IC ₅₀ (μM)
132a	0.28
132b	0.16
132c	0.41
132d	0.52
132e	0.74
132f	0.60
132g	0.60
132h	0.82
AAZ	0.0057

Nucleophilic substitution reaction of compounds **144a-k** with morpholine/thiazine produced final compounds **145a-v** (Scheme 31). Alongside the predesigned pyrazole carboxylic acids **146a-k** are reacted with morpholine-*N*-alkylamines/alkylhydroxides affording compounds **147a-s** (Scheme 32).

The designed derivatives are tested for COX-2 and 5-LOX inhibitory activities using celecoxib and zileuton as reference compounds respectively. Compared to celecoxib (IC₅₀ = 0.25 ± 0.03 μM), most of the evaluated compounds exhibited good COX-2 inhibitory activity (IC₅₀ = 0.17–7.64 μM). Amongst these, few derivatives have possessed the best activity (Table 8); particularly compound **147h** (Figure 15) has bestowed with most potent COX-2 activity. While the decent IC₅₀ values (IC₅₀ = 0.68–3.41 μM) are displayed for the tested compounds towards 5-LOX. The derivatives that exhibited remarkable IC₅₀ values better than zileuton are depicted in Table 8. The compound **147k** (Figure 15) has resulted in most potent 5-LOX inhibitory effect.

When the structure of the derivatives and their inhibitory values are correlated, the following conclusions can be drawn. The remarkable COX-2 inhibitor **147h** (Figure 16) possesses benzenesulfonamide and 4-fluorobenzene at 1- and 5-positions of pyrazole respectively; morpholine

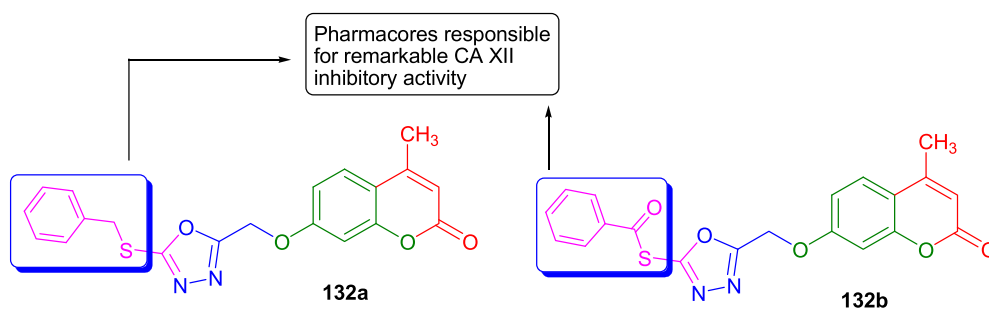
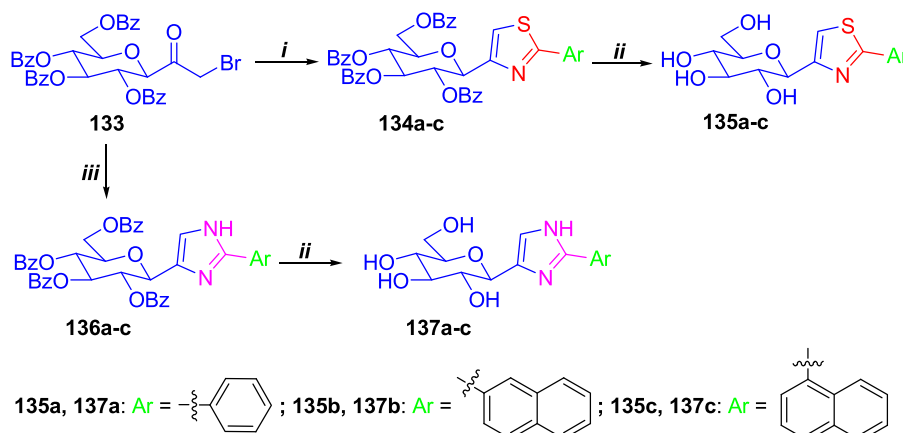


Figure 14. Structures of remarkable CA XII inhibitors.

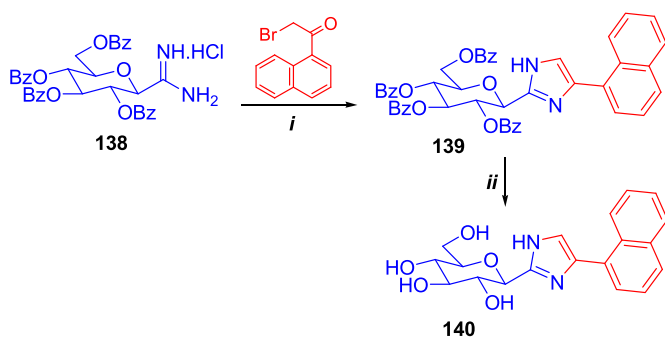


Scheme 29. Synthetic route for the synthesis of the derivatives 135a-c and 137a-c [21]; Reagents and conditions: *i*) Arylthioamides, dry DMF, 140 °C; *ii*) 1M NaOMe, MeOH, rt; *iii*) Carboxamidines, 4 Eq. K₂CO₃, THF-H₂O (4:1), rt.

is tethered to 3-position of pyrazole ethyl carboxamide fragment. Exchange of 4-fluorobenzene with 4-trifluoromethyl benzene (**147k**) and increased alkyl chain of carboxamide fragment by one unit has diminished the activity a little. There is no precise correlation between structure and activity that could be established as wide structural modification has resulted in almost similar activity. Compound **147k** having benzene sulfonamide and 4-trifluoromethylbenzene at 1- and 5-positions of pyrazole in addition to propylcarboxamide flanked by pyrazole and morpholine moiety is reported to render powerful 5-LOX inhibitory activity among the other derivatives. However, varying the substituents on pyrazole could not improve the activity.

3. Dihydroquinazoline-2-amines

Reverse transcriptase (RTase) has been reported to have its involvement in life cycle of human immunodeficiency virus type 1 (HIV-1)



Scheme 30. Synthesis of the glucopyranosyl azole derivative 140 [21]; Reagents and conditions: *i*) 4 Eq. K₂CO₃, THF-H₂O (4:1), rt; *ii*) 40 Eq. EtSH, 20 Eq. BF₃·Et₂O, dry CH₂Cl₂, rt.

wherein the RTase functions reverse transcription of its RNA genome to cDNA which is followed by integration of DNA into the host cell genome. Hence the RTase has been a major therapeutic target for HIV-1. Diarylpyrimidine scaffolds are demonstrated as second generation NNRTIs; based on structural features of these compounds, dihydroquinazoline-2-amine derivatives are designed and synthesized [23].

Partial protection of 2-amino-fluorinated acetophenone **148** with 4-methoxy-benzene methanol gave compound **149** which upon intramolecular cyclization with potassium cyanate afforded intermediate **150** and then on reflux conditions resulted in compound **151**. Cyclopropylacetylene is connected at 4-position of intermediate **151** leading to compound **152** in which protecting group is removed to obtain derivative **153**. Chlorination at 2-position of compound **153** is achieved using POCl₃ to yield 2-chloroquinazoline analog **154**; finally, various aromatic amines are utilized for nucleophilic substitution at 2-position of compound **154** to afford 2-arylaminquinazoline derivatives **155a-x** (Scheme 33).

All the synthesized molecules are tested for various strains of HIV-1 RTase using nevirapine (NVP), delavirdine (DLV), EFV and ETV as reference compounds.

In case of the RTase of IIB strain, most of the evaluated derivatives have exhibited inhibitory activity only up to micromolar level; however a

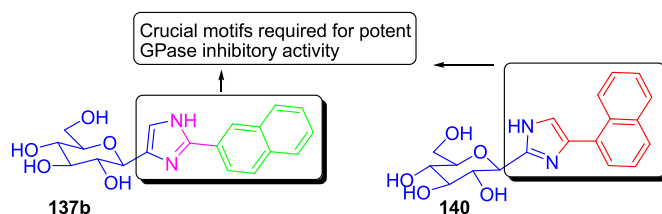
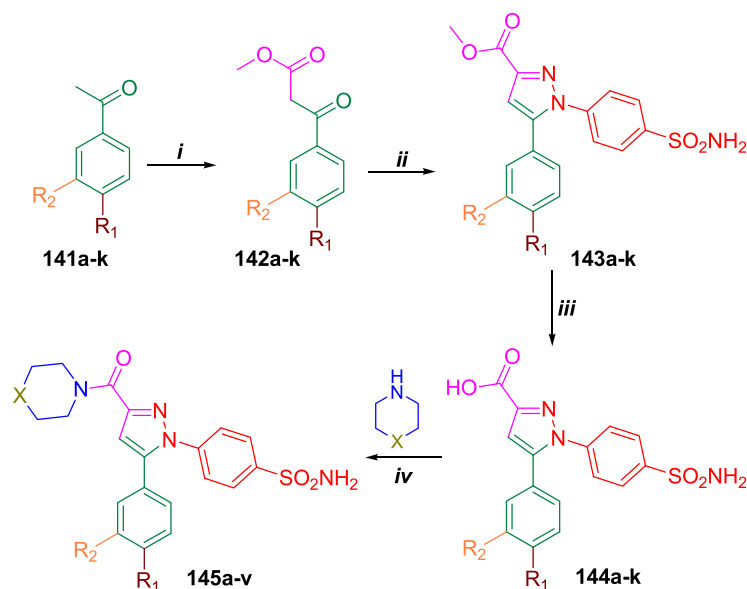


Figure 15. Structures of remarkable GPase inhibitors.



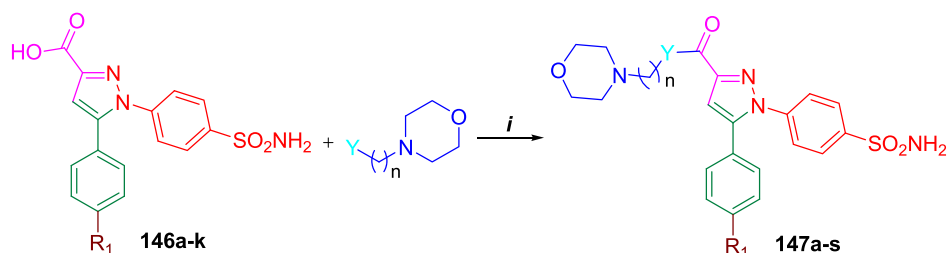
145a: $R_1 = \text{H}$, $R_2 = \text{F}$, $X = \text{S}$; **145b:** $R_1 = \text{H}$, $R_2 = \text{F}$, $X = \text{O}$; **145c:** $R_1 = \text{H}$, $R_2 = \text{Cl}$, $X = \text{S}$
145d: $R_1 = \text{H}$, $R_2 = \text{Cl}$, $X = \text{O}$; **145e:** $R_1 = \text{Cl}$, $R_2 = \text{H}$, $X = \text{S}$; **145f:** $R_1 = \text{Cl}$, $R_2 = \text{H}$, $X = \text{O}$;
145g: $R_1 = \text{CH}_3\text{CH}_2\text{O}$, $R_2 = \text{H}$, $X = \text{S}$; **145h:** $R_1 = \text{CH}_3\text{CH}_2\text{O}$, $R_2 = \text{H}$, $X = \text{O}$; **145i:** $R_1 = \text{F}$, $R_2 = \text{H}$, $X = \text{S}$
145j: $R_1 = \text{F}$, $R_2 = \text{H}$, $X = \text{S}$; **145k:** $R_1 = \text{F}$, $R_2 = \text{H}$, $X = \text{O}$; **145l:** $R_1 = \text{CH}_3$, $R_2 = \text{H}$, $X = \text{O}$
145m: $R_1 = \text{CH}_3$, $R_2 = \text{H}$, $X = \text{S}$; **145n:** $R_1 = \text{Br}$, $R_2 = \text{H}$, $X = \text{S}$; **145o:** $R_1 = \text{Br}$, $R_2 = \text{H}$, $X = \text{O}$
145p: $R_1 = \text{H}$, $R_2 = \text{CH}_3\text{O}$, $X = \text{S}$; **145q:** $R_1 = \text{H}$, $R_2 = \text{CH}_3\text{O}$, $X = \text{O}$; **145r:** $R_1 = \text{CH}_3\text{O}$, $R_2 = \text{H}$, $X = \text{S}$
145s: $R_1 = \text{CH}_3\text{O}$, $R_2 = \text{H}$, $X = \text{S}$; **145t:** $R_1 = \text{CF}_3$, $R_2 = \text{H}$, $X = \text{S}$; **145u:** $R_1 = \text{CF}_3$, $R_2 = \text{H}$, $X = \text{O}$
145v: $R_1 = \text{H}$, $R_2 = \text{H}$, $X = \text{S}$; **145w:** $R_1 = \text{H}$, $R_2 = \text{H}$, $X = \text{O}$

Scheme 31. Synthesis of the diarylpyrazoles **145a-v** [22]; **Reagents and conditions:** i) dimethyl oxalate, MeOH, reflux (6h); ii) 4-hydrazonyl benzenesulfonamide, MeOH, reflux (6h); iii) KOH, MeOH, reflux (2h); iv) EDC•HCl, HOBT, DMAP, CH_2Cl_2 , 0 °C, Revitalite, 0.5h.

few compounds are successful in exhibiting inhibitory values at as low as nanomolar drug concentration (Table 9). Among those, compound **155b** has displayed most significant inhibitory property towards IIIB strain RTase. Its activity is twice the activity of the reference compound EFV ($\text{EC}_{50} = 0.0016 \mu\text{M}$) and ETV ($\text{EC}_{50} = 0.0022 \mu\text{M}$). Meanwhile, compound **155b** ($\text{EC}_{50} = 0.0035 \mu\text{M}$) could show nanomolar inhibitory activity towards E138K RTase strain compared to EFV ($\text{EC}_{50} = 0.0020 \mu\text{M}$) and ETV ($\text{EC}_{50} = 0.0063 \mu\text{M}$). The other derivatives have shown moderate activity. Almost similar RES056 strain RTase inhibitory activity is

observed for the compound **155b** ($\text{EC}_{50} = 0.066 \mu\text{M}$) compared to EFV ($\text{EC}_{50} = 0.055 \mu\text{M}$).

The most potential RTase inhibitory activity of compound **155b** (Figure 17) towards all the HIV-1 strains is attributed to its remarkable structure. In this case, the pharmacore responsible for the strongest inhibitory properties is 4-cyanophenylamine appended to 2-position of quinazoline moiety. Electronegativity is not the sole factor to be accounted for potent activity; the position of the substituent on the phenyl ring also plays a prominent role. For instance, 3-CN-phenyl

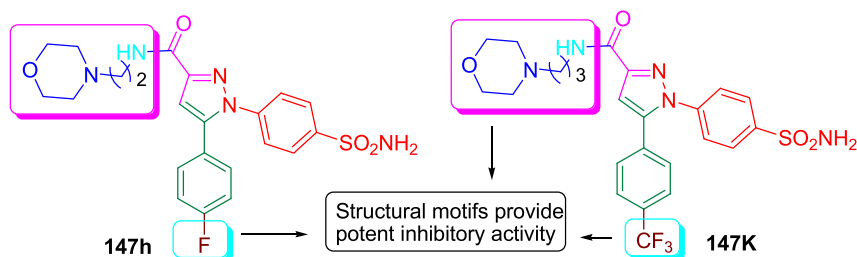


147a: $R_1 = \text{H}$, $Y = \text{NH}$, $n = 3$; **147b:** $R_1 = \text{H}$, $Y = \text{O}$, $n = 3$; **147c:** $R_1 = \text{H}$, $Y = \text{NH}$, $n = 2$
147d: $R_1 = \text{Cl}$, $Y = \text{O}$, $n = 3$; **147e:** $R_1 = \text{Cl}$, $Y = \text{O}$, $n = 2$; **147f:** $R_1 = \text{Cl}$, $Y = \text{NH}$, $n = 2$
147g: $R_1 = \text{F}$, $Y = \text{O}$, $n = 2$; **147h:** $R_1 = \text{F}$, $Y = \text{NH}$, $n = 2$; **147i:** $R_1 = \text{F}$, $Y = \text{O}$, $n = 3$
147j: $R_1 = \text{CF}_3$, $Y = \text{O}$, $n = 2$; **147k:** $R_1 = \text{CF}_3$, $Y = \text{NH}$, $n = 3$; **147l:** $R_1 = \text{CF}_3$, $Y = \text{O}$, $n = 3$
147m: $R_1 = \text{CH}_3\text{O}$, $Y = \text{NH}$, $n = 2$; **147n:** $R_1 = \text{CH}_3\text{O}$, $Y = \text{O}$, $n = 3$; **147o:** $R_1 = \text{CH}_3\text{O}$, $Y = \text{NH}$, $n = 3$
147p: $R_1 = \text{C}_2\text{H}_5\text{O}$, $Y = \text{NH}$, $n = 2$; **147q:** $R_1 = \text{C}_2\text{H}_5\text{O}$, $Y = \text{O}$, $n = 3$; **147r:** $R_1 = \text{C}_2\text{H}_5\text{O}$, $Y = \text{NH}$, $n = 3$
147s: $R_1 = \text{C}_2\text{H}_5\text{O}$, $Y = \text{O}$, $n = 2$

Scheme 32. Synthetic route for preparation of final compounds **147a-s** [22]; **Reagents and conditions:** i) EDC•HCl, HOBT, DMAP, CH_2Cl_2 , 0 °C, Revitalite, 0.5h, RT, overnight.

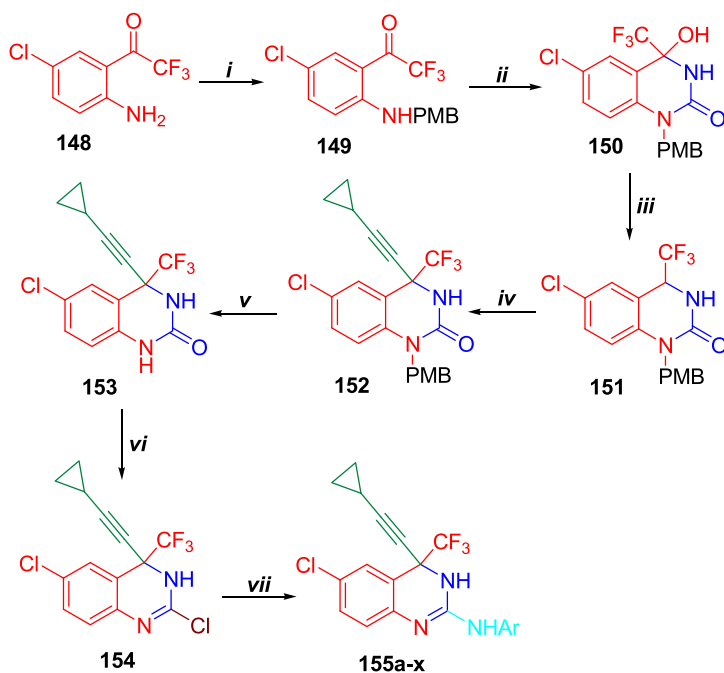
Table 8. Potent COX-2 and 5-LOX inhibitory values of diarylpyrazole derivatives.

Compd	COX-2 activity		Compd	5-LOX activity	
	IC ₅₀ (μM)			IC ₅₀ (μM)	
145a	0.19 ± 0.09		145s	0.71 ± 0.13	
145s	0.19 ± 0.02		147i	0.75 ± 0.08	
147h	0.16 ± 0.02		147k	0.68 ± 0.17	
147j	0.19 ± 0.04		147l	0.75 ± 0.12	
147k	0.17 ± 0.07		147q	0.72 ± 0.09	

**Figure 16.** Structures of pyrazole benzenesulfonamides as COX-2 and 5-LOX inhibitors.

analog **155d** ($EC_{50} = 0.44 \mu\text{M}$) has shown very weak activity compared to reference; wherein 523-fold diminished activity is observed. Besides this, 3-NO₂-phenyl derivative **155e** has not reached up to the mark although a strong electron-withdrawing group is present. Notwithstanding the above statement, the compound **155f** possessing 4-CF₃ has

displayed a decent inhibitory effect. In general consensus, the activity of the molecule and its structure may not be correlated efficiently. The linearity of the substituent CN and its para-position at phenyl ring would be beneficial for noteworthy inhibitory activity of the compound **155b**.



155a: Ar = Ph; **155b:** Ar = 4-CN-Ph; **155c:** Ar = 4-CONH₂-Ph; **155d:** Ar = 3-CN-Ph

155e: Ar = 4-NO₂-Ph; **155f:** Ar = 3-CF₃-Ph; **155g:** Ar = 3-Cl-Ph; **155h:** Ar = 4-Br-Ph

155i: Ar = 3-Br-Ph; **155j:** Ar = 2-Br-Ph; **155k:** Ar = 4-F-Ph; **155l:** Ar = 3-F-Ph

155m: Ar = 2-F-Ph; **155n:** Ar = 4-OMe-Ph; **155o:** Ar = 3-OMe-Ph; **155p:** Ar = 2-OMe-Ph

155q: Ar = 4-Me-Ph; **155r:** Ar = 3-Me-Ph; **155s:** Ar = 2-Me-Ph; **155t:** Ar = 3,4-diMe-Ph

155u: Ar = 3,5-diMe-Ph; **155v:** Ar = 3,4-diCl-Ph; **155w:** Ar = 3,4-diF-Ph

155v: Ar = 3-Cl-4-F-Ph

Scheme 33. Synthetic route for preparation of final compounds **155a-x** [23]; **Reagents and conditions:** *i*) 4-methoxy-benzenemethanol, p-Toluenesulfonic acid, acetonitrile, 60 °C (8h); *ii*) Potassium cyanate, AcOH, H₂O, 60 °C (5h); *iii*) Xylene, reflux (8h); *iv*) Cyclopropylacetylene, n-BuLi, tetrahydrofuran, -50 °C (1h); *v*) ceric ammonium nitrate, acetonitrile, H₂O, rt (4h); *vi*) POCl₃, reflux (9h); *vii*) ArNH₂, n-BuOH, reflux (5–8h).

Table 9. RTase (IIIB) inhibitory potentials of some derivatives.

Compd	RTase (IIIB)
	EC ₅₀ (μ M)
155b	0.00084
155f	0.051
155j	0.088
155o	0.063
155v	0.030

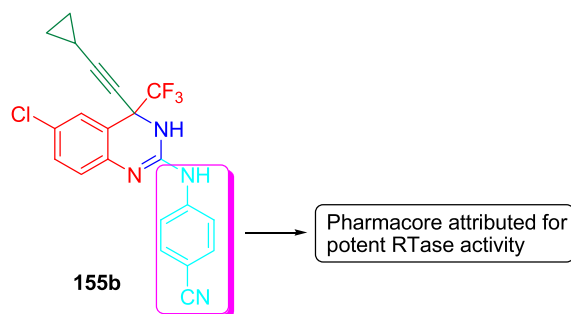
3.1. Dioxino [2,3-f]quinazoline derivatives

VEGF family ligands bind to cell receptor tyrosine kinases VEGFR-1, VEGFR-2, and VEGFR-3 which lead to activation of downstream signaling pathways to perform biological functions such as vascular development during angiogenesis. VEGFR-2 inhibitors have been emerging as potent antiangiogenic agents for the treatment of a large number of cancer types. Since previous studies have described that dioxane quinazoline scaffolds as EGFR inhibitors; phenylurea structural unit in lenvatinib is appended to dioxane quinazoline core by O-Bridge [24].

The synthesis of final compounds commences from 2,3,4-trihydroxy benzoic acid **156** which is esterified to corresponding ester **157**. The hydroxy groups of the ester **157** are protected by benzylation followed by debenylation of OH groups at 2- and 3-positions retaining benzyl protection at 4-position to yield partially protected compound **159**. Dioxane derivative **161** is prepared by intermolecular cyclization using dibromomethane with subsequent debenylation at 4-position. Compound **161** is alkylated at oxygen atom at 4-position giving derivatives **162a-l** which are nitrated at 6-position with subsequent $-\text{NO}_2$ group reduction resulted in amino dioxane derivatives **164a-l**. Intermolecular cyclization of compounds **164a-l** with formamide acetate produced compounds **165a-l** which are chlorinated upon treatment with POCl_3 rendered 4-chloroquinazoline scaffolds **166a-l**. Nucleophilic substitution of 4-chloro group of compounds **166a-l** with aromatic ring substituted urea analogs **167a-l** produced final derivatives **168a-l** (Scheme 34).

All the synthesized derivatives have been analyzed for VEGFR-2 kinase inhibitory activity using lenvatinib as a reference compound. In this activity compound, **168h** is found to be totally inactive. All the other derivatives have displayed excellent inhibitory activity except for a few derivatives compared to the reference compound ($\text{IC}_{50} = 0.0007 \mu\text{M}$).

Most of the compounds have exhibited significant inhibitory activity; among those, few derivatives (Table 10) are enough potent to reach the inhibitory effects of lenvatinib. Compound **168j** (Figure 18) has exerted the best VEGFR-2 inhibitory activity which has shown slightly diminished activity compared to the reference compound. The most remarkable VEGFR-2 kinase inhibitor **168j** possesses *N*-propylmorpholine moiety connected to oxygen at 7-position of quinazoline and 2-fluoro-4-trifluoromethyl benzene appended to the NH end of urea fragment. In addition, benzene urea is substituted by $-\text{F}$ at its 3-position. This combination of pharmacores has bestowed it with the most potent activity.

**Figure 17.** Illustration of the structure of potent RTase inhibitor.

Replacement of $-\text{F}$ group with hydrogen, retaining other structural features same, has resulted in compound **168i** with reduced activity. Chloro analog **168k** has displayed decreased inhibitory properties compared to compound **168i**. Reduction in the alkyl chain length from propyl to ethyl of morpholine paved to weakest inhibitory activity in case of compound **168h**; wherein the inhibitory activity is lowered to 1000-fold. Overall observation revealed that 2-fluoro-5-trifluoromethyl benzene moiety is crucial for potent inhibitory activity. Alongside, the compound **168c** and **168f** with methyl and methoxymethylene fragments respectively in addition to 2-fluoro-5-trifluoromethyl benzene moiety are prominent inhibitors yet lower activity compared to compound **168j**. Hence no significant inhibitor is devoid of the 2-fluoro-5-trifluoromethyl benzene moiety.

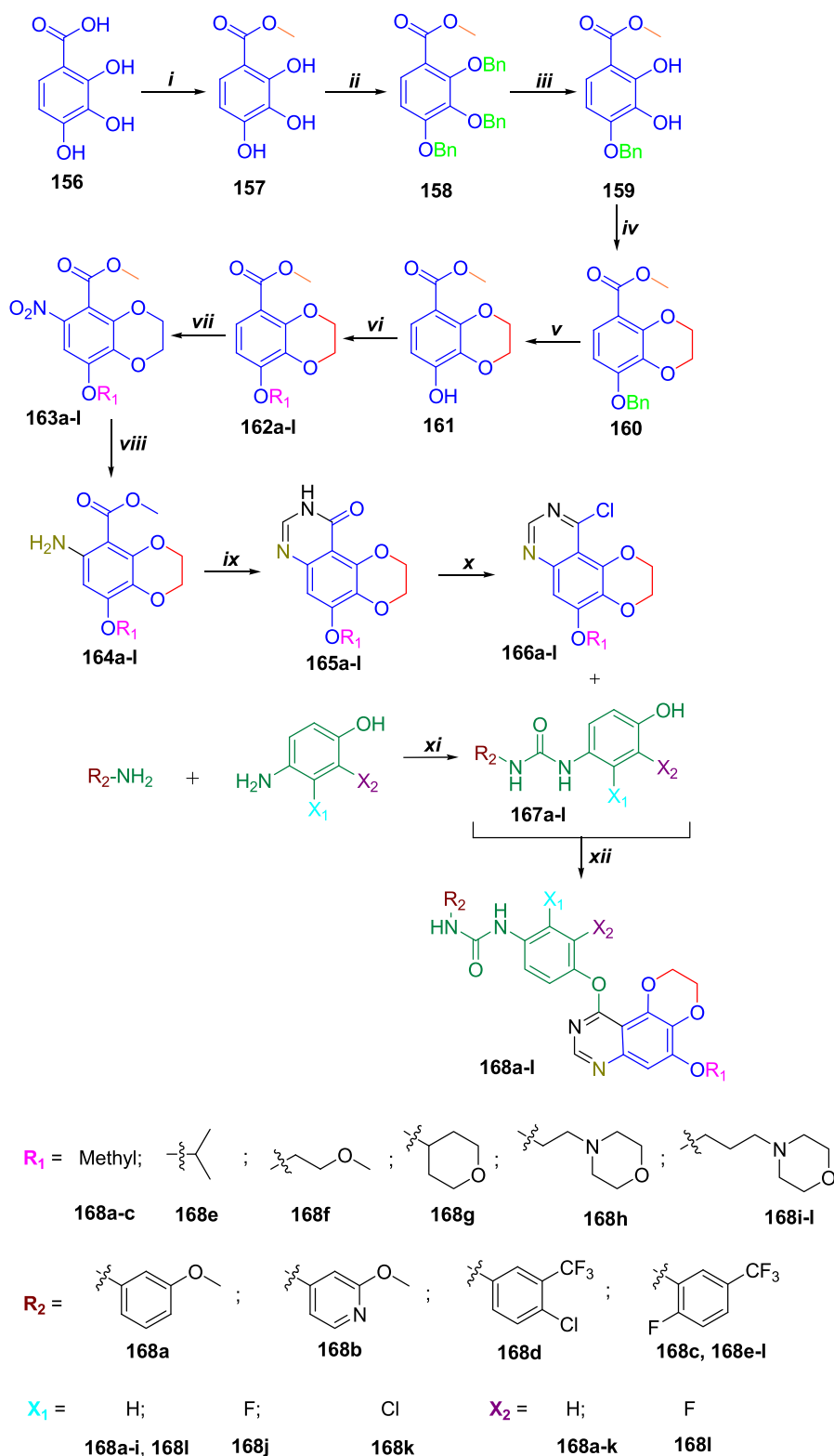
3.2. 1,2,3-Triazole analogs

Receptor tyrosine kinases such as VEGFR-2, Tie, and EphB4 are demonstrated to be overexpressed in endothelial cells which play a significant role in both vasculogenesis and angiogenesis. These also function in the process of tumor development. In order to treat metastasis and reduce angiogenesis, multi-tyrosine kinase inhibitors are designed and synthesized by incorporating 1,2,3-triazole moiety in between 3-phenyl pyridine and cyclopropylanilidine motifs [25] (Scheme 35).

The designed compounds are allowed to inhibit the VEGFR-2, Tie, and EphB4 kinases in presence of the standard tyrosine kinase inhibitor sorafenib. In the inhibitory activity towards VEGFR-2 kinase, few derivatives such as compound **174a** ($\text{IC}_{50} = 0.00163 \mu\text{M}$), **174g** ($\text{IC}_{50} = 0.00185 \mu\text{M}$), and **174m** ($\text{IC}_{50} = 0.00163 \mu\text{M}$) have elicited decent inhibitory activity. Particularly compound **175** ($\text{IC}_{50} = 0.00052 \mu\text{M}$) (Figure 19) is successful in the inhibition of VEGFR-2 with most efficiency compared to reference compound ($\text{IC}_{50} = 0.00017 \mu\text{M}$). While a good number of designed derivatives have exerted inhibitory properties stronger than sorafenib ($\text{IC}_{50} = 0.00039 \mu\text{M}$) towards Tie-2 kinase. To mention, compound **174a** ($\text{IC}_{50} = 0.00036 \mu\text{M}$), **174d** ($\text{IC}_{50} = 0.00026 \mu\text{M}$) (Figure 19), **174f** ($\text{IC}_{50} = 0.00030 \mu\text{M}$), and **174i** ($\text{IC}_{50} = 0.00028 \mu\text{M}$) are 1,2,3-triazole derivatives with potent inhibitory effects. However, only single compound **174l** ($\text{IC}_{50} = 0.00044 \mu\text{M}$) could reach the boundary of inhibitory effect shown by sorafenib ($\text{IC}_{50} = 0.00022 \mu\text{M}$) towards EphB4 kinase. Most of the other derivatives are totally inactive at this drug concentration. The most significant VEGFR-2 inhibitor **175** is appended with a 3-cyclopropylcarboxamidephenyl ring at 4-position of 1,2,3-triazole ring. Also, the decent inhibitory activity of 3-chlorophenyl analog with 6-methoxypyridine **174a**, a 3-aminophenyl derivative with 6-methoxypyridine moiety **174g**, and 3-methylphenyl analog with pyridine ring **174m** reveals that 3-substituted phenyl rings play an essential role in the VEGFR-2 inhibitory activity. 6-Fluorophenyl in combination with 5-methoxypyridine and pyridine moieties diminished inhibitory activity a lot. While the compound **174d** possessing strongest Tie-2 activity has 4-methylphenyl ring and 6-methoxypyridine motifs. Slight change of position of methyl position from 4- to 3-position of benzene ring resulted in extreme low activity (compound **174e**). Further, removal of methoxy group from pyridine 6-position in case of compound **174l** led to a greatly reduced activity. 3-Chlorophenyl moiety and pyridine combination (compound **174i**) exhibited one of the best potent activities; while its 6-methoxypyridine analog (**174a**) shown little diminished inhibitory effects. Additionally, a 4-trifluoromethylphenyl derivative with 6-methoxypyridine moiety (**174f**) can also be accounted for in most significant inhibitors. In contrast to these, only single compound **174l** bearing 4-methylphenyl and pyridine moieties could reach up to the mark with two times lower activity than that of reference compound; it reveals that it is a selective EphB4 kinase inhibitor.

3.3. Aromatic ring linked-hydroxyazole scaffolds

The disease malaria, one of the biggest infectious diseases is killing most of the people every year; wherein parasitic *Plasmodium* species



Scheme 34. Synthesis of quinazoline derivatives **168a-l** [24]; **Reagents and conditions:** *i*) CH_3I , KHCO_3 , DMF, overnight, rt; *ii*) BnCl , K_2CO_3 , KI, 60°C ; *iii*) AcOH/HCl , 45°C (8h); *iv*) CH_2Br_2 , K_2CO_3 , DMF, 70°C ; *v*) Pd/C , H_2 , EtOH, rt; *vi*) R_1X , K_2CO_3 , DMF, 70°C ; *vii*) HNO_3/AcOH , 0°C ; *viii*) Pd/C , H_2 , EtOH; *ix*) formamidine acetate, EtOH, reflux; *xi*) POCl_3 , reflux; *xii*) triphosgene, THF, triethylamine, 0°C ; *xiii*) K_2CO_3 , isopropanol, reflux.

remain the main culprit. The best approach to cure malaria is to inhibit *Plasmodium falciparum* dihydroorotate dehydrogenase (*pfDHODH*) enzyme which is essential for the biosynthesis of pyrimidine and in turn survival of the parasite. The recent discovery of acidic hydroxyazoles with potent *pfDHODH* inhibitory activity has inspired to

design novel derivatives of aromatic ring linked hydroxyazole scaffolds [26].

In the synthesis of compound 1,2,5-oxadiazole derivative **177**, the benzyloxy group at 4-position of 1,2,5-oxadiazole **176** is hydrolyzed with subsequent nucleophilic substitution reaction using 2,2-

Table 10. Potential VEGFR-2 inhibitory activity of dioxane derivatives.

Compd	VEGFR-2 activity
	IC ₅₀ (μM)
168c	0.00154
168f	0.00170
168i	0.00148
168j	0.00104
Lenvatinib	0.0007

diphenylethanamine at 4-position of oxadiazole. The cyano group at 4-position of 1,2,5-thiazole is esterified to obtain corresponding ester **179** which on nucleophilic substitution with 2,2-diphenylethanamine and benzylamine yielded final compounds **180** and **181** respectively. The 3-benzyloxy-4-pyrazole carboxylic acid derivatives **182a-b** transformed to diphenylethylamide derivatives of pyrazole **183a-b** and then benzyloxy group is hydrolyzed to corresponding 4-hydroxy pyrazole analogs **184a-b** (Scheme 36).

3-Hydroxy group of pyrazole **185** is protected using the butyloxycarbonyl group to form compound **186** in which methyl moiety at 5-position is brominated to produce compound **187**. Nucleophilic substitution of compound **187** with aromatic amines/substituted phenols produced compounds **188a-f**. Removal of -Boc group from compound **188a-f** followed by ester hydrolysis resulted in 3-hydroxy-4-pyrazole carboxylic acid scaffolds **190a-f** (Scheme 37).

The intermediate compound **189a** (one of its tautomeric forms) is made use in the design of the compounds **192a-c** (Scheme 37). The compound **189a** is alkylated at its 3-OH moiety to produce *O*-alkylated pyrazoles **191a-c** in which ester group at 4-position is hydrolyzed yielding corresponding 3-hydroxy-4-carboxylic acid derivatives **192a-c**. One of the compounds in this series, **192c** is transformed into corresponding amide **193**, followed by benzyloxy moiety hydrolysis rendered the compound **194** (Scheme 38).

In the *pf*DHODH and *h*DHODH inhibitory activity investigation using standard inhibitor DSM1, no single evaluated compound has shown the capability to inhibit the *h*DHODH enzymes. However, the designed derivatives exhibited good *h*DHODH inhibitory activity with the IC₅₀ values in the range of 2.8–75 μM. Compared to DSM1 (IC₅₀ = 0.065 μM), compound **190e** (IC₅₀ = 2.8 ± 0.3 μM) (Figure 20) is most significant *pf*DHODH inhibitor amongst the derivatives. While compound **190f** possessed remarkable activity (IC₅₀ = 5.3 ± 1.2 μM). The derivatives such as **181** (IC₅₀ = 19 ± 1 μM), **190a** (IC₅₀ = 19 ± 1 μM), and **190b** (IC₅₀ = 16 ± 1 μM) have displayed moderate inhibitory activity.

In the case of structure and its activity correlation studies, the series **192a-c** is found to be totally inactive and accordingly the compound **194** finds a place in this list. The most significant *pf*DHODH inhibitor **190e** bears 3-trifluoromethylphenol connected methyl group at 5-position of the pyrazole in addition to hydroxyl and carboxylic acid

moieties at 3- and 4-positions of pyrazole ring. The presence of 3-trifluoromethyl group rendered its most potent activity; shift of 3-trifluoromethyl from 3- to 4-position (compound **190f**) has reduced activity to half the activity of compound **190e**. Besides this, replacement of the phenol moiety with aromatic amines resulted in largely diminished inhibitory activity. In common, the 3-trifluoromethyl group makes a compound more efficient in the *pf*DHODH inhibitory properties. Although most of the pyrazole derivatives have exhibited moderate to good inhibitory activity, pyrazole could not be regarded as sole pharmacore for inhibitory properties; since, the pyrazole amide **194** has failed to show good activity. Probably the particular research team would have tried to design 3-trifluoromethylthiophenol and 3-trifluorobenzeneamine analogs to check the further improvement of the inhibitory activity.

3.4. Phenylthiazoles

Undecaprenyl Pyrophosphatase (UppPase), one of the enzymes present in the bacterial cell wall functions as a membrane protein in biosynthesis of peptidoglycan and offers resistance to chemical entities. Bacterial diseases have become most common and problematic as they have developed antibiotic resistance with most of the existed antibiotics. In this regard, a large pool of chemical entities has been engineered to encounter antibiotic resistance. Many phenylthiazole scaffolds are designed against multidrug-resistant bacteria in addition to their potential anti-MRSA properties. Targeting UppPase, novel phenylthiazoles are prepared alongside accounting for aqueous solubility property [27].

The synthetic route involves the appending of ethynylsilyl moiety to the benzene 4-position which connected at 2-position of thiazole ring (compound **195**) by sonogashira coupling to form ethynylsilyl derivative of thiazole **196**. The silyl group is cleaved to produce corresponding molecule **197** and then the free ethynyl end carbon is coupled with various aromatic/aliphatic moieties yielding compound **198**. Condensation of the intermediate **198** with aminoguanidine resulted in the final compounds **199a-z** and **200a-d** (Scheme 39).

The title compounds are tested for their anti-UppPase activity using linezolid and vancomycin as reference compounds. The most potent inhibitory activity is elicited by the compounds **199f**, **199o**, **199q** and **199x** (Figure 21) with an identical MIC value of 2 μM. The activity of most significant inhibitors is almost comparable with linezolid/vancomycin (MIC = 1 μM). The derivatives such as **199a**, **199c**, **199d**, **199s**, and **199z** have possessed remarkable inhibitory potentials with identical MIC value of 4 μM.

The noteworthy MIC values of the most significant inhibitors are attributed to a distinct functional group –OH present preferably at *meta*-position (compound **199f**). It indicates that the hydroxy group at *meta*-position offers the least steric hindrance and perfect fit into the enzyme active site. While the *meta*- and *para*-amine substituted derivatives have exhibited less striking activity (**199a** and **199c**). Also, the *meta*-methoxy substituent (**199d**) exhibited diminished activity compared to compound **199f**. If *p*-OH-phenylthiazole derivative was prepared, it would have been a furthermore potent molecule. Thiophen-2yl and 5-methyl thiophene-2yl substitutions in the case of **199o** and **199q** analogs bestowed remarkable inhibitory activity. However, activity is reduced to a greater extent by appending thiophene with its 3-position (**199p**). Chirality might have played a significant role in the case of noteworthy inhibitory potency of 2-hydroxypropyl substituted analog **199x**.

Almost half of the evaluated derivatives are weak UppPase inhibitors and exhibited inhibitory activity at drug concentration higher than 64 μM. Some of these derivatives with high MIC values possess bulky ortho substituents that can be observed in the derivatives such as **199b**, **199g**, **199i**, and **200b-c**. Also, the carbonyl substituents such as amide and acetyl in compounds **199l** and **199m** respectively rendered weak activity. Compounds derivatized with pyridine and pyrimidine substituents also failed to show good inhibitory activity.

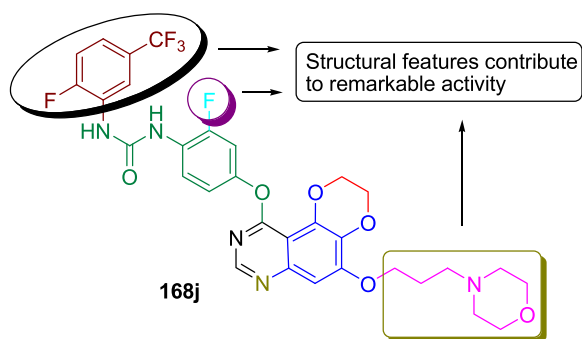
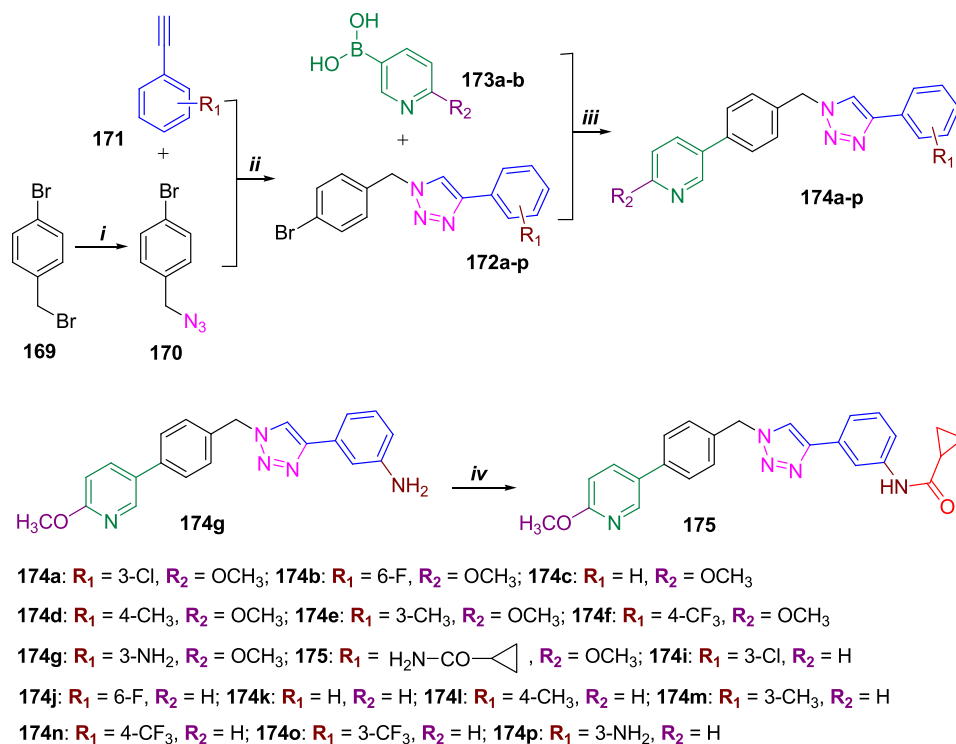


Figure 18. Demonstration of the structure of compound **168j** as potent VEGFR-2 inhibitor.



Scheme 35. Synthetic route for the preparation of compounds **174a-p** and **175** [25]; *i*) NaN_3 , DMF, rt (12h); *ii*) L-sodium ascorbate, copper sulfate pentahydrate, EtOH, H_2O , rt; *iii*) dioxane, H_2O , $\text{Pd}(\text{PdCl}_2)_2$, K_2CO_3 , reflux; *iv*) 0°C , CH_2Cl_2 , triethylamine, 30min, cyclopropyl carbonyl chloride, rt.

3.5. Pyrazole derivatives

COX-2 is an isoenzyme of the cyclooxygenases responsible for the formation of inflammatory prostaglandins such as PGE_2 . Since PGE_2 functions as an efficient inflammatory mediator, inhibition of the PGE_2 would be an effective clinical approach for inflammation treatment. Taken together the inhibitory properties of pyrazole scaffolds as COX inhibitors, novel pyrazole derivatives bearing benzenesulfonamide moiety are designed and synthesized [28].

The synthetic route commences with 4-cyano-5-amine- N_1 -benzene sulfonamidepyrazole **201**. The $-\text{NH}_2$ group of the compound **201** is treated with chloroalkane carbonyl chloride to obtain amide analogs **202a-c** which on nucleophilic substitution with morpholine afforded final compounds **203a-c**. The amine moiety of compound **201** is acylated/benzoylated in addition to acylation of the sulfonamide $-\text{NH}_2$ in one of the compounds yielded compounds **204a-b**. Condensation of compound **201** with various substituted aromatic amines produced compounds **205a-f** (Scheme 40).

All the prepared derivatives have been evaluated for COX-1 and COX-2 inhibitory activities using celecoxib. Except for a few compounds, all the evaluated derivatives exhibited decent COX-1 inhibitory effects. Compared to celecoxib, compounds **203a** ($\text{IC}_{50} = 0.064 \mu\text{M}$) (Figure 22) can be mentioned as strongest COX-1 inhibitor. Alongside, compound **204b** ($\text{IC}_{50} = 0.073 \mu\text{M}$) finds a place in significant inhibitors

list. Other derivatives have exhibited inhibitory activity ($\text{IC}_{50} = 0.104\text{--}0.169 \mu\text{M}$) as potent as celecoxib ($\text{IC}_{50} = 0.131 \mu\text{M}$). Regarding inhibitory activity towards COX-2 enzyme, except for compounds **202c**, **203c**, and **205c**, all the evaluated compounds have elicited activity almost similar to the reference compound ($\text{IC}_{50} = 0.035 \mu\text{M}$). However, most potent inhibitory potency is bestowed by compound **202a** (Figure 22).

Compound **203a** stood atop in significant inhibitors list; wherein its structural features include benzene sulfonamide connected to pyrazole N_1 -position and morpholine appended to pyrazole 5-position via methylene amide fragment. Extension of methylene amide to ethylene amide (compound **203b**) diminished COX-1 inhibitory activity 13-times compared to compound **203a**. The second most significant inhibitor **204b** possessed benzamide at 5-position of pyrazole ring in addition to benzenesulfonamide at N_1 -position. Compound **204a** obtained by connecting acetamide at pyrazole ring 5-position and N -methylation of sulfonamide functionality. Since benzenesulfonamide moiety is a prominent pharmacore for the exhibition of pharmacological activity, probably acetylation of pyrazole 5-amine would not have affected the inhibitory activity much. Hence, the design of 5-acetamide analog would be a potent try to check improvement in the activity. In the case of inhibitory activity of **202a-c** series compounds, compound **202a** ($\text{IC}_{50} = 0.104 \mu\text{M}$) has shown promising results and activity ($\text{IC}_{50} = 0.123 \mu\text{M}$) reduced a little with an extension of alkyl chain length (**202b**). Reduction of the

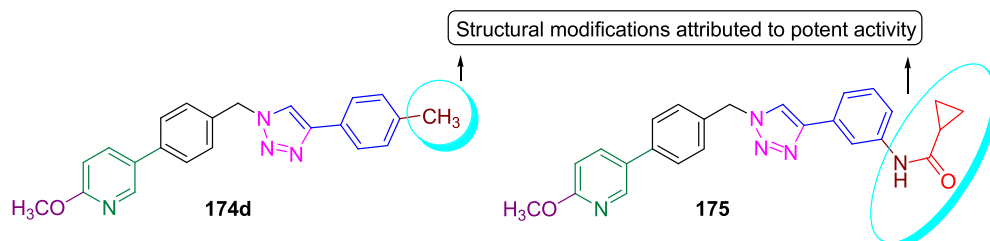
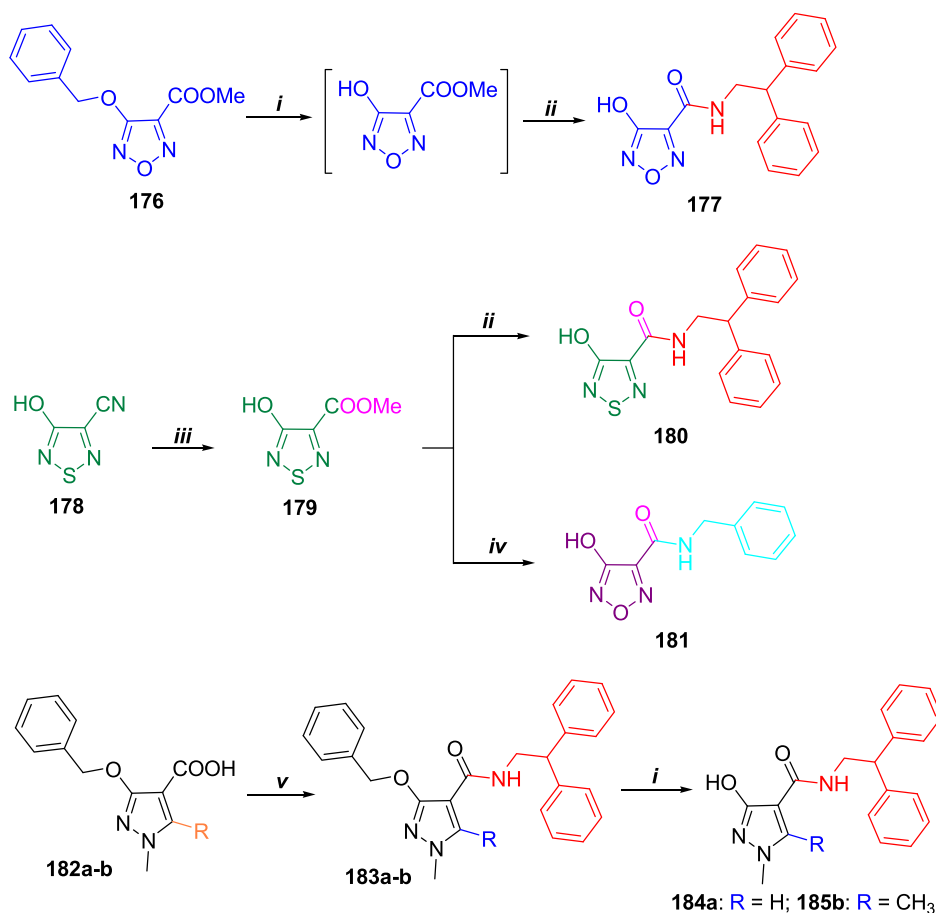


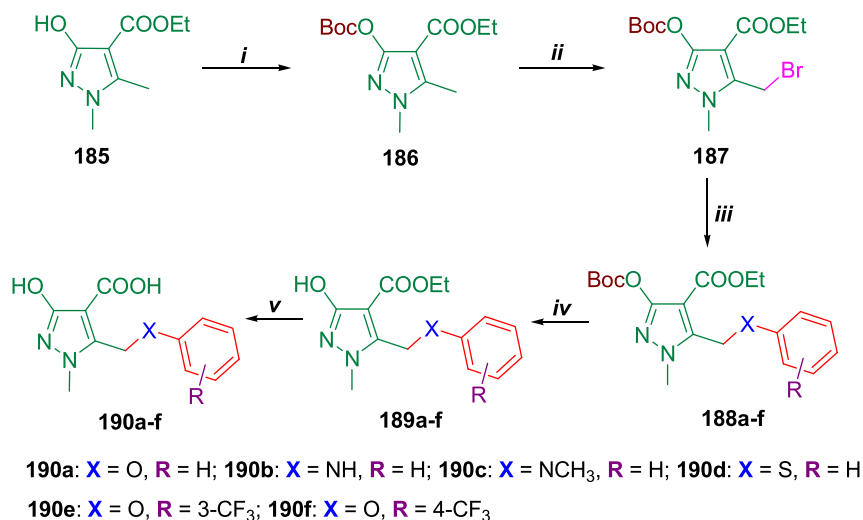
Figure 19. Structures of potent tyrosine kinase inhibitors.



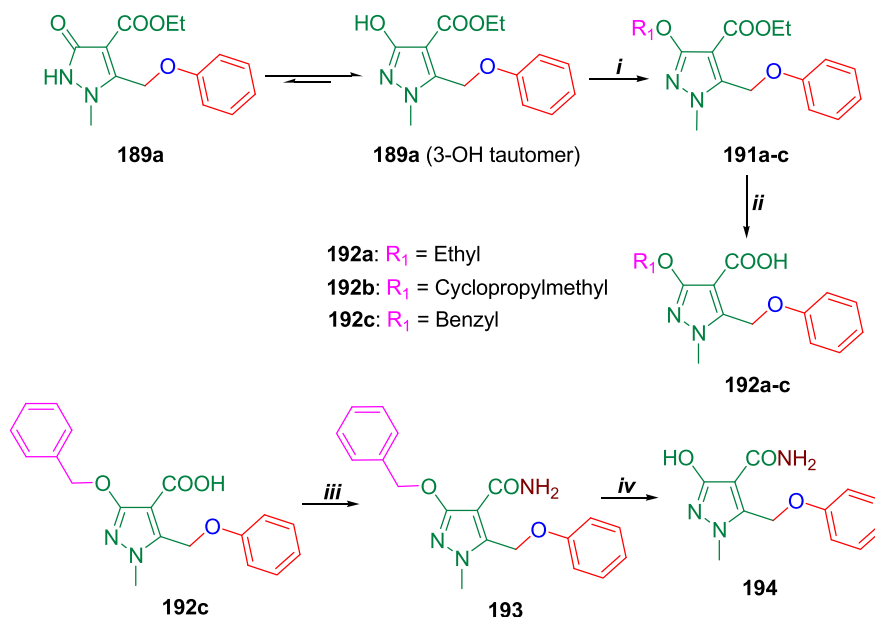
Scheme 36. Synthetic route for the preparation of hydroxyazole derivatives [26]; **Reagents and conditions:** *i*) H₂, Pd/C, dry THF; *ii*) 2,2-diphenylethanamine, 60 °C; *iii*) a) NaH, MeOH; b) 2M H₂SO₄; *iv*) benzylamine, 60 °C; *v*) HBTU, 4-(dimethylamino)pyridine (DMAP), 2,2-diphenylethanamine, dry DMF.

activity to a large extent is observed for isopropyl amide analog **202c**. A similar effect has been observed in the case of compounds **203a-c**. These facts infer that longer alkyl chain lengths deteriorated the COX-1 inhibitory activity. While compounds of **205a-f** series comprising aromatic imines of pyrazole 5-amine displayed moderate to potent inhibitory activities; amongst them, 4-bromobenzylidene derivative **205d** shown maximum inhibitory activity (IC₅₀ = 0.115 μM).

Meanwhile, in the assessment of the COX-2 inhibitory activity, the most striking inhibitory activity is observed for the compound **202a** which entails chloroacetamide fragment at 5-position of pyrazole along with benzene sulfonamide at pyrazole N₁-position. However, the inhibitory activity abated gradually for compounds **202b** and **202c** with the increased bulkiness of chloroalkylamide groups. Moderate COX-2 inhibitor **204b** has displayed diminished activity when sulfonamide amine



Scheme 37. Synthesis of the derivatives **188a-f** [26]; **Reagents and conditions:** *i*) Cs₂CO₃, BOC anhydride, dry THF, reflux; *ii*) NBS, benzoyl peroxide, dichloroethane, reflux; *iii*) R-(Ph)-XH, Cs₂CO₃, dry DMF; *iv*) TFA, DCM; *v*) 5M NaOH, EtOH.



Scheme 38. Preparation of the final compounds **192a-c** and **194** [26]; **Reagents and conditions:** *i*) R_1X , K_2CO_3 , acetonitrile; *ii*) 5M NaOH, EtOH; *iii*) a) oxalyl chloride, dry DMF, dry THF, 0 °C; b) aq NH_3 , THF; *iv*) H_2 , Pd/C, dry THF.

is methylated and pyrazole 5-amine is acetylated (**204a**). Pyrazole derivatives in which benzylidene substituted by both electron-withdrawing -F (**205b**) and electron-donating $-OCH_3$ (**205e**) are successful in exhibiting remarkable COX-2 inhibitory activity which is almost similar to that of the reference compound. Hence correlation of structure and activity, in this case, could not be established.

3.6. Phthalimide-1,2,3-triazole hybrid compounds

The hydroxylation of L-tyrosine to L-DOPA and oxidation of L-DOPA to dopaquinone are carried out in melanin biosynthesis by multifunctional metalloenzyme tyrosinase. However, abnormal secretion of the melanin enzyme leads to skin disorders and esthetic problems in human beings. Thereby inhibition of the tyrosinase in such conditions is crucial to address these problems. Considering the prominent pharmacological properties of phthalimide and antityrosinase effects of triazole scaffolds, the design of phthalimide-1,2,3-triazole hybrid compounds is accomplished [29].

In the synthesis of target molecules, phthalimide **206** connected to propargyl fragment to form *N*-propargyl phthalimide **207**. Substituted benzyl chlorides **208a-m** are transformed into substituted benzyl azides **209a-m** in which azide functionality is utilized to create a triazole with alkyne moiety of compound **207** to render final compounds, triazole linked phthalimide scaffolds **210a-m** (Scheme 41).

The designed derivatives are allowed to inhibit tyrosinase using kojic acid as a standard inhibitor. More than half of the evaluated molecules have not shown good tyrosinase inhibitory activity compared to kojic acid. Methyl, methoxy and fluoro benzyl substituted triazole phthalimides (**210a-f**) and dichlorobenzyl scaffolds **210i** and **210j** would be included in the inactive molecules list with the inhibitory activity >50 μM . While -Br, -Cl and $-NO_2$ benzyl substituted triazole phthalimides

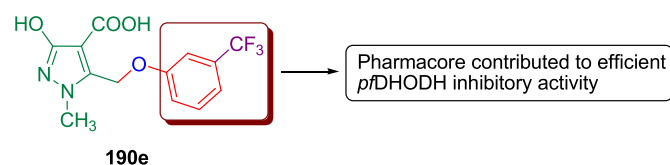


Figure 20. Structure of compound **190e** possessing efficient $p7DHODH$ inhibitory activity.

displayed decent inhibitory activities. Amongst them, compound **210k** ($IC_{50} = 26.55 \pm 2.31$ μM) bearing 2-bromobenzyl moiety and its 2- NO_2 analog **210m** ($IC_{50} = 26.20 \pm 1.55$ μM) (Figure 23) are having almost similar inhibitory potencies but comparatively threefold lower activity than that of kojic acid ($IC_{50} = 9.28 \pm 1.15$ μM). In both the potent inhibitors bulky electron-withdrawing substituents such as -Br, $-NO_2$ groups have exhibited favorable effects. Less bulky groups 2-Cl and 3-Cl-benzyl substituted derivatives **210g** and **210h** rendered moderate activity.

3.7. Purine-Pyrazole hybrids

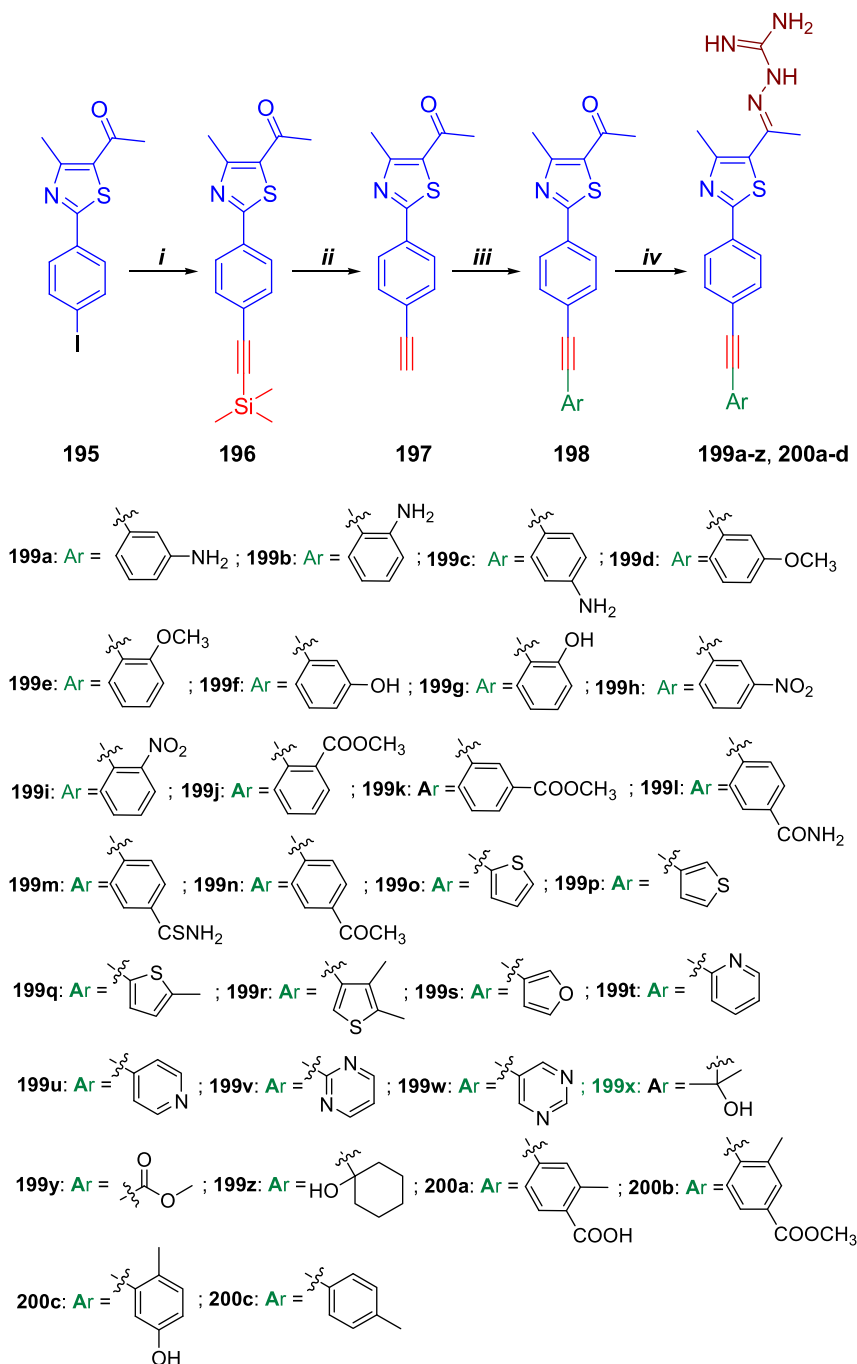
15-LOX, one of the isoenzymes of lipoxygenases promotes invasion of tumor cells into lymphatic vessels and induction of lymph node metastasis. Through the LOX pathway hydroxyeicosatetraenoic acids (HETEs) or leukotrienes (LTs) are produced from Arachidonic acid (AA). Hence best chemotherapeutic agents include 15-LOX inhibitors. Purines have been reported as first-class 15-LOX inhibitors. Previously demonstrated purine derivatized pyrazoles possessing anticancer properties and antioxidant effects triggered the design of a new series of purine-pyrazole hybrid derivatives [30].

In the first series, purine derivative **211** is treated with various substituted acetophenones to yield benzylidene derivatives of purine **212a-d** which upon cyclization using $POCl_3/DMF$ resulted in pyrazole carbaldehyde analogs **213a-d** (Scheme 42).

The pyrazole carbaldehydes **213a-d** are reacted with thiazolone-benzenesulfonamide and thiazolone acetic acid to obtain the corresponding thiazolone incorporated pyrazole-purine derivatives **214a-d** and **215a-d** respectively (Scheme 43).

Likewise, the compounds **213a-d** on condensation with substituted thiosemicarbazide resulted in substituted thiosemicarbazone analogs **216a-h**. The thiosemicarbazone fragment is utilized in the formation of thiazole ring using *p*-bromo phenacyl bromide and ethyl bromoacetate to produce finally purine-pyrazole scaffolds (**217a-h** and **218a-h**) linked to thiazole moiety through hydrazone spacer (Scheme 44).

Some selected compounds were investigated for their 15-LOX inhibitory activity using zileuton, quercetin, and meclufenamate sodium. All the evaluated derivatives have exhibited higher potential values compared to reference compounds. However, with respect to the standard inhibitor zileuton ($IC_{50} = 3.98$ μM), except for a few derivatives, all



Scheme 39. Synthetic route for the preparation of thiazole derivatives **199a-z** and **200a-d** [27]; **Reagents and conditions:** *i*) $\text{PdCl}_2(\text{PPh}_3)_2$, ethynyltrimethylsilane (2 Equiv), 50°C (24h); *ii*) *iii*) $\text{PdCl}_2(\text{PPh}_3)_2$ (5% mol), CuI (7.5% mol), Et_3N for 6–24h; *iv*) aminoguanidine HCl, EtOH .

other screened molecules have shown potent inhibitory properties ($\text{IC}_{50} = 1.76\text{--}3.42\ \mu\text{M}$). The first series of compounds **213a-d** have failed to reach a decent inhibitory level mark. It indicates that pyrazole carbaldehydes would not fit exactly into the enzyme active site. Whereas, compounds of purine-pyrazole linked to benzenesulfonamide **214a-d** have displayed the striking inhibitory activities. In those, compound **214a** ($\text{IC}_{50} = 1.96\ \mu\text{M}$) bearing phenyl ring at pyrazole 3-position elicited excellent activity. But the inhibitory activity reduced gradually with an increase in bulkiness at phenyl 4-position. Similar effects are observed in the case of the compounds in the **215a-d** series. In these derivatives, purine-pyrazole scaffolds are appended to thiazole acetic acid moiety, wherein simple phenyl analog **215a** ($\text{IC}_{50} = 2.62\ \mu\text{M}$) is the most potent inhibitor in the series. The 4-substituted phenyl analogs have exhibited

diminished activity. Out of the thiosemicarbazones derivatized purine-pyrazoles, compound **216a** ($\text{IC}_{50} = 2.81\ \mu\text{M}$) possessing simple phenyl ring connected to pyrazole 3-position exhibited promising inhibitory effects. Again inhibitory effects of 4-substituted phenyl analogs could be repeatedly observed to be similar to previous series compounds. A good account of inhibitory properties is displayed by **217a-h** series derivatives. Amongst these derivatives, compound **217d** ($\text{IC}_{50} = 1.76\ \mu\text{M}$) (Figure 24) bearing 4-methoxyphenyl ring at pyrazole 4-position has bestowed with the most remarkable activity out of all evaluated molecules. Contrary to previous series compounds, the bulkiness at benzene 4-position appended to pyrazole 3-position has led to moderate activity. Final series of compounds **218a-h** wherein purine-pyrazole scaffolds are linked to thiazolone via diazo spacer has exerted decent inhibitory

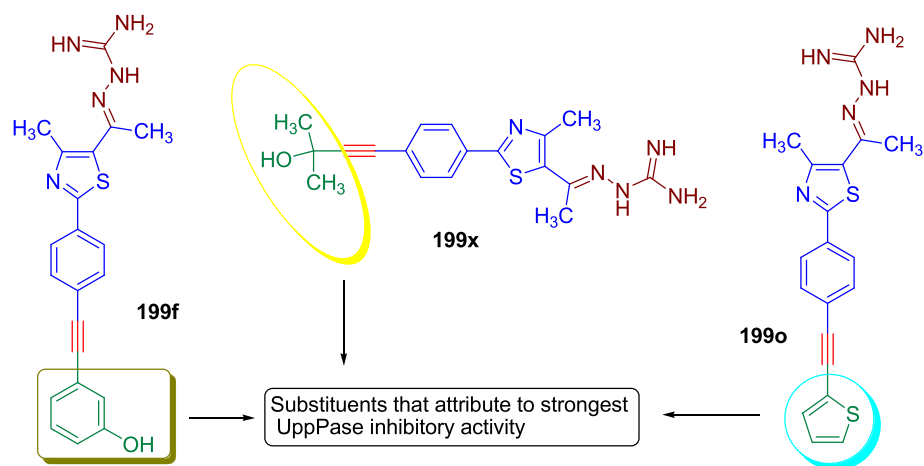
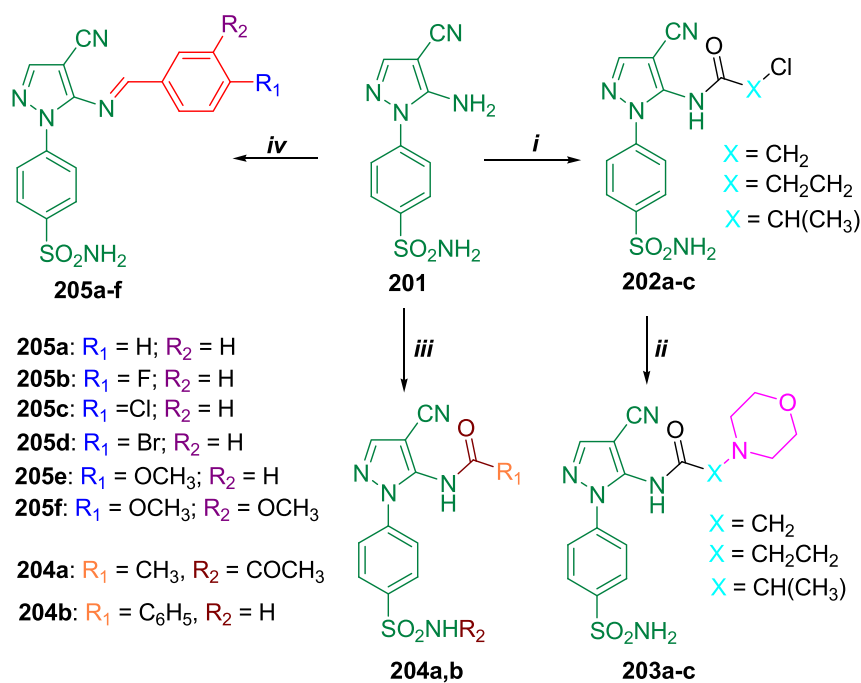


Figure 21. Demonstration of structures of most significant inhibitors.



Scheme 40. Strategic design and synthesis of the pyrazole-benzenesulfonamide derivatives [28]; **Reagents and conditions:** i) Chloroalkane carbonyl chloride, DMF, rt (24h); ii) Morpholine, anhyd. K_2CO_3 , DMF, 80 °C (16 h); iii) Acetyl chloride or benzoyl chloride, pyridine, 80 °C, (24h); iv) Aromatic aldehyde, glacial acetic acid, reflux (8–24h).

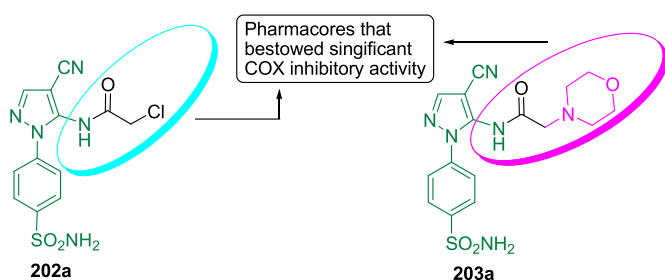
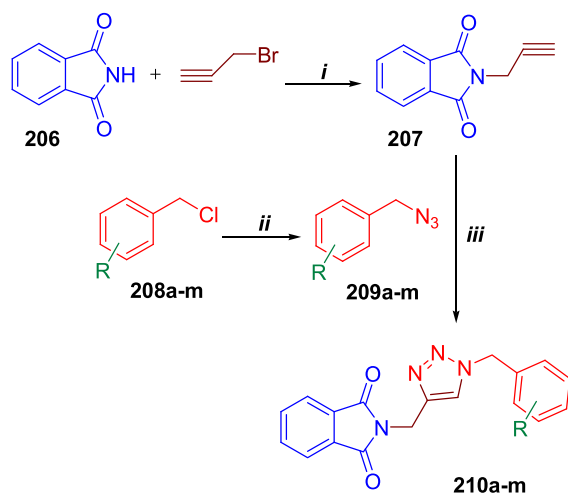


Figure 22. Structures of most potent COX inhibitors.

activity. Even in this series of compounds, 4-substituted phenyl analog **218d** ($IC_{50} = 1.98 \mu M$) exhibited better activity.

3.8. Pyrazole and pyrazolo [1,5- α] pyrimidine scaffolds

Protein kinases function transfer of γ -phosphate group wherein transfer of γ -phosphate from a nucleoside triphosphate (ATP) to the side chain of an amino acid residue in the substrate proteins such as serine, threonine, histidine and tyrosine residues. The cyclin-dependent kinases (CDK) related to serine/threonine kinase family are responsible for the initiation and succession of each cell cycle phase; amongst these, CDK2 is essential for progress through G1 to S phase. However, hyperactivation of CDK2 in a large number of human cancer types is attributed to the



210a: R = 2-methyl; **210b:** R = 4-methyl; **210c:** R = 4-methoxy
210d: R = 2-Fluoro; **210e:** R = 3-Fluoro; **210f:** R = 4-Fluoro
210g: R = 2-Chloro; **210h:** R = 3-Chloro; **210i:** R = 2,3-Dichloro
210j: R = 3,4-dichloro; **210k:** R = 2-Bromo; **210l:** R = 4-Bromo
210m: R = 2-Nitro

Scheme 41. Synthesis of phthalimide-triazoles as COX inhibitors [29]; **Reagents and conditions:** i) K_2CO_3 , DMF, 80 °C (2h); ii) NaN_3 , $H_2O/t-BuOH$, NEt_3 ; iii) intermediates **209a-m**, CuI.

overexpression of the particular enzyme. Pyrazolo [1,5- α] pyrimidines have been reported as pharmacologically important scaffolds especially in case of inhibition of CDK2/Cyclin A. Based on these facts novel pyrazolo-pyrimidine derivatives are designed and synthesized [31].

Synthesis of the first series of compounds involves condensation of ethyl acetoacetate with phenylisothiocyanate to give compound **219** which on cyclization using hydrazine hydrate produced pyrazole derivative **220**. The compound **220** is utilized in the synthesis of the derivatives **221a-g** and **222a-c** by reacting with triethyl orthoformate and aromatic amines and aromatic aldehydes respectively (Scheme 45).

Further, cyanoacetamide **223** is transformed into compound **224** using phenylisothiocyanate followed by treatment with dimethyl sulfate. The compound **224** is allowed to undergo intermolecular cyclization with hydrazine pyrazole amide analog **225** and subsequent fusion of pyrimidine ring pyrazole 1,5-position produced pyrazolo-pyrimidine derivatives **226a-d** (Scheme 46). Finally, in the synthesis of compounds **229a-e**, similar reaction sequences with similar reaction conditions are observed; wherein malononitrile is used as a starting material (Scheme 47).

The final derivatives designed are investigated for their anti-CDK2 inhibitory activity using dinaciclib. The inhibition percentage of the reference compound is considered as 100%. Most of the evaluated derivatives have exhibited poor inhibition percentages. In the list of potent inhibitors list, compounds **221d** (Inhibition = 60%) (Figure 25) and **221g** (Inhibition = 44%) could be mentioned. While compound **226c**

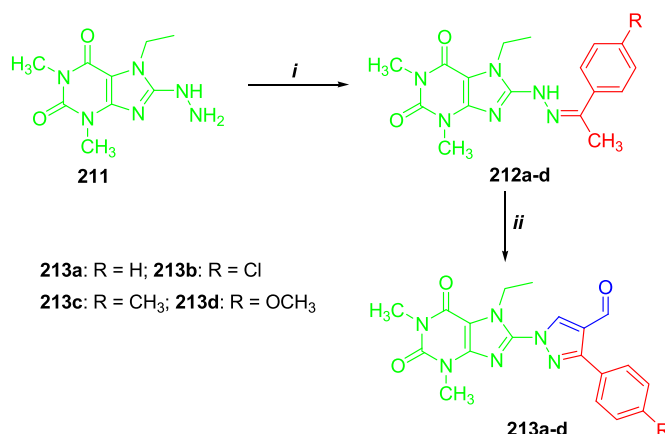
(Inhibition = 28%) has shown some significance. The compound **221d** bearing phenylamine moiety at pyrazolone 3-position and 4-hydroxy-phenyl ring through methylene amine fragment at 4-position bestowed the significant activity. Most of the poor CDK2 inhibitors possessed bulky groups at benzene amino methylene moiety, while the -OH functionality is small and distinct group. However, the compound **221g** with bulky and hindered pyrimidine sulfonamide moiety has elicited the most promising activity; it might be attributed to the prominent pharmacological activity of pyrimidine sulfonamide. No single pyrazolopyrimidine derivative has displayed good inhibitory activity except for compound **226c**. The two significant inhibitors **221d** and **221g** pertain to the series wherein pyrazolone is derivatized with a benzene amine group and phenylamino-methylene moiety at 3- and 4-positions respectively.

3.9. Dihydropyran fused pyrazole derivatives

Non-steroidal anti-inflammatory drugs (NSAIDs) are being used for inhibition of inflammation wherein cyclooxygenases play a significant role in the mediation of inflammation through the release of prostaglandins. Since such drugs exhibit gastrointestinal and renal toxicity, design of new NSAIDs is crucial for inhibition of cyclooxygenases. In view of promising pharmacological activity of pyrazole scaffolds such as celecoxib, deracoxib towards COX-2 enzyme, dihydropyran derivatized pyrazole derivatives are synthesized [32].

The synthetic route commences from ethyl acetoacetate wherein it is cyclized with substituted hydrazines **230a-b** to produce *N*-substituted pyrazolone **231a-b** and fusion of dihydropyran to the pyrazolone at its 4- and 5-positions via multicomponent reaction to render fused derivatives **232a-o**. The amine group present at fused derivatives **232a-o** is condensed with various aromatic aldehydes to obtain the final compounds **233a-o** (Scheme 48).

The target molecules have been tested for COX-1 and COX-2 inhibitory properties using celecoxib. Compared to the reference compound ($IC_{50} = 0.34 \mu M$), no single investigated derivative has exhibited potent



Scheme 42. Design and synthesis of the compounds **212a-d** [30]; **Reagents and conditions:** i) 4-substituted $C_6H_5COCH_3$; ii) $POCl_3/DMF$.

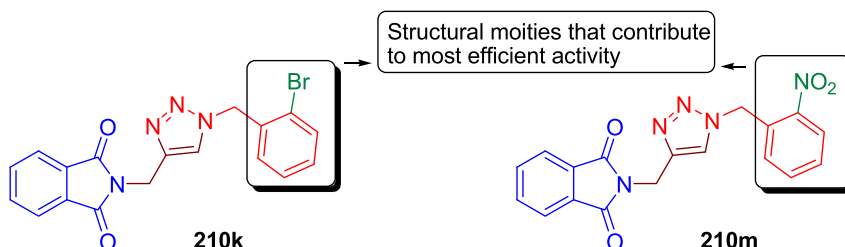
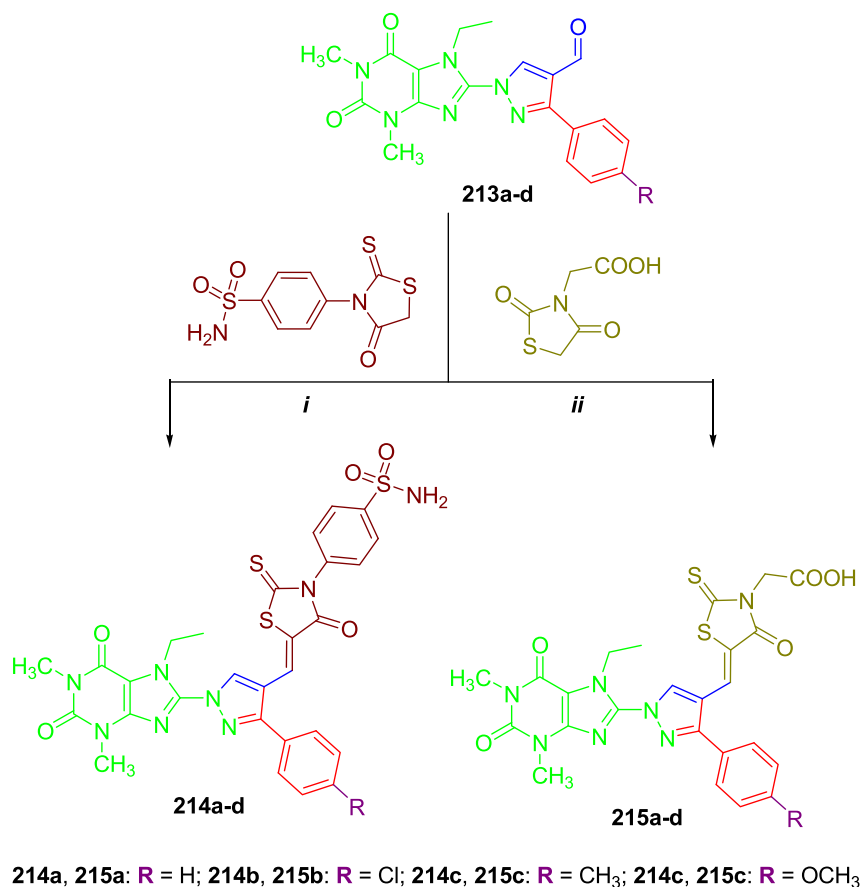
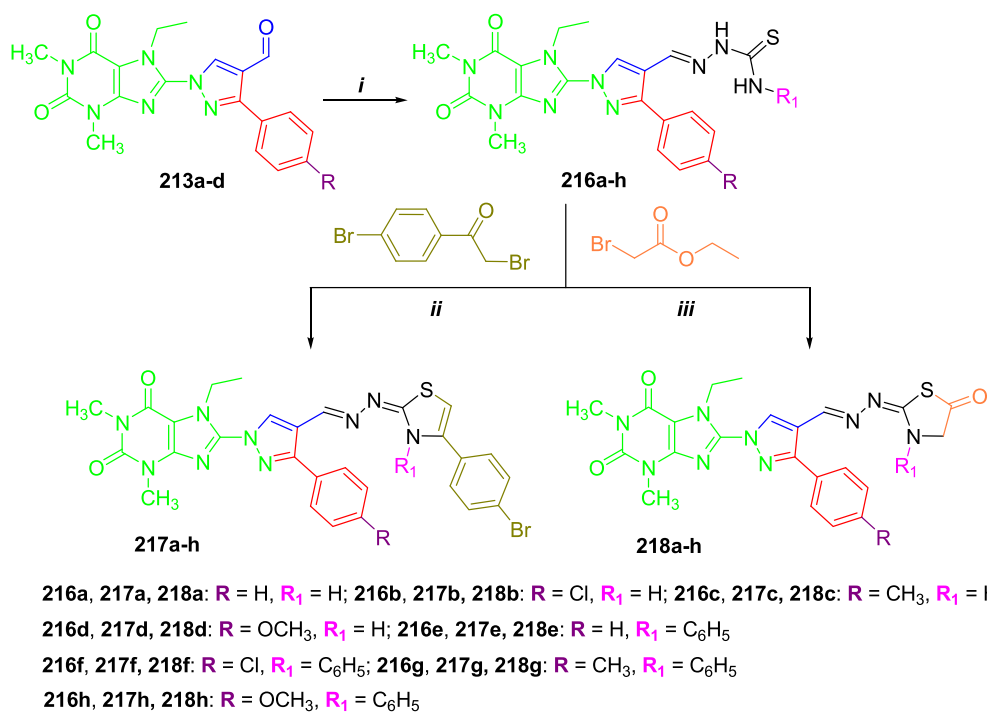


Figure 23. Structures of remarkable tyrosinase inhibitors.



Scheme 43. Synthetic route for the preparation of the compounds **214a-d** and **215a-d** [30]; **Reagents and conditions:** *i*) Dry dioxane, piperidine (catalyst) *ii*) Dry dioxane, CH₃COONH₄ (catalyst).



Scheme 44. Synthesis of the purine-pyrazolothiazoles **216a-h** and **217a-h** [30]; **Reagents and conditions:** *i*) *N*-substituted thiosemicarbazide, dry dioxane, glacial acetic acid (catalyst), reflux; *ii*) dry dioxane, anhyd. CH₃COONa, reflux; *iii*) dry dioxane, anhyd. CH₃COONa, reflux.

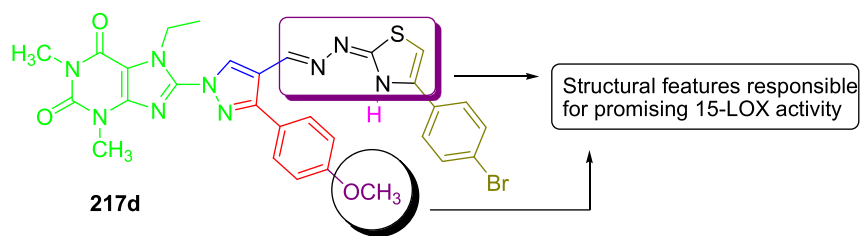
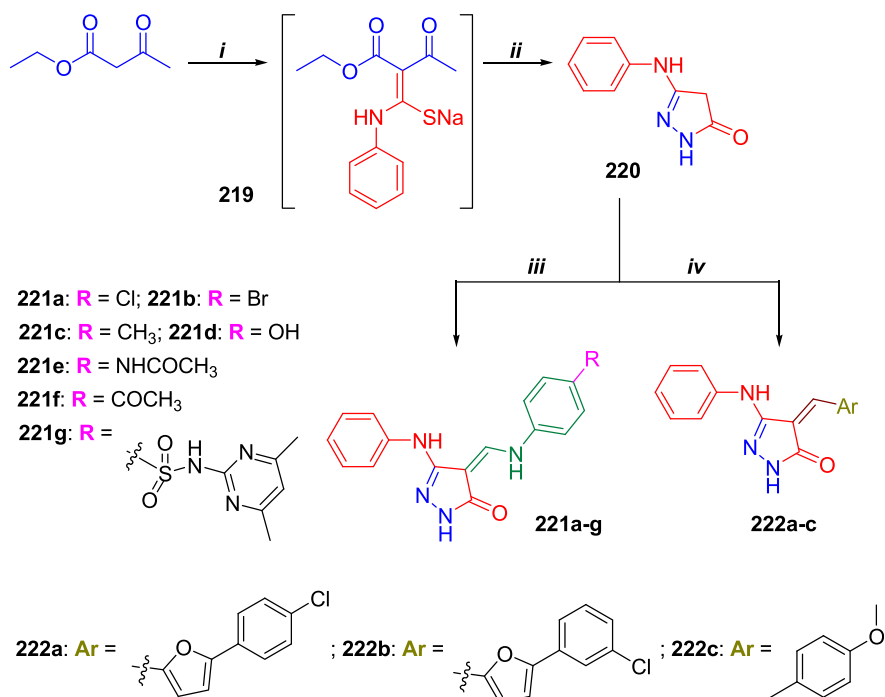
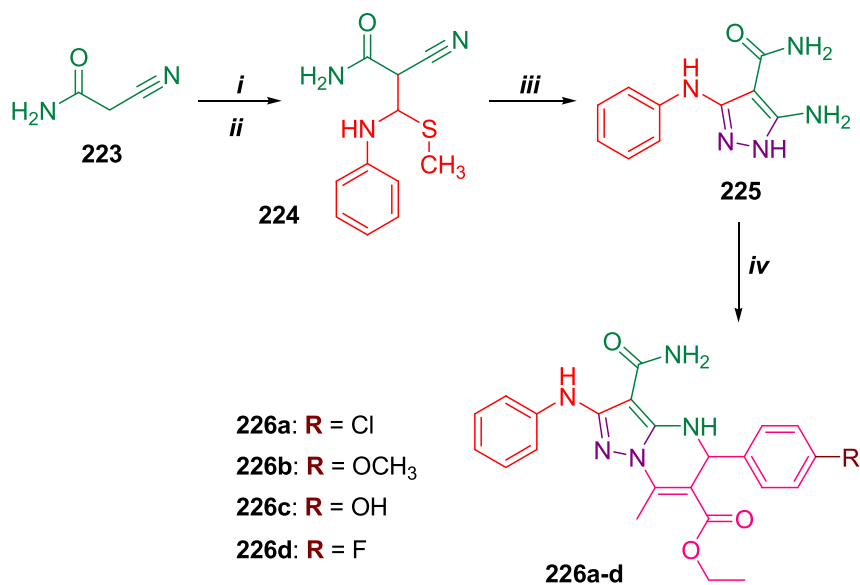


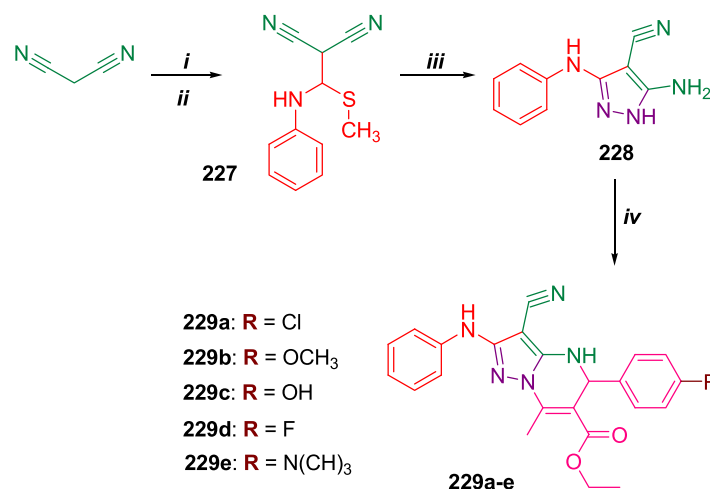
Figure 24. Demonstration of the structure of significant 15-LOX inhibitor.



Scheme 45. Strategic design and synthesis of final compounds **221a-g** and **222a-c** [31]; **Reagents and conditions:** *i*) Na, CH₃OH, phenyl isothiocyanate, reflux 1/2 h, cool; *ii*) Hydrazine hydrate, reflux 1 h; *iii*) Aryl amine, triethyl orthoformate, DMSO, Oil Bath, 2.5–4.5 h, *iv*) Aromatic aldehyde, sodium acetate, AcOH, reflux 6 h.



Scheme 46. Synthesis of the pyrazolopyrimidines **226a-d** [31]; **Reagents and conditions:** *i*) KOH, DMF, phenyl isothiocyanate, stirring, RT, 24 h; *ii*) Dimethyl sulfate, stirring, RT, 8 h, *iii*) Hydrazine hydrate, 3–4 h, *iv*) Hydrochloric acid, aromatic aldehyde, ethyl acetoacetate, ethanol, reflux, 4–8 h.



Scheme 47. Synthetic design and preparation of final compounds **229a-e** [31]; **Reagents and conditions:** *i*) KOH, DMF, phenyl isothiocyanate, stirring, RT, 24 h; *ii*) Dimethyl sulfate, stirring, RT, 8 h, *iii*) Hydrazine hydrate, 3–4 h, *iv*) Hydrochloric acid, aromatic aldehyde, ethyl acetoacetate, ethanol, reflux, 4–8 h.

inhibitory activity. However, compound **233j** ($IC_{50} = 2.56 \mu\text{M}$) stood top in the inhibitors list with IC_{50} value sevenfold weaker compared to the standard inhibitor. Although, the activity of derivative **233h** ($IC_{50} = 4.32 \mu\text{M}$) is poor; however, its activity is second to the strongest COX-2 inhibitor **233j**. When structural modification of the derivatives is correlated with their pharmacological activity the following conclusions are made; the most significant inhibitor **233j** bears phenyl ring at fused scaffold N_1 -position, 3,4,5-triOCH₃-phenyl moiety and 4-hydroxyphenyl-methanimine entity at 4- and 6-positions of dihydropyran-fused pyrazolone. Meanwhile, compound **233h** is appended with phenyl rings and phenylmethanimine moiety at N_1 , 4 and 6-positions of the fused pyrazolone-dihydropyran moiety. Within the inhibitors list, the derivatives with 4-hydroxyphenyl rings at 4- and 6-positions possessed somewhat good inhibitory properties. In the case of COX-1 inhibitory properties, few compounds exhibited inhibitory activity stronger than celecoxib ($IC_{50} > 50.0 \mu\text{M}$). The strongest inhibitory activity ($IC_{50} = 33.58 \mu\text{M}$) is elicited by the compound **233n** (Figure 26). Likewise the compound **233c** (Figure 26) ($IC_{50} = 37.72 \mu\text{M}$) stood next to potent COX-1 inhibitors list. While the compound **233e** ($IC_{50} = 51.32 \mu\text{M}$) shown activity as potent as the standard inhibitor. The inhibitory values of these compounds infer that these derivatives are selective COX-1 inhibitors. The remarkable COX-1 inhibitor **233n** possessed with phenyl ring at N_1 -position in addition to a 3-chlorophenyl moiety and 4-hydroxyphenylmethanimine at 4- and 6-positions respectively. However, the derivative **233c** comprising unsubstituted phenyl and phenylmethanimine moieties but 2-NO₂-phenyl rings at N_1 , 4- and 6-positions respectively bestowed the best result. Similar to COX-2 inhibitors, compounds having 4-OH-phenyl rings either at N_1 or 4- or 6-positions of fused pyrazolone scaffold have displayed moderate inhibitory activity.

4. Heterocycle-fused pyrazole analogs

Acetylcholinesterase enzyme's involvement in the dementia disease is confirmed by the cholinergic hypothesis; in this regard, cholinesterase inhibitors have been synthesized to treat Alzheimer's and its sister diseases. Human carbonic anhydrases catalyze the reversible interconversion of carbon dioxide and bicarbonate. Isoenzyme of *hCA* functions in the tumorigenesis in addition to pH regulation, bone resorption, and some biosynthetic reactions. Thereby, based on the pharmacological history of pyrazoles towards cholinesterases and carbonic anhydrases, fused pyrazole derivatives are engineered and tested for corresponding biological activity [33].

Pyrazole-3,4-dicarboxylic acid **234** is transformed to acyl chloride **235** with SOCl₂ and then treatment with ammonia led to pyrazole-diamide **236**. Dehydration of dihydride **236** produced dinitrile **237**

and subsequent cyclization rendered the final compound **238**. One of the intermediate **235** is converted to corresponding diester **239** which upon cyclization with hydrazine yielded the fused pyrazolopyridazinone **240**.

The starting material pyrazole dicarboxylic acid **234** is utilized in the design of another series of molecules. Here fused cyclic anhydride **241** is synthesized from dicarboxylic acid using a mixture of SOCl₂ and DMF followed by primary amine insertion into cyclic anhydride to give fused-pyrazolo cyclic imide **242a-b** (Scheme 49).

The engineered molecules are evaluated for *hCA* and AChE inhibitory activity using acetazolamide and tacrine respectively. A good account of carbonic anhydrase-I & II inhibitory activity has been reported. All the synthesized derivatives have shown *hCA* inhibitory activity higher than reference compounds. In the case of *hCA* I inhibitory activity, compound **235** ($IC_{50} = 0.83 \mu\text{M}$) (Figure 27) is found to be the most significant *hCA* I inhibitor exhibiting 25-fold greater potency compared to reference compound ($IC_{50} = 21.13 \mu\text{M}$). The remarkable *hCA* I inhibitors include compound **234** ($IC_{50} = 3.54 \mu\text{M}$) (Figure 27), **238** ($IC_{50} = 6.66 \mu\text{M}$), **239** ($IC_{50} = 5.04 \mu\text{M}$), and **241** ($IC_{50} = 6.01 \mu\text{M}$). Surprisingly, the most significant *hCA* I inhibitor **235** ($IC_{50} = 1.36 \mu\text{M}$) has succeeded in eliciting the most potent *hCA* II activity; wherein its inhibitory activity is 21-fold stronger than the acetazolamide ($IC_{50} = 28.55 \mu\text{M}$). Meanwhile the derivatives **234** ($IC_{50} = 5.52 \mu\text{M}$), **238** ($IC_{50} = 9.02 \mu\text{M}$), and **239** ($IC_{50} = 7.88 \mu\text{M}$) managed to exhibit noteworthy *hCA* II potency. When the inhibitory activities towards both *hCA* I and *hCA* II are observed, it is evident that dual inhibitory effect has prevailed in the molecules **234**, **235**, **238**, and **239**. The most significant *hCA* I & *hCA* II dual inhibitor **235** comprises 3,4-dimethyl benzene and phenyl ring at pyrazole N_1 and C_5 positions of pyrazole. Alongside, 3- and 4-positions of pyrazole are occupied by acyl chloride moieties. The structural modifications infer that acid chlorides are more potent than corresponding carboxylic acids and again inhibitory activity reduced to a large extent for diamide analog **236**. Gradual increment in *CA* inhibitory activity is observed for dinitrile **237**, followed by pyrazolo-

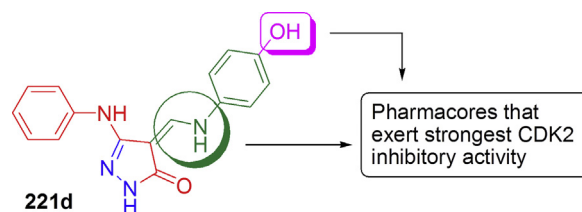
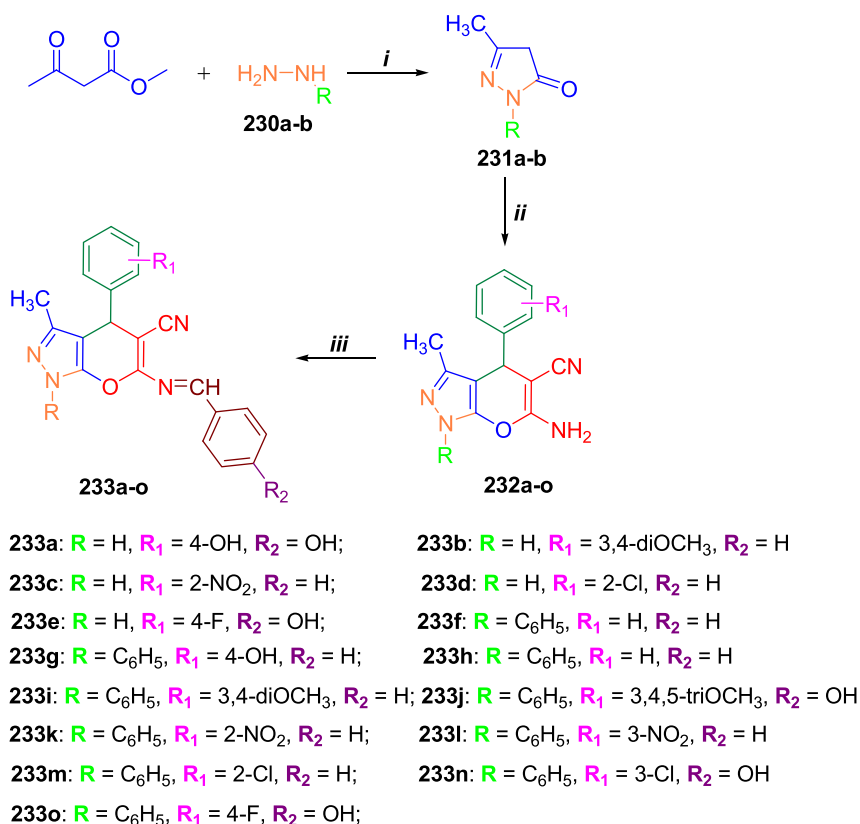


Figure 25. Structure of most promising CDK2 inhibitor.



Scheme 48. Design and synthesis of the target compounds **233a-o** [32]; **Reagents and conditions:** *i*) stirring at room temperature *ii*) substituted aromatic aldehydes, malononitrile, piperidine, 2 h *iii*) substituted aromatic aldehydes, EtOH, AcOH, 3 h, Reflux.

pyridazine diamine **238**. The huge diminished activity has been observed for the diester derivative **239** and the effects are continued to the pyrazole pyridazinone derivative **240**.

In one more series of derivatives, cyclic anhydride formation (**241**) possessed decent activity although its activity is less than that of dicarboxylic acid **234**; further, decrement in the activity is observed for derivatives (**242a** and **242b**) wherein primary amine is inserted into cyclic anhydride.

In spite of the large IC₅₀ values of the evaluated derivatives in the AChE inhibitory investigation, comparatively the compounds are reported to be better inhibitors than tacrine. Amongst these compounds, derivative **239** (IC₅₀ = 60.26 μM) stood atop in the inhibition activity with 2.76-fold higher inhibitory effect than tacrine. The diester derivative **237** (IC₅₀ = 64.04 μM) has exhibited almost similar inhibitory potential compared to compound **239**. Further, dicarboxylic acid **234**, pyridazinone analog **240**, pyrazole derivatized with fused cyclic imide **242b** have displayed slightly reduced inhibitory activity.

4.1. Pyrazole linked-benzothiazole-β-naphthol derivatives

Topoisomerases are enzymes responsible for the process of DNA replication. As the DNA is most essential for highly proliferative cells, inhibition of topoisomerase leads to cell apoptosis. Hence topoisomerases are effective chemotherapeutic candidates for corresponding drug discovery. In addition, topoisomerase I functions the process of cleavage and stitching back the single strands of double-stranded DNA. Pyrazole derivatives are demonstrated to possess DNA binding ability and anticancer properties. In addition to this, remarkable anticancer activity and DNA binding ability of benzothiazoles and potent cytotoxicity of β-naphthol scaffolds towards breast cancer have prompted to design benzothiazole-β-naphthol derivatives linked to pyrazoles [34].

In a multi-component reaction, pyrazole-3-aldehydes **243**, substituted benzothiazole-2-amines **244** and β-naphthol are reacted to bestow final compounds **245a-ad** (Scheme 50).

Employing circular dichroism (CD) the conformational changes in DNA with derivatives is studied; wherein the CD spectrum of the calf

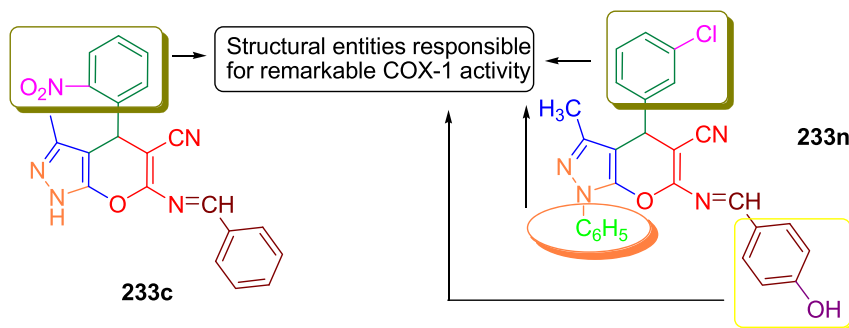
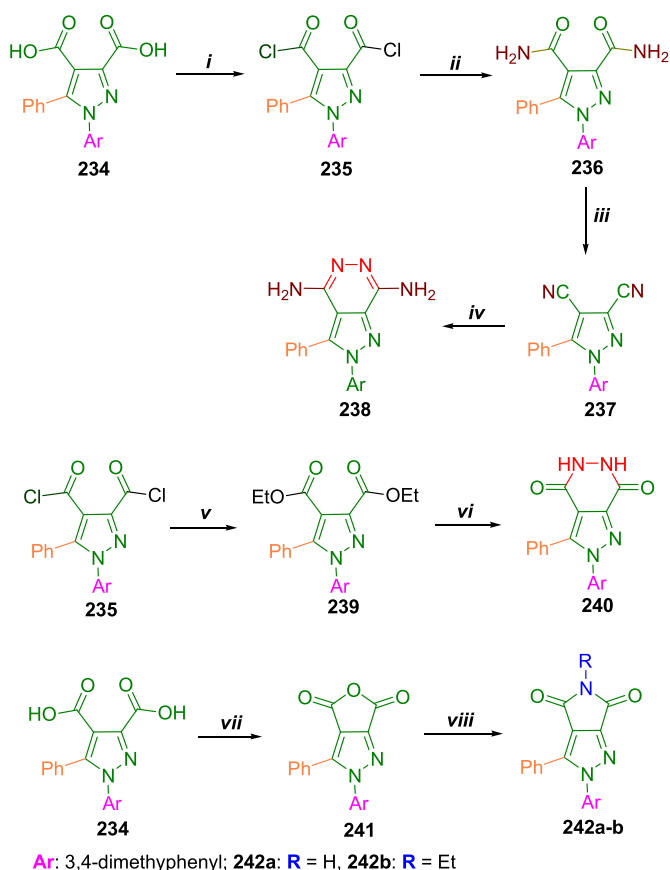


Figure 26. Illustration of structures of molecules with remarkable COX-1 inhibitory activity.



Scheme 49. Design and synthesis of fused pyrazole scaffolds [33]; **Reagents and conditions:** i) SOCl_2 , reflux (5h); ii) NH_3 , xylene, reflux (5h); iii) SOCl_2 +DMF, rt (10h); iv) NH_2NH_2 , reflux (5h); v) NH_2NH_2 , toluene, reflux (5h); vi) SOCl_2 +DMF, rt (12h); vii) R_1NH_2 , reflux (48h).

thymus DNA (CT-DNA) gives a positive band at 175 nm and a negative band at 245 nm due to π - π base stacking and right-hand helicity. In this study, the addition of compounds **245j**, **245k**, and **245l** (Figure 28) at a concentration of 10 μM of CT-DNA solution, a positive band is obtained at 275 nm which indicates slight hypochromicity; this, in turn, is a positive indication of melting of the DNA-derivative complex. Further, the positive band at 275nm got reduced in its intensity on the increase of concentration of the derivatives, revealing that further unwinding of DNA on derivative interaction. In addition to this, negative band intensity is altered at 245 nm; it indicates the ability of the designed derivatives to bring the change in the DNA helix. The viscosity studies of the Ct-DNA-derivative complexes are carried out using Hoechst 33258. The addition of the compounds **245j**, **245k**, and **245l** a small amount of increment in the viscosity of DNA is observed and these facts infer that they possess groove binding capability to DNA.

The topoisomerase I inhibitory activity is carried out on synthesized derivatives considering Camptothecin as a reference compound. In this study also, the compounds **245j**, **245k**, and **245l** have excelled in an exhibition of the remarkable topoisomerase enzyme inhibitory. These derivatives have displayed topoisomerase I inhibitory activity at 100 μM concentration compared to camptothecin which has inhibited the corresponding enzyme at 150 μM . Hence these compounds have proved themselves as efficient topoisomerase I inhibitors and subsequently potential anticancer agents. The potent topoisomerase I inhibitor **245k** bears N_1 -phenyl 3-(4-fluorophenyl) pyrazole-4-yl moiety and β -naphtholyl and 2-amino-6-methoxy benzothiazole moieties appended to methane. Structural features of other two potent inhibitors **245j** and **245l** entail identical moieties except for 4-chlorophenyl and 4-fluorophenyl moieties at pyrazole 3-position respectively. These structural features have bestowed them with the striking topoisomerase I inhibitory activity.

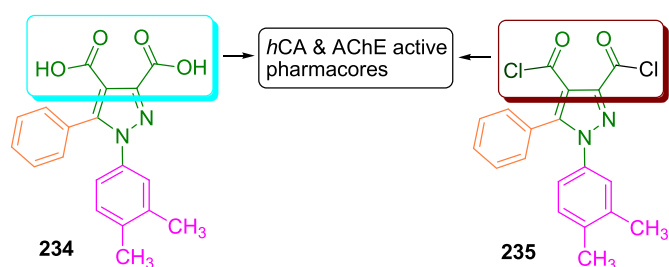


Figure 27. Illustration of structures of molecules possessing hCA and AChE inhibitory activities.

4.2. Pyrazoles and pyrazolo [3,4-*b*] pyridines

NSAIDs comprise a large pool of drugs including inflammatory drugs. However, many complications have been reported with the prescription of NSAIDs and this led to the design and discovery of non-selective COX inhibitors. COX-2 enzymes are predominantly released at sites of inflammation and COX-2 inhibitors are demonstrated to exert anti-inflammatory and analgesic effects. Pyrazole and pyrazolo-pyrimidine derivatives have been shown to possess multi-potent anti-inflammatory agents; encouraged by these scaffolds and to enhance the inhibitory properties, novel pyrazoles and pyrazolo [3,4-*b*] pyridines have been devised [35].

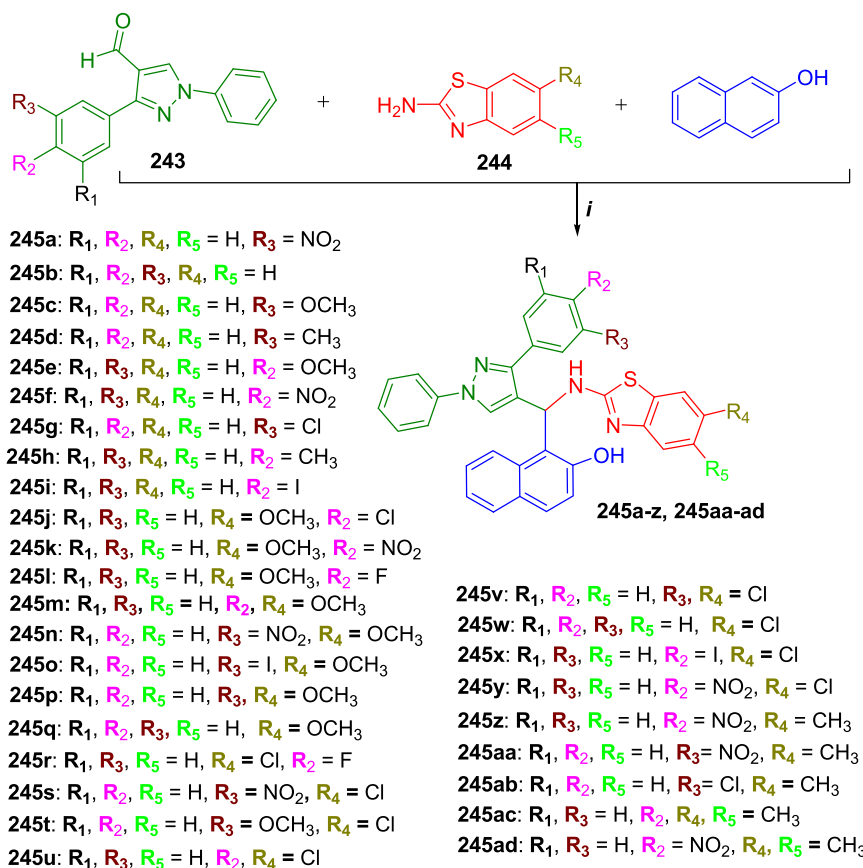
3-Aminopyrazole **246** is appended with 2-fluoroaniline via nucleophilic substitution to obtain an intermediate **247** which on coupling reaction with various substituted benzene diazonium chlorides has yielded pyrazolone-hydrazone **248a-f** (Scheme 51). These final compounds are utilized as starting material to design mannich products **249a-l** via mannich reaction with substituted anilines (Scheme 52).

The intermediate compound **247** is allowed to undergo a multi-component reaction with 4-substituted benzaldehydes and malononitrile in the presence of ammonium acetate rendering fused pyrazolo-pyridine derivatives **250a-f** (Scheme 53).

All the designed final derivatives have been evaluated for COX-I and COX-2 inhibitory properties in the presence of standard COX inhibitors celecoxib, diclofenac sodium, and indomethacin. No single evaluated derivative has enough COX-I potency ($\text{IC}_{50} = 4.9$ – $13.2 \mu\text{M}$) to reach an inhibitory value of indomethacin ($\text{IC}_{50} = 0.041 \mu\text{M}$). Compounds such as **248d** ($\text{IC}_{50} = 4.9 \mu\text{M}$), **250a** ($\text{IC}_{50} = 5.1 \mu\text{M}$), and **250f** ($\text{IC}_{50} = 4.9 \mu\text{M}$) have displayed COX-I activity almost similar to that of diclofenac sodium ($\text{IC}_{50} = 3.8 \mu\text{M}$). However, all the tested compounds could exert stronger inhibitory potentials compared to that of celecoxib ($\text{IC}_{50} = 15.1 \mu\text{M}$). On keen observation of inhibitory values of the compounds of three series, the compounds of **248a-f** and **250a-f** have exhibited stronger potentials compared to derivatives of **249a-l** series. In the derivatives of **249a-l**, the pyrazole NH is utilized for the design of mannich products with subsequent reduction of pyrazole basicity. Whereas in other series, **248a-f** and **250a-f**, the pyrazole NH is free that might be essential for apt fit into the active site of COX-I enzyme and hence these derivatives are the selective COX-I inhibitors.

In the case of COX-2 inhibitory effects, a collection of potent inhibitors are noticed ($\text{IC}_{50} = 0.046$ – $0.055 \mu\text{M}$) (Table 11); wherein the IC_{50} values are almost identical with that of standard COX-2 inhibitor ($\text{IC}_{50} = 0.049 \mu\text{M}$). All tested derivatives have exhibited remarkable inhibitory values ($\text{IC}_{50} = 0.046$ – $0.34 \mu\text{M}$). Contrary effects are noticed in the case of COX-2 inhibitory properties.

The strongest inhibitory properties are exerted by mannich derivatives **249a-l**. Although a good account of COX-2 inhibitory properties has been observed for all the synthesized derivatives, comparatively the derivatives of the series **249a-l** have elicited excellent inhibitory properties. The results infer that the mannich products of pyrazolones have COX-2 selectivity. It also indicates that N_1 -substituted pyrazoles and particular N -mannich bases of pyrazoles have essential pharmacophores. Amongst the potent inhibitors, compound **249j** (Figure 29) possessing 3-



Scheme 50. Synthetic route for the design of preparation of compounds 245aa-ad [34]; Reagents and conditions: i) Methanol, 2-naphthol, 2-aminobenzothiazole reflux (5h).

fluoroaniline, 4-bromophenylhydrazone moiety at 3, 4-positions respectively in addition to *N*-methylene 2,6-dimethylaniline at *N*₁-position has excelled in exhibiting most significant activity which is higher activity compared to celecoxib. Similarly, almost identical inhibitory effects are noticed for the compound **248b** (Figure 29) wherein 4-bromophenylhydrazone motif and *N*-methylene aniline are appended to pyrazole at 4- and *N*₁-positions respectively. Only slight increment/decrement is observed on the variation of substituents on phenyl of phenylhydrazone and *N*-methylene aniline. Irrespective of the substituents on these phenyl rings, all mannich derivatives possessed remarkable COX-2 inhibitory properties.

4.3. Pyrazoles-containing thiophene, thienopyrimidine, and thienotriazolopyrimidine

Inflammation is a common symptom in most of the pathological diseases. COX-2 enzyme plays a prominent role in the mediation of inflammation through prostaglandins, thromboxanes, and leukotrienes.

It is more fruitful to inhibit the COX-2 enzyme without interfering with COX-1 activity. Pyrazoles and pyrazolines are the most efficient choice of starting material to design potent anti-inflammatory agents. Inspired by the significant COX inhibitory of active thiophene-pyrazoles, design of pyrazoles incorporating thiophene, thienopyrimidine, and thienotriazolopyrimidine is accomplished [36].

The synthetic route involves the conversion of thiophene ester **251** to corresponding thiophene hydrazide **252** which is used as intermediate for the design of its derivatives. The thiophene hydrazide **252** is allowed to undergo intramolecular cyclization in the presence of diethyl ethoxymethylenemalonate and acetylacetone to form corresponding thiophene-pyrazole analogs **253** and **255** respectively. In another way, thiophene hydrazide is condensed with ethyl ethoxymethylenecyanoacetate and pyrazole carbaldehydes to yield compounds **254** and **256a-c** (Scheme 54).

Fused thiophene-pyrimidine chloride **257** is transformed into analogous hydrazide **258** which is considered as an intermediate for further synthesis of derivatives. The -NH-NH₂ fragment of compound **258** is utilized in the intermolecular cyclization with ethoxymethylene

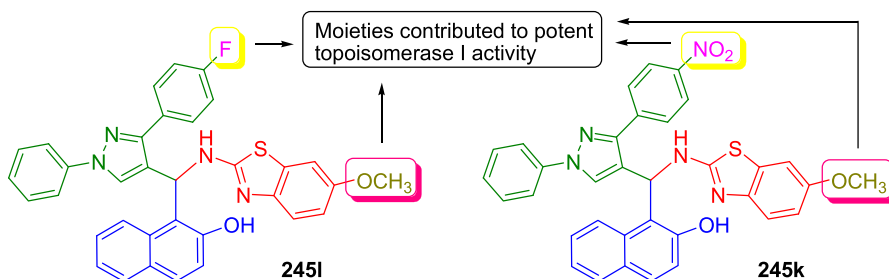
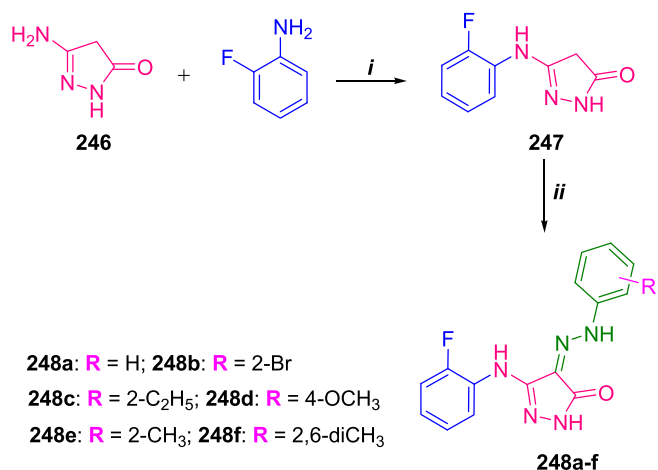


Figure 28. Demonstration of significant topoisomerase I inhibitors.



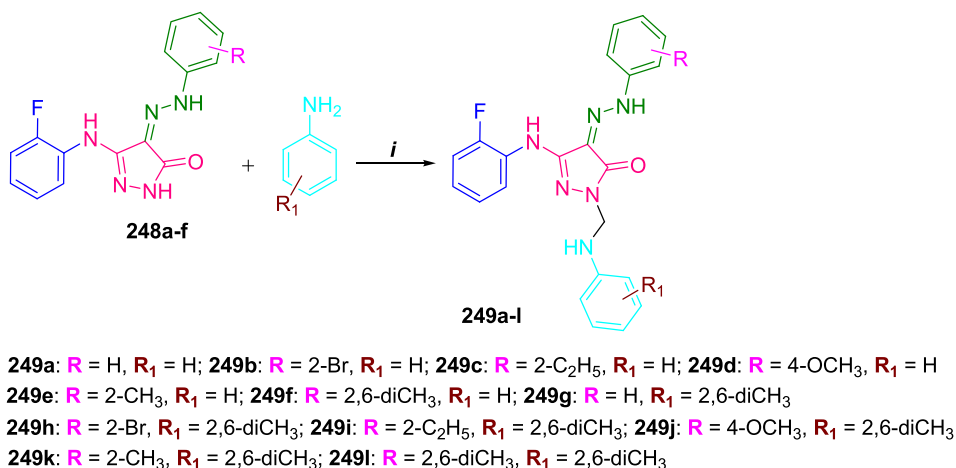
Scheme 51. Synthesis of final compounds **248a-f** [35]; **Conditions and reagents:** *i*) HCl/H₂O, reflux (3h); *ii*) substituted benzene diazonium chlorides, EtOH, CH₃COONa.

malononitrile and ethyl ethoxymethylene cyanoacetate producing fused thiophene-pyrimidine pyrazoles **259** and **260** respectively. Likewise, treatment of the intermediate **258** with diethyl ethoxymethylene malonate and acetylacetone has resulted in the formation of compounds **261** and **262** respectively. Condensation of compound **258** with pyrazole aldehyde **263** has produced corresponding hydrazone derivative **264** which on intramolecular cyclization rendered compound **265** (Scheme 55).

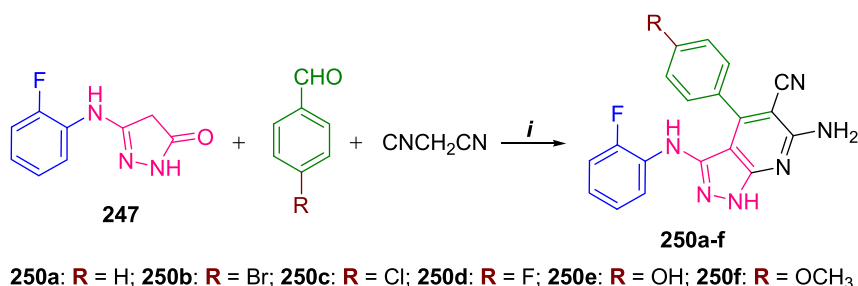
In the COX inhibitory activity investigation of the designed derivatives, good inhibitory activity is obtained towards the COX-1 enzyme;

and all the evaluated molecules have exhibited stronger inhibitory potentials (IC₅₀ = 7.52–11.91 μM) compared to celecoxib (IC₅₀ = 14.70 μM). Comparatively, compound **253** (IC₅₀ = 7.52 μM) and **262** (IC₅₀ = 7.53 μM) are noteworthy derivatives to be mentioned. However, no single derivative evaluated has enough inhibitory potency that could be compared with standard COX inhibitor indomethacin (IC₅₀ = 0.10 μM). Regarding COX-2 inhibitory effects, a set of molecules (Table 12) has produced IC₅₀ values of high impact. Amongst them, compound **264** (Figure 30) has bestowed with the strongest inhibitory value which is almost comparable to that of celecoxib (IC₅₀ = 0.048 μM).

Compound **253** has exhibited the most significant COX-1 inhibitory activity wherein its structural features comprise 3-amino-4-phenylthio-5-hydroxypyrazole and 4-carbomethoxy-5-hydroxypyrazole connected via the carbonyl group. Besides this, most of the derivatives (except for a few) have displayed almost similar COX-I inhibitory properties irrespective of their structural differences. Regarding COX-2 activity, compound **264** possessing 7-phenylthienopyrimidine moiety appended to N₁-phenyl-3-(4-chlorophenyl) pyrazole at 4-position through methylene-hydrazine fragment has elicited promising activity. Unfortunately, cyclization (compound **265**) carried out in order to check the further improvement of the activity is in vain. This fact shows that methylene-hydrazine fragment is essential for potent activity. It is also evident from the striking COX-2 inhibitory activity of **256c** (Table 12) bearing methylene-hydrazine fragment. However similar analogy could not hold good for the compound **254** probably attributed to the presence of electron-withdrawing –CN and –COOEt groups at the methylene-hydrazine fragment end. Triplet of derivatives **259–261** has exhibited decent activity wherein these derivatives possessed 3,4-substituted pyrazole at thienopyrimidine 4-position. Particularly compound **260** (Figure 30) having carbomethoxy moiety and –NH₂ at 3- and 4-positions of pyrazole has shown nice activity. While the compounds **259** and **261** in which carbomethoxy and –NH₂ groups are substituted by –CN and –OH moieties respectively resulted in lowered inhibitory activity compared to compound **260**. The



Scheme 52. Synthetic route for the preparation of the molecules **249a-l** [35]; **Reagents and conditions:** *i*) HCHO/EtOH, stirring, 60 °C (6h).



Scheme 53. Design and synthesis of the pyrazole derivatives **250a-f** [35]; **Reagents and conditions:** *i*) CH₃COONH₄, EtOH, reflux (15h).

Table 11. Inhibitory values of potent COX-2 inhibitors.

Compd	COX-2 inhibitory activity	
	IC ₅₀ (μM)	
249b	0.048	
249c	0.055	
249d	0.051	
249j	0.046	
249l	0.054	
Celecoxib	0.046	

observation reveals the essence of the carbethoxy and -NH₂ groups at pyrazole 3- and 4-positions.

4.4. Pyrazoline benzene sulfonamides

The membrane-bound enzyme, acetylcholinesterase found in many types of tissues is responsible for the termination of cholinergic signaling wherein the enzyme acetylcholinesterase hydrolyzes acetylcholine. This

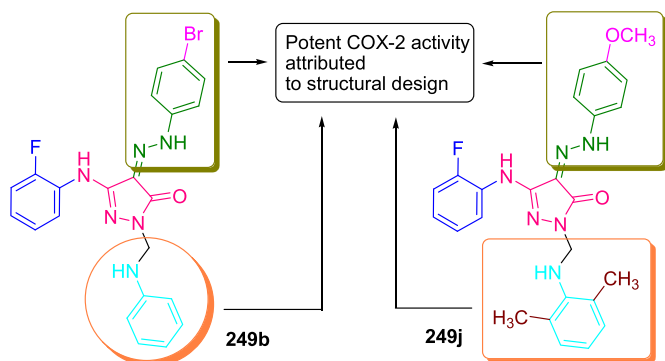
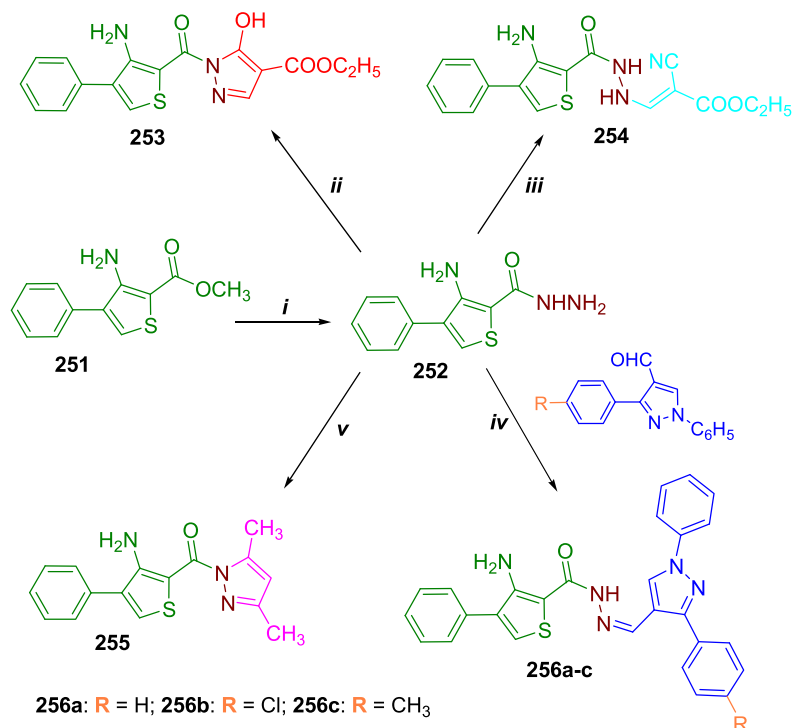


Figure 29. Demonstration of structures of excellent COX-2 inhibitors.

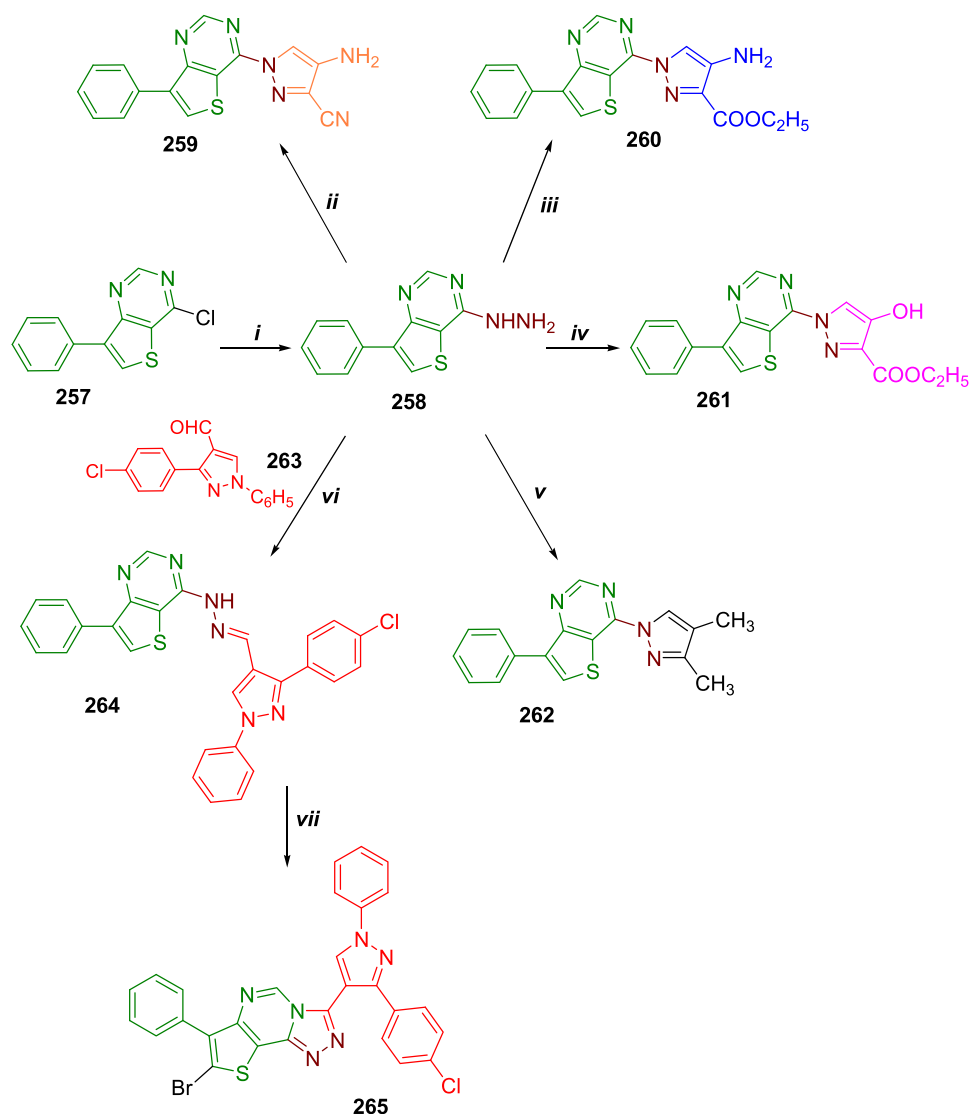


Scheme 54. Preparation of pyrazole-thiophene derivatives [36]; **Reagents and conditions:** *i*) NH₂NH₂·H₂O, EtOH, reflux (5h); *ii*) EtOCH=C(COOEt)₂, Anhyd.K₂CO₃, EtOH, reflux (6h); *iii*) EtOCH=C(CN)COOEt, Anhyd.K₂CO₃, EtOH, reflux (6h); *iv*) EtOH, reflux (12h); *v*) CH₃COCH₂COCH₃, EtOH, reflux (10h).

subsequently leads to AD and inhibition of a particular enzyme would be an effective approach for the cure of AD. Celecoxib possessing pyrazoline and sulfonamide has been demonstrated to have stimulatory effects on brain AChE levels and β-amyloid peptide in addition to COX-2 inhibitory properties. Alongside, pyrazole, pyrazoline, and sulfonamide derivatives have exhibited carbonic anhydrase and AChE inhibitory properties. In light of these observations, a research team has aimed at a new series of pyrazolines derivatized with benzene sulfonamides [37].

The synthetic pathway involves condensation of 4-substituted acetophenones **266** with trisubstituted benzaldehydes **267** to obtain corresponding chalcones **268a-h**. An α, β-unsaturated fragment in chalcones **268a-h** is utilized in the intermolecular cyclization producing dihydropyrazole-sulfonamide derivatives **269a-h** (Scheme 56).

All the final compounds are tested for hCA I, hCA II and AChE inhibitory properties using acetazolamide and tacrine as the reference compounds for CA and AChE enzymes respectively. In case of hCA I and hCA II, all the evaluated molecules displayed decent inhibitory activity (hCA I: IC₅₀ = 0.0347–0.0769 μM, hCA II: IC₅₀ = 0.0301–0.491 μM) which are better than that of AAZ (hCA I: IC₅₀ = 0.169 μM, hCA II: IC₅₀ = 0.149 μM). In particular compound **269d** (IC₅₀ = 0.0347 μM) has exhibited the most significant hCA I inhibitory activity. Except for compound **269e** (IC₅₀ = 0.0769 μM) (Figure 31), other derivatives have almost similar hCA I inhibitory properties. While compound **269a** (Figure 31) stood atop of the hCA II inhibitors with IC₅₀ value 0.0301 μM. Analogous to hCA I inhibitors, all the evaluated molecules have shown almost similar IC₅₀ values towards hCA II. Observation of the hCA I and hCA II inhibitory properties infer selective inhibition. Except for compound **269e**, all other derivatives have selectivity towards only one CA type. Alongside, in general, with some exceptions, the compounds with the 2,4-dimethoxy phenyl ring attached to dihydropyrazole 5-position have excelled in hCA II inhibitory potencies. In that, compound **269a** possessing phenyl ring connected to dihydropyrazole 3-position bestowed the strongest activity. However, the substitution of phenyl ring at dihydropyrazole 3-position with 4-fluorobenzene/4-chlorobenzene rings has diminished the activity gradually. Whereas



Scheme 55. Synthesis of fused thiophene-pyrimidine incorporated pyrazole derivatives [36]; **Reagents and conditions:** *i*) $\text{NH}_2\text{NH}_2 \cdot \text{H}_2\text{O}$, reflux (1h); *ii*) $\text{EtOCH}=\text{C}(\text{CN})_2$, Anhyd. K_2CO_3 , EtOH, reflux (6h); *iii*) $\text{EtOCH}=\text{C}(\text{CN})\text{COOEt}$, Anhyd. K_2CO_3 , EtOH, reflux (6h); *iv*) $\text{EtOCH}=\text{C}(\text{COOEt})_2$, Anhyd. K_2CO_3 , EtOH, reflux (12h); *v*) $\text{CH}_3\text{COCH}_2\text{COCH}_3$, EtOH, reflux (10h); *vi*) EtOH, reflux (6h); *vii*) Anhyd. CH_3COONa , Br_2 in AcOH, stir (overnight).

dihydropyrazole analogs with 3,4-dimethoxy phenyl moiety at 5-position have led to potential *hCA* I inhibitors.

Further, the AChE inhibitory activity ($\text{IC}_{50} = 0.082\text{--}0.233 \mu\text{M}$) of the final compounds indicates that every tested molecule is an efficient inhibitor compared to tacrine ($\text{IC}_{50} = 0.698 \mu\text{M}$). However, the compounds **269b** ($\text{IC}_{50} = 0.0822 \mu\text{M}$) and **269d** ($\text{IC}_{50} = 0.086 \mu\text{M}$) possessed most remarkable AChE inhibitory activities. When the inhibitory values of *hCA* I, *hCA* II and AChE are checked and correlated, an interesting observation is made wherein there is direct synchronization of *hCA* I, and AChE inhibitory values for compounds **269a-e**. These may suggest that a potent *hCA* I inhibitor may be also a potent AChE inhibitor.

4.5. Pyrazolopyrimidine scaffolds

The cyclooxygenases are mediators of inflammation many times. The drugs for reduction of the risks that arise with the usage of NSAIDs to cure inflammatory-related diseases are being designed and discovered. Besides this, selective COX-2 inhibitors have been developed to reduce adverse effects. The pyrazole scaffolds possessing fused pyrazolopyrimidine core are described as potent anti-inflammatory agents alongside possessing other prominent pharmacological properties. In this regard,

pyrazolopyrimidine scaffolds are synthesized to check the improvement in COX inhibitory properties [38].

Synthetic pathway commences from compound **270** wherein dinitrile ethylene **270** is allowed to undergo intermolecular cyclization with phenylhydrazine or its 4-methylsulfonyl derivative to form pyrazole derivatives **271a-b** which are transformed into fused pyrazolopyrimidinone scaffolds using formic acid to yield **272a-b**. Fused pyrimidinones **272a-b** are transformed into fused pyrazolochloropyrimidines **273a-b** followed by nucleophilic substitution of $-\text{Cl}$ with α -aminoester yielding compounds **274a-b**. Hydrolysis of the ester functionality with hydrazine produced corresponding hydrazides **275a-b** (Scheme 57). Hydrazides of fused pyrazole-pyrimidines **275a-b** are used intermediates to design condensed products **276a-f** with various aldehydes. The intermolecular cyclization of compounds **275a-f** with ethyl isothiocyanate produced pyrazole-pyrimidines-linked triazole thiol **277a-b**. α -Amino hydrazide fragment is utilized in which it is cyclized with appropriate phenyl or 4-substituted phenyl isothiocyanate to obtain corresponding triazole analogs **278a-f** (Scheme 58).

The intermediates **275a-b** are cyclized with CS_2 to obtain oxadiazoles linked to fused pyrazole-pyrimidine derivatives **279a-b**. While cyclization of intermediates **275a-b** with ethyl acetoacetate resulted in fused

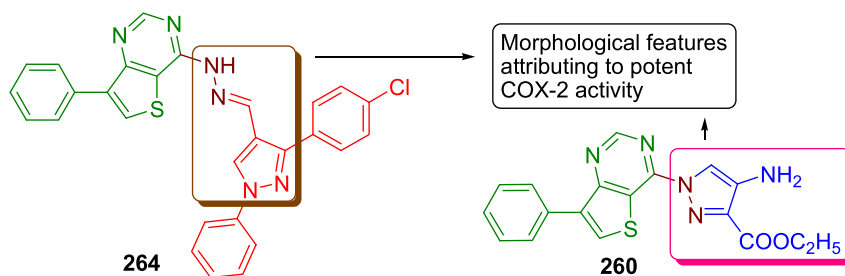
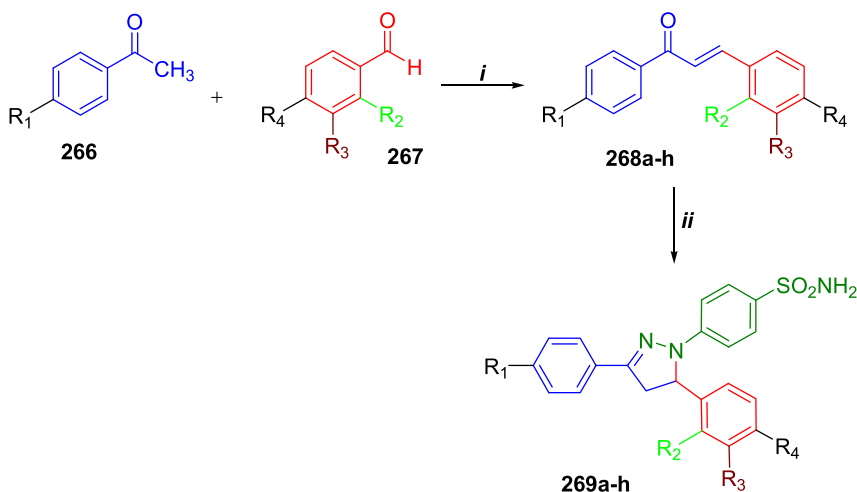
Table 12. Inhibitory values of potent COX-2 inhibitory values.

Compd	COX-2 inhibitory activity	
	IC ₅₀ (μM)	
256c	0.071	
259	0.063	
260	0.059	
261	0.098	
Celecoxib	0.045	

pyrazole-pyrimidines linked to pyrazole **280a-b** (Scheme 59). The expected regioisomers **281** and **282** are not formed. Except for a few derivatives, all the compounds have inhibitory activities with small differences. In structure-activity studies, it is evident that the hydrazone analogs **276a-f** (except for compound **276a**) are reported to possess comparatively weak COX-1 activity indicating that the hydrazone fragment is not favorable for potent activity.

Using standard COX inhibitors celecoxib, diclofenac disodium and indomethacin, COX-1 and COX-2 inhibitory properties are evaluated. Although COX-I inhibitory properties of final compounds (IC₅₀ = 5.28–13.11 μM) are poor compared to indomethacin (IC₅₀ = 0.041 μM); compared to celecoxib (IC₅₀ = 8.1 μM) and diclofenac sodium (IC₅₀ = 3.8 μM) potent activities have been exhibited by the target molecules. The most significant COX-I inhibitory activity (IC₅₀ = 5.28 μM) is displayed

by the compound **278e**. Meanwhile, in the case of triazole thiol analogs, compound **277a** (IC₅₀ = 7.35 μM) rendered significant activity; its methylsulfonyl analog exhibited diminished inhibitory property. When it comes to **278a-f** series of compounds, all the derivatives (except for compound **278a**) have shown decent COX-I inhibitory properties. In these compounds, the presence of triazole thiol *N*₁-(4-aryl) substituted moiety or methylsulfonyl motif must be crucial. Particularly, compound **278e** possessing 4-fluorophenyl ring at triazole thiol *N*₁-position and 4-methylsulfonylphenyl ring on fused pyrazole-pyrimidine moiety is most remarkable among evaluated molecules. Fortunately, potential IC₅₀ values are observed towards COX-2 activity. All the tested compounds have exerted noteworthy inhibitory properties which are higher than that of diclofenac sodium (IC₅₀ = 0.84 μM) and indomethacin (IC₅₀ = 0.51 μM). However, the inhibitory values are weak compared to standard inhibitor celecoxib (IC₅₀ = 0.049 μM). In these, **276a-f** series compounds (except for compound **276a**) have excelled in the COX-2 inhibitory activity (Table 13). Compounds of other series possessed more or less similar potencies. The aromatic hydrazone analogs of the series **276a-f** have exhibited excellent COX-2 inhibitory activity which might be attributed to hydrazone fragment as well as the methylsulfonyl moiety. Particularly these compounds with methylsulfonyl moiety have resulted in a well-established activity. Besides this series, the triazole thiol analog **278a** bearing phenyl ring at triazole *N*₁-position possessed identical inhibitory activity compared to the **276a-f** series. However, the substitution of 4-fluorophenyl/4-chlorophenyl or presence of methylsulfonyl

**Figure 30.** Structures of remarkable COX-2 inhibitors.

269a: R₁, R₃ = H, R₂, R₄ = OCH₃; **269b:** R₁, R₂ = H, R₃, R₄ = OCH₃

269c: R₁ = F, R₃ = H, R₂, R₄ = OCH₃; **269d:** R₁ = F, R₂ = H, R₃, R₄ = OCH₃

269e: R₁ = Cl, R₃ = H, R₂, R₄ = OCH₃; **269f:** R₁ = Cl, R₂ = H, R₃, R₄ = OCH₃

269g: R₁ = Br, R₃ = H, R₂, R₄ = OCH₃; **269h:** R₁ = Br, R₂ = H, R₃, R₄ = OCH₃

Scheme 56. Synthesis of dihydropyrazole-benzenesulfonamide derivatives [37]; **Reagents and conditions:** *i*) EtOH, aq. NaOH (20%), rt. *ii*) *p*-hydrazinobenzene sulfonamide hydrochloride, EtOH, glacial acetic acid, reflux (4–19h).

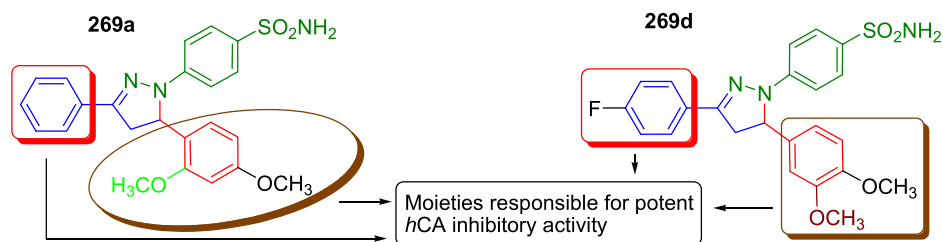


Figure 31. Structures of remarkable hCA inhibitors.

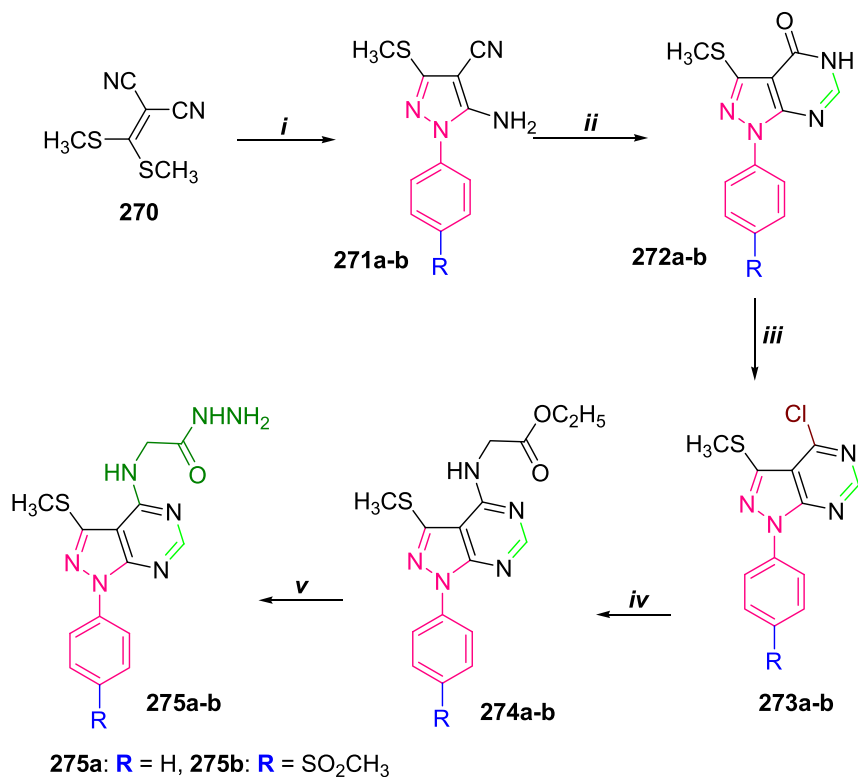
moiety at N_1 -position of the fused pyrazole-pyrimidine scaffold has diminished the activity to a greater extent. Along with these, compound **280a** has managed to exhibit the strongest inhibitory activity which might be attributed to the pyrazole ring linked to pyrimidine moiety in addition to 4-sulfonyl-methyl phenyl ring at fused pyrazole-pyrimidine N_1 -position. In general consensus, the evaluated derivatives are selective inhibitors.

4.6. Pyrazolyl pyrimidinetriones and thioxopyrimidinediones

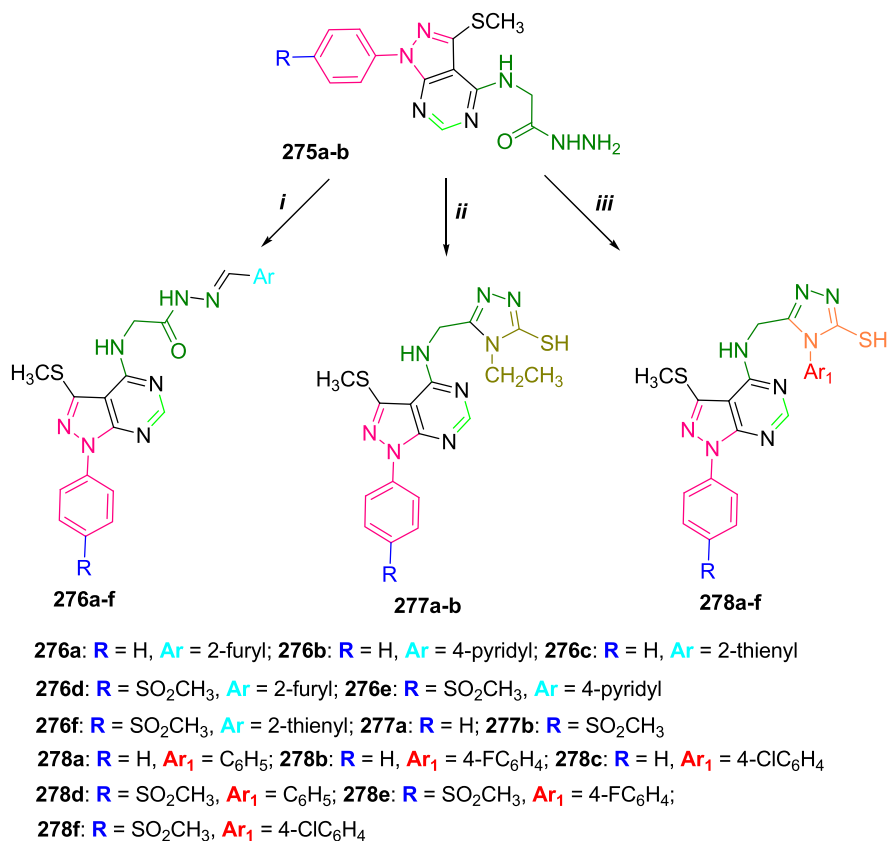
Ecto-nucleotidases perform P2 purinergic signaling in addition to maintaining cell function. Cell activation, apoptosis, proliferation, and degenerative neurological and immunological responses are some of the disorders attributed to the overexpression of the ectonucleotidases. Hence to address such problems, the design of ectonucleotidase inhibitors is achieved. Ecto-nucleotide pyrophosphatases/phosphodiesterases (NPPs) entail seven various subtypes (NPP1-7). Among these, NPP-1 and NPP-3 perform the hydrolysis of pyrophosphatases and phosphodiester in various nucleotides. NPP-3 are associated with a number of physiological functions such as nucleotide recycling, stimulating cell motility and modulation of purinergic receptor signaling. Particularly NPP1 performs

the biological processes including insulin receptor signaling, bone mineralization, and immune modulation; however overexpression of the enzyme NPP1 results in the ectopic calcification, calcium pyrophosphate dehydrate crystal deposition and cancer cell proliferation. While the NPP3 is reported as tumor marker since its overexpression led to carcinogenesis and cancer cell metastasis. Alkaline phosphatases catalyze the dephosphorylation of nucleotide phosphates and phosphomonoesters. In the alkaline phosphatase family of enzymes, tissue-nonspecific alkaline phosphatases (TNAP) are an important type of enzymes. Overexpression of human alkaline phosphatases in cancer cells, Paget's disease, and osteoblastic bone metastasis. Pyrazole pharmacore has been in limelight because of its versatile pharmacology alongside ectonucleotidase inhibitory properties. To address all these problems of alkaline phosphatases and nucleotide pyrophosphatases, novel pyrazolyl pyrimidinetriones and thioxopyrimidinediones are designed and synthesized [39].

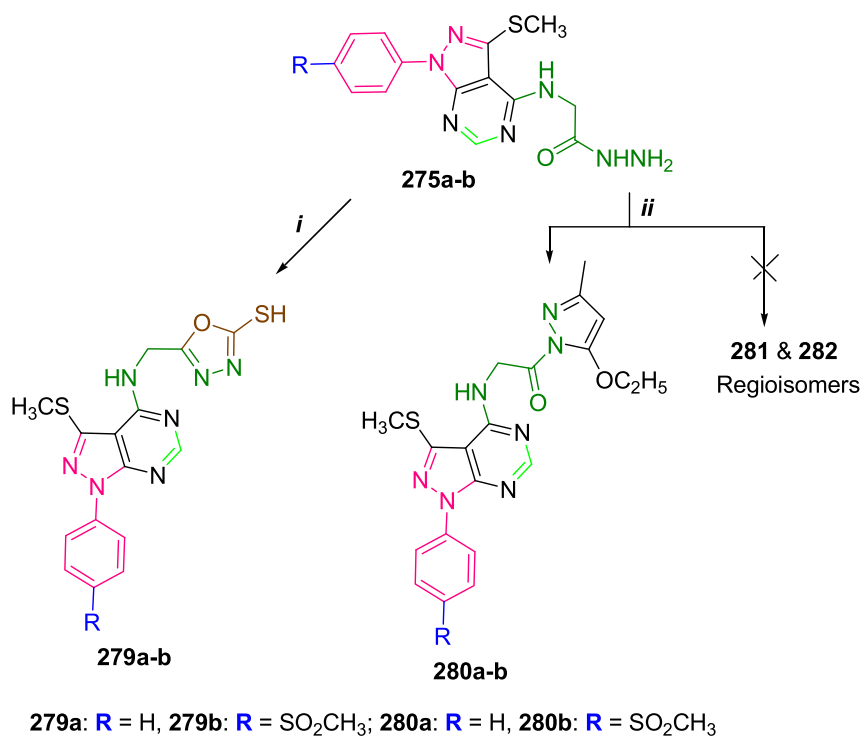
The synthetic route involves condensation of phenylhydrazine with 4-substituted acetophenones **281a-g** giving corresponding hydrazones **282a-g**. Cyclization of the hydrazone fragment using formylating mixture yielded pyrazole derivatives **283a-g** followed by condensation with pyrimidine triones/thiopyrimidine dioxanes resulted in final compounds **284a-n** (Scheme 60).



Scheme 57. Synthetic pathway for preparation of compounds **275a-b** [38]; Reagents and reaction conditions: *i*) phenylhydrazine hydrochloric (R = H) and *p*-methane sulfonyl hydrochloride (R = SO₂CH₃), sodium acetate, 95% ethanol, reflux (5h); *ii*) formic acid (85%), reflux (10h); *iii*) POCl₃, DMF, reflux (4h); *iv*) glycine ethyl ester hydrochloride, TEA, absolute ethanol, reflux (5–6h); *v*) hydrazine hydrate, EtOH, reflux (10h).



Scheme 58. Synthesis of the pyrazolo-pyrimidine derivatives [38]; **Reagents and conditions:** i) appropriate aldehyde, absolute EtOH, gl. Acetic acid, reflux (4h); ii) ethyl isothiocyanate, absolute ethanol, TEA, reflux (3h); iii) appropriate phenyl or 4-substituted phenyl isothiocyanate, absolute ethanol, TEA, reflux (3h).



Scheme 59. Preparation of target molecules 279a, b and 280a, b [38]; **Reagents and conditions:** i) CS₂, KOH, absolute ethanol, reflux (3h); ii) ethyl acetoacetate, absolute ethanol, reflux (10h).

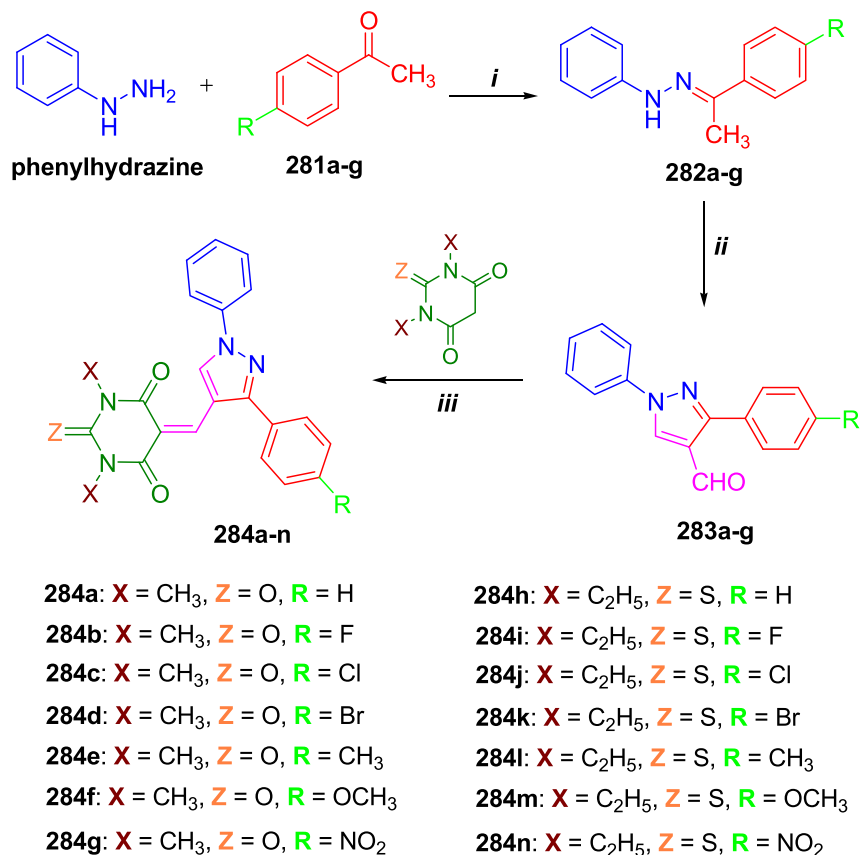
Table 13. COX-2 inhibitory values of most potent inhibitors.

Compd	COX-2 inhibitory activity	
	IC ₅₀ (μM)	
276b	0.19	
276c	0.11	
276d	0.10	
276e	0.12	
276f	0.10	
278a	0.10	
280a	0.10	

The designed derivatives are investigated for their alkaline phosphatases and nucleotide phosphatase inhibitory properties using sumarin, levamisole and L-phenylalanine as reference compounds (Table 14). Almost half of the synthesized molecules could exhibit strong inhibitory values compared to corresponding standard inhibitors. Among the potent *h*-TNAP inhibitors, compound **284a** in which *N*₁, *N*₃-dimethyl-2,4,6-pyrimidinetrione is tethered to pyrazole 4-position via methylene group alongside phenyl ring at pyrazole 3-position is found to possess most significant IC₅₀ value; while the compound **284n** possessing 4-nitrophenyl ring and *N*₁, *N*₃-diethyl-2-thioxo-4,6-pyrimidinetrione at 3- and 4-positions of pyrazole stands next to it in exhibition of *h*-TNAP inhibitory activity. Compound **284a** has shown 61 times greater inhibitory potential than that of levamisole. In the case of *N*₁, *N*₃-dimethyl-2,4,6-pyrimidinetrione analogs, compounds with a 4-bulky group (irrespective of electron environment) substituted phenyl ring at pyrazole 3-position have failed to exhibit good inhibitory values. Meanwhile, the activity could not be correlated with the *N*₁, *N*₃-diethyl-2-thioxo-4,6-

pyrimidinetrione derivatives. Surprising facts are observed in the case of *h*-IAP inhibitory activities. All the potent *h*-IAP inhibitors are *h*-TNAP inactive revealing that the synthesized molecules are selective inhibitors. The most potent inhibitor **284d** comprises *N*₁, *N*₃-dimethyl-2,4,6-pyrimidinetrione connected to pyrazole 4-position and 4-bromophenyl ring at 3-position of pyrazole; it is ~ 175 fold higher activity compared to the standard inhibitor. The results described in this way; the presence of pyrimidinetrione and 4-bulky electron-withdrawing group substituted phenyl ring is a must for remarkable *h*-IAP inhibitory activity.

Regarding *h*-NPP1 activity, some compounds have rendered promising activity; amongst them, compound **284b** (Figure 32) has bestowed with most striking inhibitory activity. Its significant activity is attributed to the *N*₁, *N*₃-dimethyl-2,4,6-pyrimidinetrione connected to pyrazole 4-position and 4-bromophenyl ring at 3-position of pyrazole possessing 175-fold higher activity compared to the standard inhibitor. Compound **284d** is found to exhibit *h*-IAP and *h*-NPP1 dual inhibitory potential. Further, *N*₁, *N*₃-diethyl-2-thioxo-4,6-pyrimidinetrione derivative **284j** having 4-chlorophenyl moiety at pyrazole 3-position has got its place in potential inhibitors list. Regarding inhibitory properties towards *h*-NPP3, only two compounds **284b** and **284h** have exhibited higher inhibitory potentials compared to sumarin; compound **284h** entailing structural moieties phenyl ring and *N*₁, *N*₃-diethyl-2-thioxo-4,6-pyrimidinetrione elicited noteworthy inhibitory value; it is followed by compound **284b** with respect to potential inhibitory values. Thereby compound **284b** is considered as NPP1 and NPP3 dual inhibitor. Other derivatives have managed to show moderate to decent IC₅₀ values. Overall *N*₁, *N*₃-dimethyl-2,4,6-pyrimidinetrione analogs of pyrazole have excelled in eliciting higher alkaline phosphatase/nucleotide pyrophosphatase inhibitory potentials compared to *N*₁, *N*₃-diethyl-2-thioxo-4,6-pyrimidinetrione derivatives.



Scheme 60. Synthesis of the target molecules **284a-n** [39]; Reagents and conditions: *i*) AcOH, EtOH, 70 °C; *ii*) a. DMF, POCl₃, 0→70 °C (3h); b. aq NaOH/aq NaHCO₃; *iii*) DCM/MeOH (8:1), EDA (0.2 mmol), AcOH (2 mM).

Table 14. Depiction of alkaline phosphatase and nucleotide phosphatase inhibitory values of final compounds.

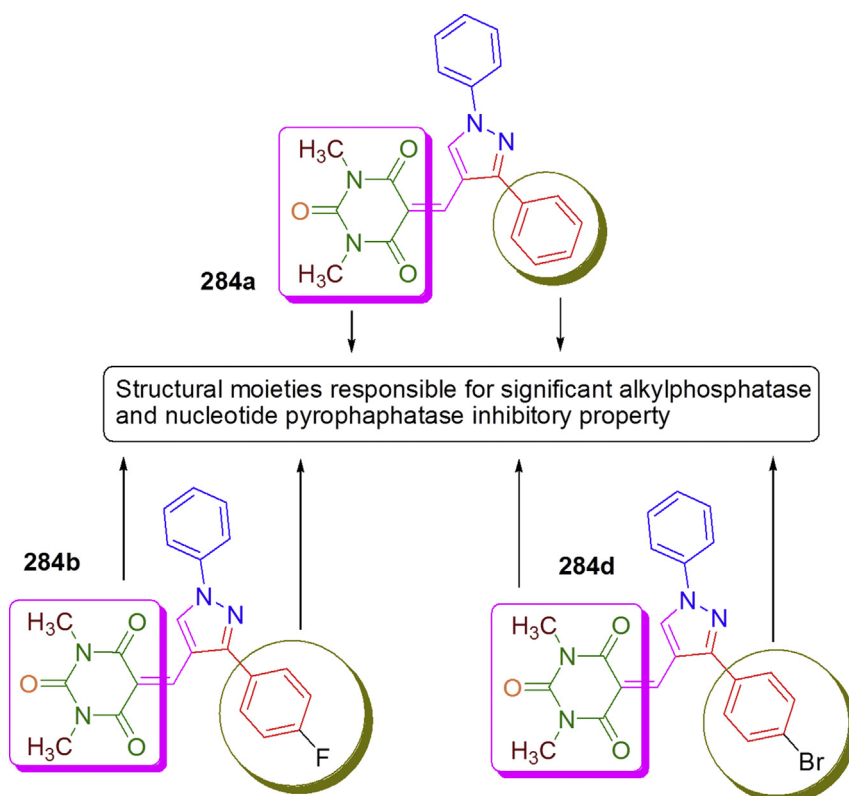
Comp	<i>h</i> -TNAP IC ₅₀ (μM)	<i>h</i> -IAP	<i>h</i> -NPP1	<i>h</i> -NPP3
284a	0.33	-	-	1.36
284b	2.21	-	0.61	0.66
284c	-	0.86	-	-
284d	-	0.57	1.21	2.27
284e	5.83	-	1.86	-
284f	-	-	-	-
284g	-	12.7	-	2.49
284h	2.99	-	4.61	0.57
284i	-	-	-	2.03
284j	-	33.6	1.01	-
284k	3.07	-	-	6.36
284l	5.26	6.33	-	4.55
284m	-	1.31	-	2.86
284n	1.78	21.2	-	2.11
Sumarin	-	-	8.67	1.27
Levamisole	20.2	-	-	-
L-Phenylalanine	-	100	-	-

4.7. Pyridinylimidazoles

Glycogen synthase kinase 3β (GSK3β) is an enzyme of synthase kinase enzyme family, associated with hyperphosphorylation tau protein and its overexpression has been led to increased production of β-amyloids. The p38α mitogen-activated protein (MAP) kinase plays a significant role in the biosynthesis of proinflammatory cytokines at translational and transcriptional levels. Overactivity of p38α MAP kinase is responsible for the tau protein hyperphosphorylation in addition to neuroinflammation. The research revealed that selective p38α MAP kinase inhibitors have

diminished tau phosphorylation. In this regard, pyridinyl imidazoles have been demonstrated as versatile pharmacores that target several kinases including p38α MAP kinases. Hence, in order to reduce the problems associated with the enzymes GSK3β and p38α MAP kinase, a pool of pyridinyl imidazoles are designed and synthesized [40].

In the synthetic pathway, Boc-protected 4-methyl-2-aminopyridine 285 is again protected by 4-methoxybenzyl moiety to form compound 286 which is treated with ethyl-4-fluorobenzoate to yield a carbonyl compound 287. Hydroxylamine moiety is introduced adjacent to the carbonyl group in compound 287 using sodium nitrite to render

**Figure 32.** Representation of structures of potent alkaline phosphatase/nucleotide pyrophosphatase inhibitors.

compound **288** followed by reduction of hydroxylamine functionality into corresponding ammonium salt **289**. α -Aminocarbonyl fragment of compound **289** is utilized for cyclization using potassium thiocyanate to produce imidazole-2-thione **290** with subsequent nucleophilic substitution with methyl chloride/benzyl chloride to obtain compounds **291a-b**. Finally, the removal of NH-Boc gave the molecules **292a-b** (Scheme 61).

Pyridine-carboxamide derivatives **294a-u** and **295a-e** are prepared from commercially available compounds **292a-b/293a-b** using the reagents mentioned in the Scheme 60. The alkyl thiol moiety is oxidized to thioxane analogs **296a-b** (Scheme 62).

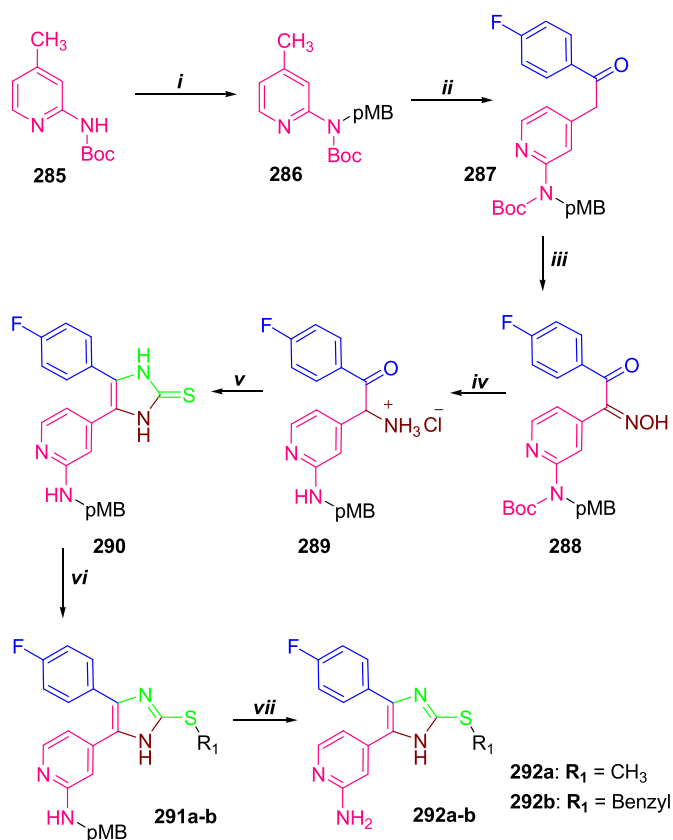
The commercially available compounds **297** is reacted with cyclopropanecarbonyl chloride to design pyridine-2-cyclopropylcarboxamide of imidazole thiol derivative **299**; likewise, compound **298** is coupled with cyclopropanecarboxamide producing carboxamide derivative **300** (Scheme 63).

The pyridine carbonyl intermediate **287** is oxidized at the adjacent position of the carbonyl group to produce diketo analog **301** from which removal of NH-Boc led to the formation of diketo derivative of pyridine-2-amine **302**. *N*-Cyclopropylcarboxamide derivative **303** and *N,N'*-dicyclopropyl carboxamide derivative **304** are obtained from diketone derivative **301** using cyclopropanecarbonyl chloride in which diketone pharmacore of compound **304** is utilized in the design of imidazole ring subsequently yielding final compounds **305a-g** (Scheme 64).

NH group protection of 2-methylimidazole **306** gave compound **307**; wherein tributyltin moiety is appended at imidazole 5-position to obtain compound **308**. *N*-(4-Bromopyridin-2-yl) cyclopropane carboxamide is coupled with 2-methylimidazole at 5-position followed by hydrolysis of 2-(trimethylsilyl) ethoxymethyl protection group bestowed target molecule **310** (Scheme 65).

All the synthesized molecules are evaluated for their GSK3 β and p38 α MAP kinase inhibitory activities using SB203580 (IC₅₀ = 0.041 μ M) and SB216763 (IC₅₀ = 0.089 μ M) as reference compounds for p38 α MAP kinase and GSK3 β respectively. In the first series of pyridineimidazole derivatives **294a-u**, an excellent account of p38 α MAP kinase inhibitors molecules is found to exhibit potent p38 α MAP kinase inhibitory activity. Amongst them **294e** (IC₅₀ = 0.013 μ M), **294k** (IC₅₀ = 0.015 μ M) and **294l** (IC₅₀ = 0.015 μ M) shown most remarkable inhibitory activity. Except for compound **294a**, all other derivatives displayed almost similar inhibitory potencies. This series of molecules comprise imidazole-2-thiomethane in addition to 4-fluorobenzene at imidazole 4-position and pyridine carboxamide at imidazole 5-position to which various moieties are attached. Compound **294e** (Figure 33) finds its place in this series as the most significant inhibitor wherein the structural significance includes 3,4,5-trimethoxy-methylenebenzene carboxamide. An increase in the alkyl chain length from methylene to ethylene (compound **294a**) resulted in a large extent of reduced activity (IC₅₀ = 0.088 μ M). Alongside, the removal of methoxy groups (compound **294f**) has led to diminished activity (IC₅₀ = 0.055 μ M). The carboxamides with cyclopropyl ring and cyclobutyl rings have possessed decent inhibitory activity. The derivatives of the sub-series **295a-e** which contain 2-benzylimidazole ring are only moderate inhibitors. However, compound **295e** possessing 4-fluoro-methylene benzene motif appended to carboxamide moiety is strongest p38 α MAP kinase inhibitory value (IC₅₀ = 0.003 μ M) among all the pyridineimidazole scaffolds which has 30-fold higher potency compared to reference compound and compound **295e** is found to be selective p38 α MAP kinase inhibitor. The series of compounds **305a-g**, pyridine-cyclopropyl carboxamides bearing 2-substituted imidazole rendered finest inhibitory activities which are almost similar with respect to IC₅₀ values (IC₅₀ = 0.016–0.027 μ M). *N*-Methylimidazole-pyridine cyclopropylcarboxamide derivatives **299** and **300** are out of the boundary of the good inhibitory potencies.

In the case of GSK3 β inhibitory properties, most of the derivatives are poor inhibitors compared to the standard inhibitor. In the **294a-u** series, all the molecules have displayed a very weak inhibitory property except for compound **294c** (IC₅₀ = 0.040 μ M) entailing cyclopropylcarboxamide attached to pyridine possessed noteworthy inhibitory effects. Along with



Scheme 61. Preparation of the compounds **292a-b** [40]; **Reagents and conditions:** i) NaH, 4-methoxybenzyl chloride, DMF, 0 °C, rt, (18h); ii) NaHMDS, ethyl 4-fluorobenzoate, THF, 0 °C, rt, (2h); iii) NaNO₂, AcOH, rt, (1h); iv) H₂, Pd/C, methanolic HCl, 45 °C, (6h); v) KSCN, DMF, 160 °C (2h); vi) CH₃I, NaOtBu, MeOH, 55 °C (2h); (in case of preparation of **292a**) or benzyl bromide, Cs₂CO₃, DMF, rt (36h) (in case of preparation of **292b**); vii) TFA, 45 °C.

it, compound **294q** (IC₅₀ = 0.073 μ M) could also exhibit the finest inhibitory property wherein cyclopentanone ring is appended to carboxamide fragment. 2-Thiobenzylimidazole derivatives **295a-e** have failed to exhibit good inhibitory effects. Half of the compounds of **305a-g** series exerted remarkable GSK3 β inhibitory properties; particularly compound **305c** (IC₅₀ = 0.035 μ M) (Figure 33) is reported to have the strongest inhibitory potency which is better than that of standard inhibitor. Structurally compound **305c** comprises pyridine-cyclopropyl amide connected to 2-ethylimidazole at 5-position. Hence pyridine-cyclopropyl amide and 2-alkyl substituted imidazole motifs favor for GSK3 β /p38 α MAP kinase dual inhibitory potentials. The compound devoid of 4-fluorobenzene at imidazole 4-position (compound **310**) has shown complete wash out with respect to both inhibitory properties which confirms mandate of 4-fluorobenzene at imidazole 4-position for good inhibitory activity.

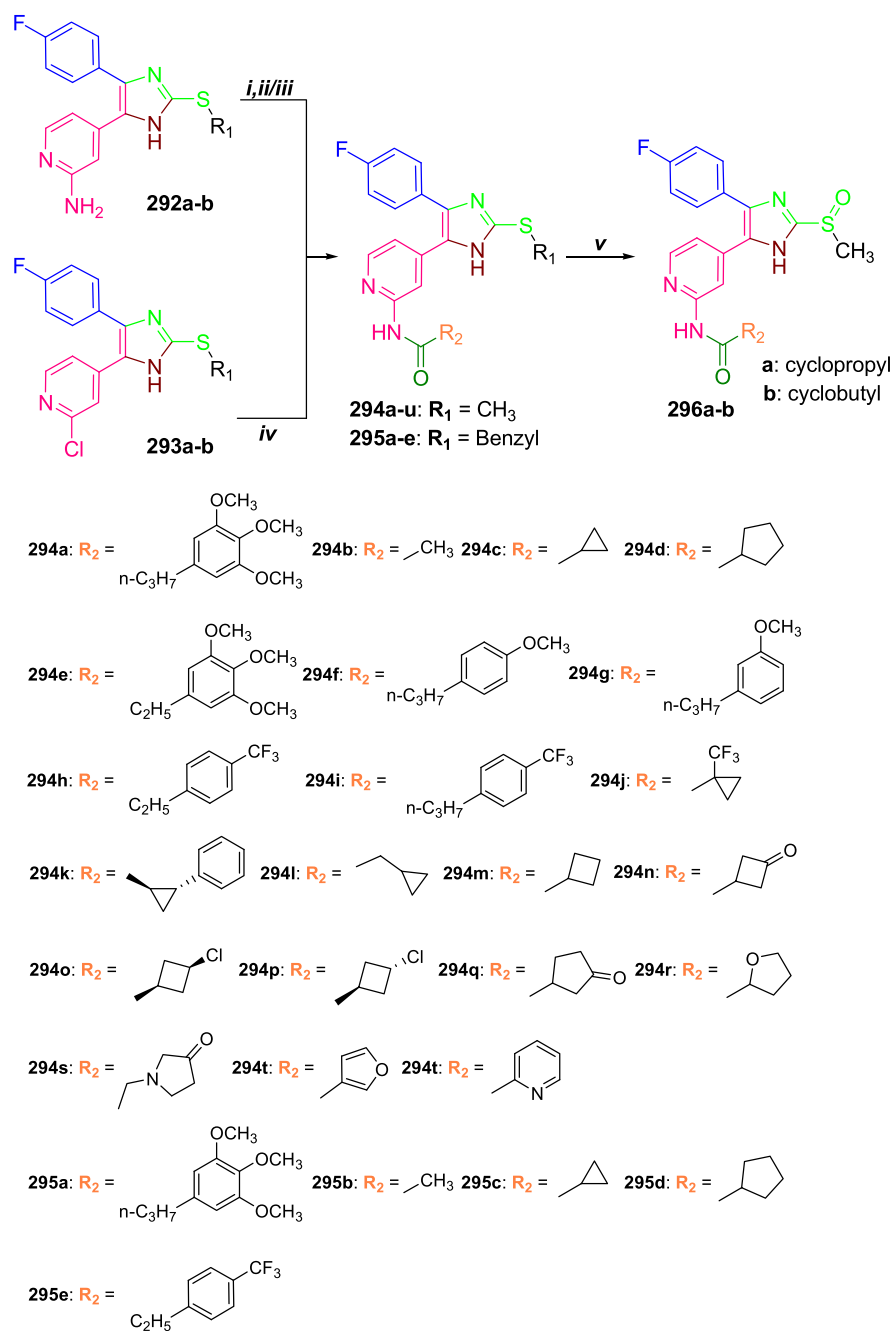
4.8. Quinazolin-4(3H)-one derivatives

Urease, a metalloenzyme associated with nickel performs hydrolysis of urea to carbon and ammonia; increased pH attributed to liberated ammonia paves for the survival of *Helicobacter pylori*. It has been reported that *Helicobacter pylori* is responsible for many gastroduodenal disorders such as peptic ulcer, gastric cancer, and duodenal ulcers and so forth. Hence, the need of the hour is to design the urease inhibitors. In order to counter such issues, the plethora of heterocyclic molecules are being synthesized including quinazolinones that have possessed anti-cancer properties along with other prominent pharmacological properties. In

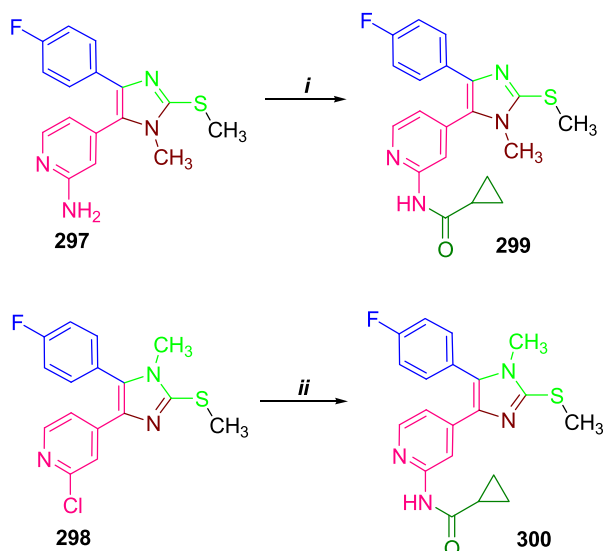
this regard, urease inhibitory investigation is continued with the design and preparation of quinazolinone derivatives linked to thiadiazole/triazole moiety [41].

Pyrimidinone appended with 4-substituted benzyl at pyrimidinone 2-position **311a-e** are treated with bromoethylacetate to get corresponding ester **312a-e**. The ester functionality of compounds **312a-e** is transformed to hydrazide **313a-e** with subsequent treatment using ethyl isothiocyanate rendered thiosemicarbazide analogs **314a-e**. The thiosemicarbazide fragment of compounds **314a-e** is utilized for cyclization to produce final compounds **315a-e** and **316a-e** in presence of NaHCO_3 and H_2SO_4 respectively (Scheme 66).

The prepared molecules are evaluated for urease inhibitory effects in the presence of urea and acetohydroxamic acid. Compared to reference compounds, all the tested compounds have exhibited strong urease inhibitory properties. In the three series of compounds, the thiosemicarbazide analogs **314a-e** displayed comparatively weak activity ($\text{IC}_{50} = 6.00\text{--}6.42 \mu\text{M}$); indicating that thiosemicarbazide fragment is not favorable for anti-urease activity. Again pyrimidinone-thiadiazole **316a-e** derivatives could show higher inhibitory activity ($\text{IC}_{50} = 2.24\text{--}2.98 \mu\text{M}$) compared to thiosemicarbazide analogs but inferior inhibitory effects with respect to triazole thione derivatives **315a-e**. Fortunately, pyrimidinone-linked thiadiazoles **315a-e** exerted most significant

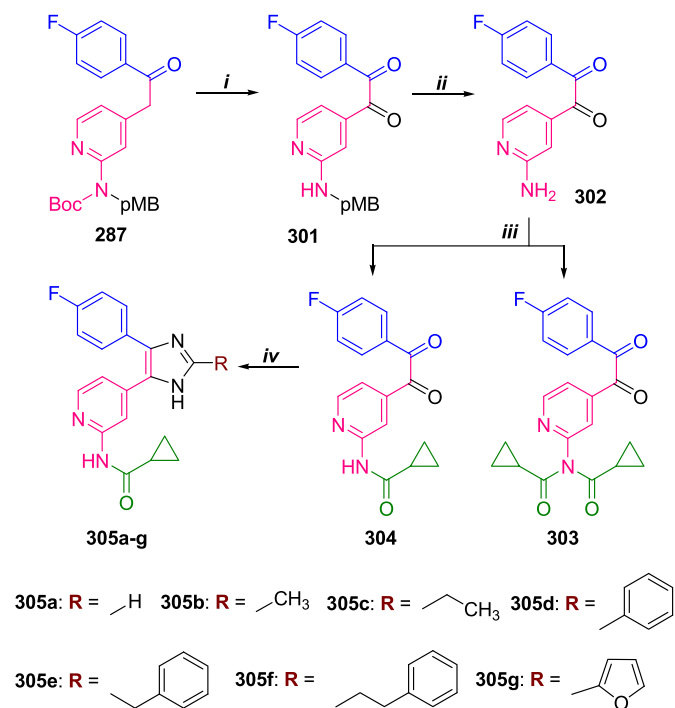


Scheme 62. Synthetic route for preparation of compounds **295a-u** [40]; **Reagents and conditions:** *i*) carboxylic acid, PyBOP, DIPEA, DCM, rt; *ii*) carboxylic acid, HATU, DIPEA, DCM, rt; *iii*) acyl chloride, pyridine, 0°C , rt; *iv*) amide, $\text{Pd}_2(\text{dba})_3$, XantPhos, Cs_2CO_3 , DMF, 100°C (16h); *v*) H_2O_2 , MeCN, rt.

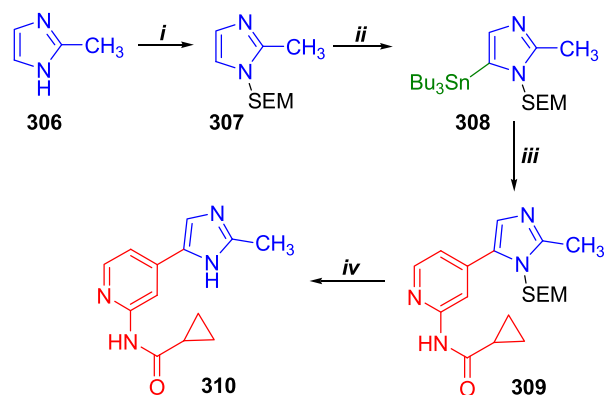


Scheme 63. Design and synthesis of compound **299** and **300** [40]; **Reagents and conditions:** *i*) cyclopropanecarbonyl chloride, pyridine, 0 °C, rt (2h); *ii*) cyclopropanecarboxamide, Pd₂(dba)₃, XantPhos, Cs₂CO₃, DMF, 100 °C (16h).

inhibitory potencies (IC₅₀ = 1.90–2.00 μM). These observations show that pyrimidine linked to triazole-thiones have a beneficiary influence on urease inhibitory properties. An interesting thing observed in these pyrimidinone derivatives is a similarity in the inhibitory effects in a particular series. This similarity within a series of compounds infers that 4-substitution of benzyl ring has influenced only to a very small extent on the anti-urease activity. Hence, the inhibitory properties of corresponding pyrimidinone derivatives are dependent on the basic structure of the derivative.



Scheme 64. Preparation of the compounds **305a-g** [40]; **Reagents and conditions:** *i*) SeO₂, acetic acid, 130 °C, 1.5h; *ii*) TFA, rt; *iii*) cyclopropanecarbonyl chloride, DIPEA, DCM, rt (18h); *iv*) R-CHO, NH₄OAc, acetic acid, 130 °C (3–4h).



Scheme 65. Synthetic route for the preparation of pyridineimidazole derivative **310** [40]; **Reagents and conditions:** NaH, 2-(trimethylsilyl)ethoxymethyl chloride, THF, 0 °C, rt (18h); *ii*) n-butyllithium, tributyltin chloride, Et₂O, 0 °C, rt (2h); *iii*) N-(4-bromopyridin-2-yl)cyclopropanecarboxamide, Pd(PPh₃)₄, 1, 4-dioxane, 105 °C (18h); *iv*) TFA, DCM, rt (6h).

4.9. Quinoline based 4,5-dihydropyrazoles

Out of a large number of tyrosine kinases, epidermal growth factor receptor (EGFR) is one of the enzymes involved in the regulation of several cellular functions like cell growth, survival, proliferation, and apoptosis. Downstream activation of EGFR would occur with the binding of ligands as EGF; which leads to MAP kinase activation and in turn phosphorylation of protein will result. Many of cancer types have been demonstrated due to significant mutations through MAPK or EGFR pathways. Drugs like afatinib and dacomitinib are designed as irreversible second-generation EGFR inhibitors. Taking consideration of anticancer properties of quinoline along with other pharmacological properties and pyrazolythiazole derivatized naphthalene, quinoline based 4,5-dihydropyrazoles are synthesized [42].

Synthesis of target molecules commenced with 2-Chloro-3-formyl-6-methoxyquinoline **317** wherein compound **317** is condensed with 4-methyl acetophenone to yield analogous chalcone **318** followed by hydrolysis with glacial acetic acid to produce chalcone of 2-hydroxyquinoline **319** (Scheme 67).

An α,β-unsaturated moiety of intermediate chalcone **318** is made to undergo intermolecular cyclization with semicarbazide/thiosemicarbazide yielding dihydropyrazole-quinoline derivatives **320a-b**. In continuation, cyclization of the chalcone **318** with hydrazine and acetic acid rendered compound **321** (Scheme 68). Further, the thioamide functionality on dihydropyrazole of compound **320b** on cyclization with appropriate phenacyl bromides obtained corresponding thiazole derivatives **322a-d**. Treatment of compound **320b** with appropriate 3-chloropentane-2,4-diones yielded compounds **323a-c**. Again reaction of compound **320b** with appropriate 2-oxo-N-arylpropanehydrazonyl chloride resulted in compounds **324a-d** (Scheme 69).

All the synthesized molecules are first tested for their cytotoxicity on cancer cell lines such as MCF7, HeLa, DLD1, and WT-38. Based on cytotoxicity of derivatives, some compounds which exhibited excellent activity have been selected for inhibition of EGFR. Among the chosen compounds, derivative **322b** (Figure 34) has exhibited the most significant EGFR potency (IC₅₀ = 0.0318 μM). The molecule entails 4-tolyl and 2-chloro-6-methoxyquinoline at dihydropyrazole 3- and 5-positions in addition to substituted thiazole-2-yl motif at N₁-position as a basic structure; besides, compound **322b** is connected to 4-fluorophenyl ring at thiazole 5-position. Its activity is almost identical with that of the reference compound gefitinib (IC₅₀ = 0.0291 μM). Substitution of the 4-fluorophenyl ring at dihydropyrazole 5-position with phenyl ring led to the total washout of the EGFR inhibitory activity. Slightly diminished activity is observed with substitution of the 4-fluorophenyl ring with ester and anilide moieties in the case of compounds **323b** and **323c**. The

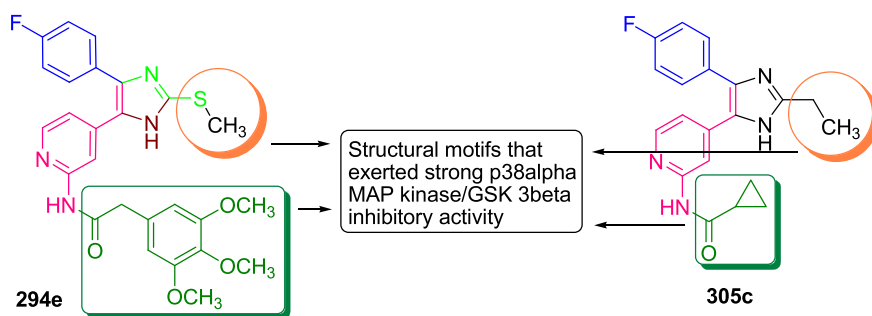


Figure 33. Illustration of structures of noteworthy GSK3 β /p38 α MAP kinase inhibitors.

molecule **323c** possessing anilide at thiazole 4-position has shown remarkable inhibitory activity ($IC_{50} = 0.0425 \mu\text{M}$). However, the exchange of aniline with ethyl carboxylate at thiazole 4-position (**323b**) has led to further reduced activity ($IC_{50} = 0.063 \mu\text{M}$). Chalcone **318** has stood second in the potent inhibitors list with IC_{50} value of $0.037 \mu\text{M}$. Replacement of 2-chloro group of compound **318** with $-\text{OH}$ resulted in a diminished activity. Diazophenyl thiazole scaffold **324a** could only render a weak EGFR inhibitory activity.

5. Radioiodinated benzo[d] imidazole-quinoline derivatives

Among the transmembrane receptor tyrosine kinases, platelet-derived growth factor receptor β (PDGFR β) is one that assumes responsibility with highly regulated cell expression. The enzyme is associated with angiogenesis and embryonic growth in addition to other functions such as the formation of blood vessels, kidneys, adipocytes. A large number of cancer types are associated with overactivity of PDGFR β . Currently, versatile probes have been developed for cancer imaging and targeting tyrosine kinases such as EGFR and PDGFR β . Radiolabelled tyrosine kinase inhibitors (TKIs) have been demonstrated to possess a high affinity for PDGFR β . In this regard, radioiodinated benzo[d] imidazole-quinoline derivatives are designed and synthesized [43].

8-Hydroxyquinoline linked to benzimidazole derivative **325** is triflated using *N*-phenyl-bis(trifluoromethanesulfonamide) yielding compound **326**. Substitution of triflate of compound **326** followed by coupling of secondary amines at quinoline 8-position has produced compounds **327a-g** (Scheme 70). 8-Hydroxy group of compound **325** is coupled with various mesylates to render compounds **328a-b** (Scheme 71).

In another series, the precursor **327a** is iodinated at quinoline 5-position to give compound **329** followed by NH protection by $-\text{Boc}$ group (**329**). Iodine at quinoline 5-position is replaced by *t*Butyltin moiety to obtain compound **331**. Final compound **333** is synthesized by radioiodinating the compound **331** to get compound **332** with subsequent NH $-\text{Boc}$ protection removal (Scheme 70). In a similar fashion, **327d** is radioiodinated at quinoline 5-position to form compound **333** (Scheme 72) (see Scheme 73).

The non-iodinated benzimidazole-quinoline derivatives **327a-g** and **328a-b** have been tested for the ability to reduce PDGFR β -overexpressed cell line viability. Out of the derivatives evaluated, compounds **327a** and **327d** (Figure 35) exhibited enhanced inhibitory potencies on PDGFR β positive cells. Hence, these compounds are selectively radioiodinated at quinoline 5-position to check the further improvement of the inhibitory activity; unfortunately, the radioiodinated derivatives could hardly express good binding to PDGFR β . The results indicate that the introduction of iodine diminished the affinity towards PDGFR β . The correlation between PDGFR β affinity and structural versatility of the designed molecules goes in this way; the presence of piperazine and morpholine at quinoline 8-position in compounds **327a** and **327d** respectively bestowed them the most remarkable inhibitory potentials. Replacement of piperazine with *N*-methyl piperazine in case of compound **327e** abated affinity is observed. Alongside, diaminopiperazine analogs **327b** and

327c have lost activity. Further, diaminoethylene derivatized benzimidazole-quinolines **327f** and **327g** have failed to elicit potent affinity properties. All these results infer that the increased size of the secondary amine at quinoline 8-position has led to the conformation that lowered activity.

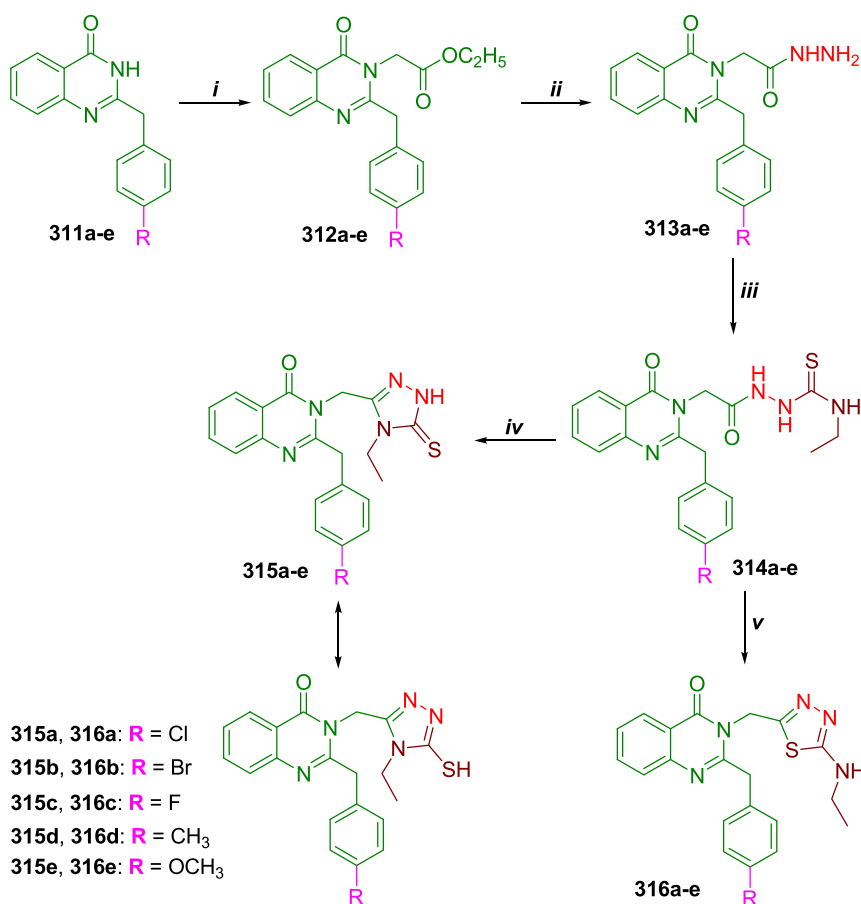
5.1. SLC-0111 thiazole and thiadiazole analogs

Carbonic anhydrases play significant roles such as lipogenesis, gluconeogenesis, ureagenesis, and tumorigenicity. Carbonic anhydrases have become versatile drug targets for AD treatment. SLC-0111 is a selective inhibitor of CA isoforms IX and XII; it possesses ureido substituted benzene sulfonamide motif. Considering the potentiality of SLC-0111 as CA inhibitors, the design and synthesis of novel SLC-0111 thiazole and thiadiazole derivatives are accomplished [44].

The synthesis of the thiazole-benzenesulfonamide derivatives commences from compound **337**. Carboxylic acid group of compound **337** is chlorinated to corresponding benzoyl chloride analog **338** which is converted to benzoyl azide derivative **339**. The Curtius rearrangement of the compound **339** led to the formation of isocyanate derivative **340** which is used as intermediate for the preparation of urea derivative of thiazole **341a-d** and thiadiazole derivatives **342a-d** using thiazoles and thiadiazoles respectively (Scheme 74).

The synthesis of the thiazole-benzenesulfonamide derivatives commences from compound **337**. Chlorination of carboxylic acid group of compound **337** and attachment of *N,N*-dimethyl methylene group to the NH of sulfonamide moiety resulted in corresponding benzoyl chloride analog **343** which is converted to benzoyl azide derivative **344**. The Curtius rearrangement of the compound **344** led to the formation of isocyanate derivative **345** which is used as intermediate for the preparation of urea derivative of thiazole **346a-d** and thiadiazole derivatives **347a-d** using thiazoles and thiadiazoles respectively (Scheme 75).

The synthesized derivatives are subjected to inhibition of CA isoforms using SLC-0111 and AAZ as reference compounds. Compared to SLC-0111 (*h*CA I: $K_I = 5.08 \mu\text{M}$, *h*CA II: $K_I = 0.250 \mu\text{M}$) thiazole derivatives of benzenesulfonamide have shown potent *h*CA I and *h*CA II inhibitory activity (*h*CA I: $K_I = 0.162\text{--}0.713 \mu\text{M}$; *h*CA II: $K_I = 0.009\text{--}0.833 \mu\text{M}$). However, in comparison with AAZ ($K_I = 0.250 \mu\text{M}$) towards *h*CA I, compounds **341c** ($K_I = 0.191 \mu\text{M}$) and **342b** ($K_I = 0.162 \mu\text{M}$) (Figure 36) are reported to have remarkable *h*CA I inhibitory agents. The significant *h*CA I inhibitor **342b** comprises benzenesulfonamide on one end of the urea and 3-phenylthiazole-5-yl on the other end. Amongst the thiazole analogs, compound **341c** possessing 4-fluorophenyl moiety at thiazole 2-position has exhibited notable activity. Removal of $-\text{F}$ or substitution with $-\text{Cl}$ on thiazole and substitution of phenyl with 4-F/4-Cl phenyl ring have led to slightly diminished inhibitory activity. However, plane thiazole/thiadiazole derivatives of urea have shown very poor *h*CA I activity. 4-Fluorophenyl derivatization at 5- and 3-positions of thiazole **341c** ($K_I = 0.0092 \mu\text{M}$) and thiadiazole **342c** ($K_I = 0.009 \mu\text{M}$) respectively resulted most potent *h*CA II inhibitory potentials compared to AAZ ($K_I = 0.0125 \mu\text{M}$). Remaining derivatives have not shown good activity. In the case of *h*CA IX and *h*CA XII isoenzymes, thiadiazole analogs have



Scheme 66. Design and synthesis of quinazolinone moiety linked to thiazole derivatives [41]; **Reagents and conditions:** i) BrCH₂COOC₂H₅, K₂CO₃, acetone; ii) NH₂NH₂•H₂O, EtOH; iii) C₂H₅NCS, EtOH, reflux; iv) 1M NaHCO₃, reflux; v) dil. H₂SO₄.

shown excellent inhibitory activity; whereas, thiazole derivatives exhibited comparatively less potent activity. In the *hCA IX* activity, phenyl (compound **342b**) and 4-chlorophenyl (compound **342d**) ring connected at thiazazole 3-position has elicited decent inhibitory activities with K_i values of 0.0083 μ M and 0.0079 μ M respectively. The same molecules **342b** and **342d** could also exhibit the strongest *hCA XII* inhibitory properties with K_i values of 0.0094 μ M and 0.0099 μ M respectively. Keen observation of the structure and activity inferred that 4-fluoro/4-chlorophenyl appendants on thiazole and thiazazole ring bestowed with decent CA inhibitory activity and the further improvement may be checked with the design of -fluoro and -chloro disubstituted phenyl thiazole/thiazazole derivatives. Unfortunately, the thiazole and thiazazole derivatives in which NH of benzenesulfonamide substituted with *N, N*-methyl methylene have totally failed to show CA inhibitory

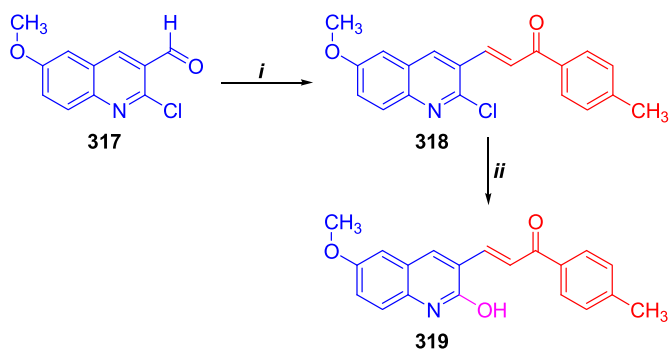
activity. It indicates that free sulfonyl amide pharmacore is crucial for CA inhibitory activity.

5.2. Tetrazole-peptidomimetics

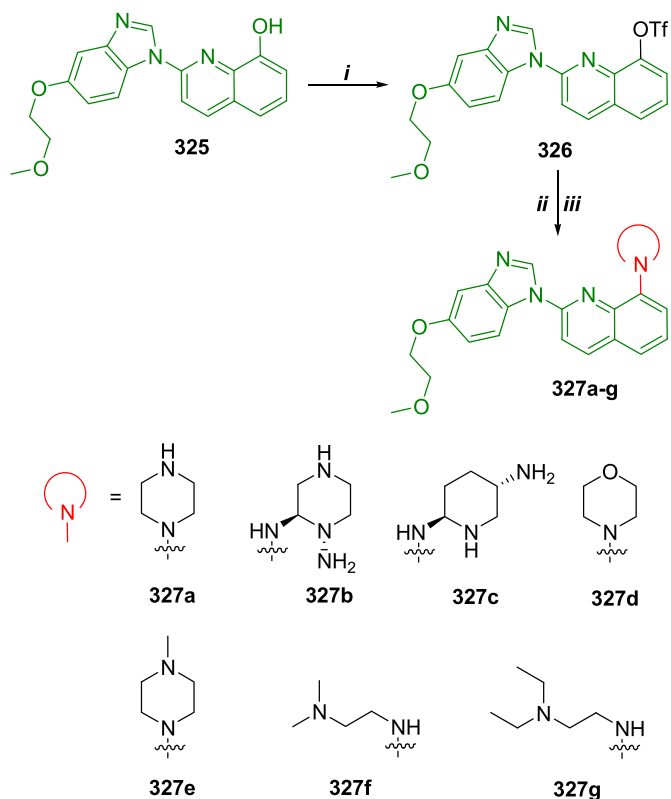
Neutral M1-alanyl aminopeptidase (ePepN) is a bacterial protease from a gram-negative bacterium (*E. Coli*) studied mostly. It catalyzes the removal of polypeptide *N*-terminal amino acid throughout the nucleophilic attack of a water molecule activated by a Zn²⁺ cation. ePepNs are not only crucial for bacterial survival, but they are also essential for *E. Coli* and *Plasmodium falciparum*. Hence, ePepN could be an attractive therapeutic target for the efficient control of bacterial diseases. Recently, tetrazole scaffolds have been highlighted to possess inhibitory properties against pathogenic bacteria and protozoa. Having considered these facts, tetrazole-peptidomimetics are designed and synthesized [45].

Amino acid derivatives protected with Fmoc **348** is deprotected to yield resin-bound amino acid derivatives **349**. Ugi reaction of compound **349** with substituted aldehydes, isocyanides, and TMSN₃ resulted in tetrazole derivatives **350** followed by treatment with TFA to produce amino acid derivatives of tetrazole **351a-u** (Scheme 76) (see Figure 36).

All the prepared tetrazole derivatives are investigated for ePepN inhibitory properties using bestatin. Here, compound **351b** (Figure 37) and **351d** are reported as remarkable ePepN inhibitors with IC₅₀ values of 1.4 \pm 0.2 μ M and 2.2 \pm 0.3 μ M respectively possessing threefold and fivefold activities respectively compared to bestatin (IC₅₀ = 7 \pm 4 μ M). Further compound **351i** has possessed good inhibitory activity (IC₅₀ = 7.2 \pm 0.9 μ M) as potent as a reference compound. Surprisingly, derivative **351k** (Figure 37) has elicited strongest ePepN inhibitory activity (IC₅₀ = 0.00026 μ M) possessing a 27-fold higher inhibitory activity compared to bestatin. Strongest ePepN inhibitor **351k** entails benzyl moiety at the



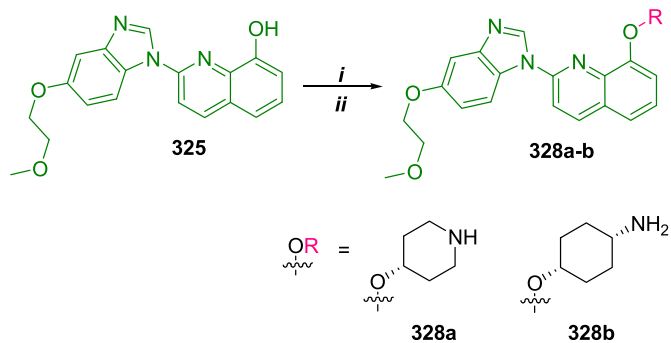
Scheme 67. Synthesis of compound quinoline derivative **319** [42]; **Reagents and conditions:** i) NaOH, CH₃COC₆H₄CH₃, RT (4h); ii) gl. AcOH, reflux (10h).



Scheme 70. Preparation of benzo[*d*]imidazole-quinoline derivatives [43]; **Reagents and conditions:** *i*) *N*-phenyl-bis(trifluoromethanesulfonylimide), rt (2d); *ii*) tris(dibenzylideneacetone) dipalladium(0), cesium carbonate, *rac*-BINAP, reflux (3d); *iii*) TFA.

cancers. Phosphatidylinositol-3-kinase (PI3K)/Akt is a prominent signaling pathway in most of the human cancer types. Akt is demonstrated to have overexpression in a wide variety of human cancer types such as lung, ovarian, gastric and pancreatic carcinomas. Thereby inhibition of PI3K/Akt would result in apoptosis and tumor cell growth inhibition. Subsequently, the design of anti-Akt derivatives leads to potential anticancer agents. Several substituted thiazole scaffolds have been highlighted as antitumor agents in addition to other pharmacological properties. Besides, hydrazone derivatives have possessed anticancer properties against cancer cell lines such as A549, MCF-7, U-373, SK-OV-3, and so forth. These findings have allowed the researchers to prepare thiazole derivatives linked to diaryl ethers *via* hydrazone tether [46].

The synthetic pathway that led to the design of title molecules goes in this way; diaryl ether with aldehyde functionality on one of the aryl ring



Scheme 71. Synthetic route for the preparation of compounds 327a-b [43]; **Reagents and conditions:** *i*) R-OMs, Cesium carbonate, reflux, overnight; *ii*) TFA.

352 is condensed with thiosemicarbazide to produce the corresponding thiosemicarbazone of diaryl ether **353**. Intermolecular cyclization of thiosemicarbazone with substituted phenacyl bromide rendered thiazoles derivatives tethered to diaryl ethers **354a-j** (Scheme 77).

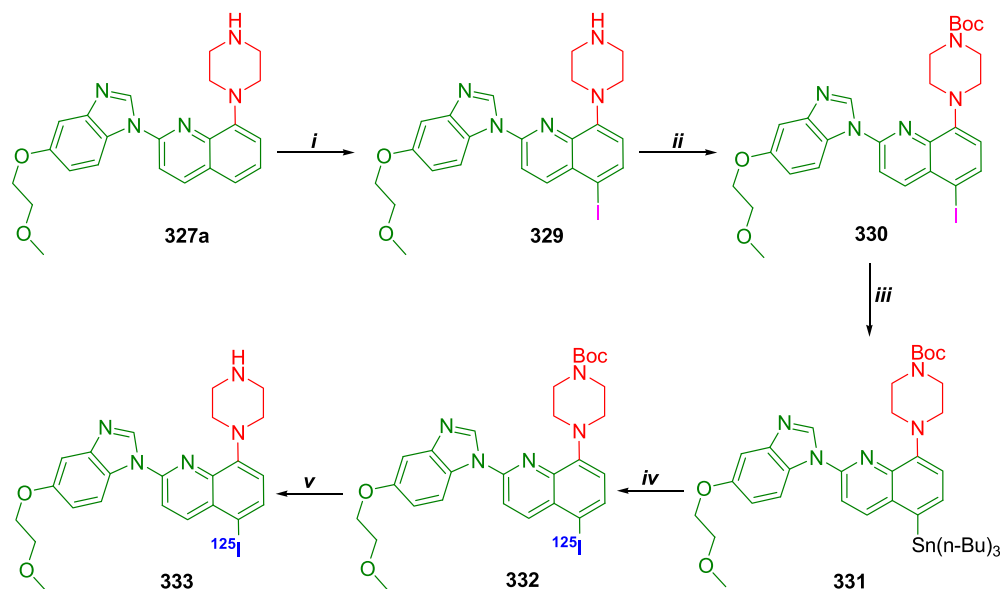
The newly prepared compounds **354a-j** along with compound intermediate **353** are screened for Akt inhibitory effects using Cisplatin as a standard compound. Firstly, the derivatives are checked for their cytotoxicity on cancer cell lines A549, C6, and NIH/3T3 comparing with standard anticancer agent cisplatin ($IC_{50} = 17.33 \pm 2.08 \mu\text{M}$). In this activity, compound **354f** (Figure 38) has exhibited the most remarkable inhibition ($IC_{50} = 12 \pm 1.73 \mu\text{M}$) towards A549 cell line and other derivatives have totally failed to show decent cytotoxicity. Whereas, the same compound **354f** has produced enough activity ($IC_{50} = 3.83 \pm 0.76 \mu\text{M}$) to become the most toxic derivative towards the C6 cell line. Along with this, the compound **354h** (Figure 38) has found its place in the notable cytotoxic compounds list with IC_{50} value of $5.83 \pm 0.76 \mu\text{M}$. While compounds **353** ($IC_{50} = 26.33 \pm 1.53 \mu\text{M}$) and **354g** ($IC_{50} = 16 \pm 5.66 \mu\text{M}$) have shown moderate cytotoxicity. Unfortunately, no single designed derivative has rendered good cytotoxicity towards the cell line NIH/3T3. The compound which exhibited notable cytotoxicity towards both A549 and C6 cell lines possesses 4-benzonitrile at thiazole 4-position; while the derivative having the strongest cytotoxicity towards C6 cell line yet comparatively lower than compound **354f** bearing 4-hydroxyphenyl moiety at thiazole 4-position. The precise correlation between the structure of the compound and its cytotoxicity cannot be established as both electron-withdrawing groups and electron-donating groups have produced good cytotoxic effects. The compounds which have exhibited decent cytotoxicity towards the cancer cell lines have been chosen for inhibition of Akt on the cell lines A549 and C6 cell lines. The intermediate compound **353** has elicited excellent percent inhibition ($68.08 \pm 2.48\%$) which is twofold stronger compared to cisplatin ($31.01 \pm 3.18\%$). Annoyingly, most A549 cell line cytotoxic molecule **354f** has displayed good activity but lower activity ($45.77 \pm 10.58\%$) compared to compound **353**. Besides, 4-hydroxyphenyl analog has exhibited decent inhibition percentage ($57.37 \pm 17.30\%$). Regarding inhibition of the C6 cell line, most cytotoxic compound **354f** bestowed strongest inhibition percentage ($71.66 \pm 4.09\%$) which is a slightly diminished activity compared to cisplatin ($77.25 \pm 5.75\%$). Compound **354g** is also one of the finest C6 inhibitors with percentage inhibition of $70.42 \pm 10.37\%$.

5.4. Thiazol-hydrazono-coumarin

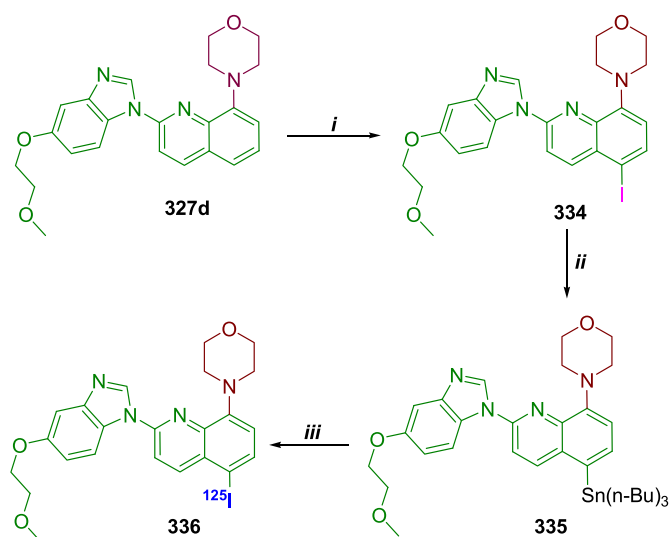
Out of a large number of signaling pathways that are essential for the proliferation of cancer cell lines, cyclin-dependent kinases (CDKs) play a significant role. Hence CDKs are attractive molecular targets for efficient cancer therapy; thereby extensive study of these is being taken up. Many research outputs have proved the overexpression of CDKs in malignancies such as lung, ovarian and pancreatic carcinoma and so forth. Considering the CDKs inhibitory properties of thiazole scaffolds and coumarin hydrazone derivatives, the design and synthesis of thiazol-hydrazono-coumarin analogs are achieved [47].

In the synthesis of title compounds, 3-acetyl-6-halocoumarin **355** is condensed with thiosemicarbazone to yield intermediate thiosemicarbazone of coumarin **356**. Further, the intermediate **356** on intramolecular cyclization with the reagents $\text{CH}_3\text{COCH}_2\text{Cl}$, phenacyl bromide, 4-bromo phenacyl bromide, 2-bromoacetyl tetralin, 3-chloroacetylacetone, and ethyl-2-chloroacetoacetate formed the thiazol-hydrazono-coumarins **357a-c**, **358a-c**, **359a-c**, **360a-c**, **361a-c**, and **362a-c** respectively. The intermolecular cyclization of intermediate **356** with ethyl bromoacetate has resulted in thiazolidinone derivatives **363a-c** (Scheme 78).

The title molecules are subjected to anticancer activity followed by evaluation of CDK2 inhibitory properties of some selected compounds. In the anti-proliferative activity of designed derivatives on HeLa cell line considering doxorubicin as a standard compound, all the tested compounds have shown decent anti-proliferative activity. Compared to



Scheme 72. Synthesis of radioiodinated compound $[^{125}\text{I}]$ **333** [43]; **Reagents and conditions:** *i*) NCS, NaI, 50 °C, overnight *ii*) Boc_2O , TEA, rt (3d) *iii*) hexabutylstannane, $\text{Pd}[\text{P}(\text{C}_6\text{H}_5)_3]_4$, reflux (24h) *iv*) $[^{125}\text{I}]\text{NaI}$, NCS, acetic acid, rt (15min) *v*) TFA, rt (30min).



Scheme 73. Synthetic pathway for preparation of radioiodinated compound **336** [43]; **Reagents and conditions:** *i*) NCS, NaI, 50 °C, overnight *ii*) hexabutylstannane, $\text{Pd}[\text{P}(\text{C}_6\text{H}_5)_3]_4$, reflux (48h) *iii*) $[^{125}\text{I}]\text{NaI}$, NCS, acetic acid, rt (15min).

doxorubicin compound **362c** (Figure 39) can be mentioned as a compound with the highest activity (Table 15). Little diminished activity is observed for the compound **362b** and derivatives **361c** and **362a** have exhibited almost similar anti-proliferative activity. Among the various thiazole derivatives designed, thiazole-4-methyl-5-ethyl carboxylate **362a-c** have been found to be significant anti-proliferative compounds; particularly compound **362c** with -Br atom at coumarin 6-position stood atop of the potent anti-proliferative molecules possessing approximately 115-fold greater activity compared to doxorubicin. Replacement of -Br in compound **362c** with -Cl (**362b**) led to twofold reduced activity and substitution of halogen with -H (**363a**) has resulted in a slightly diminished anti-proliferative property.

The molecules with the dominant anti-proliferative property are chosen for inhibition of the enzyme CDK2 using staurosporine as standard compound CDK2 inhibitor (Table 15). Compound **361c** and **362a** have exhibited weak inhibitory potentials compared to staurosporine. However, synchronization of anti-proliferative property and inhibitory activity is observed in the case of compounds **362b** and **362c** wherein compound **362c** is bestowed with excellent inhibitory activity. Its activity is twofold stronger in comparison with standard inhibitor. Moderate inhibitory CDK2 activity is shown by compound **362b**. These observations reveal the importance of size and electronegativity of -Br. Decreased halogen size and increased electronegativity diminished the CDK2 inhibitory activity.

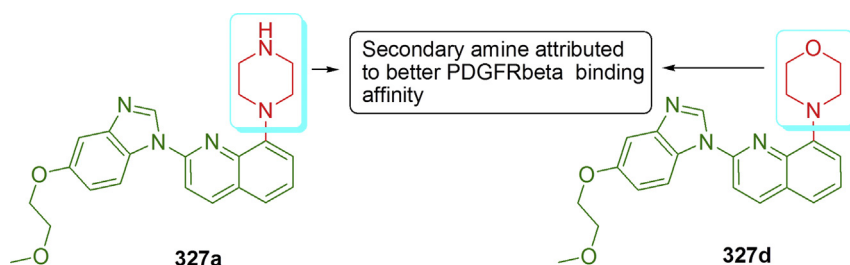
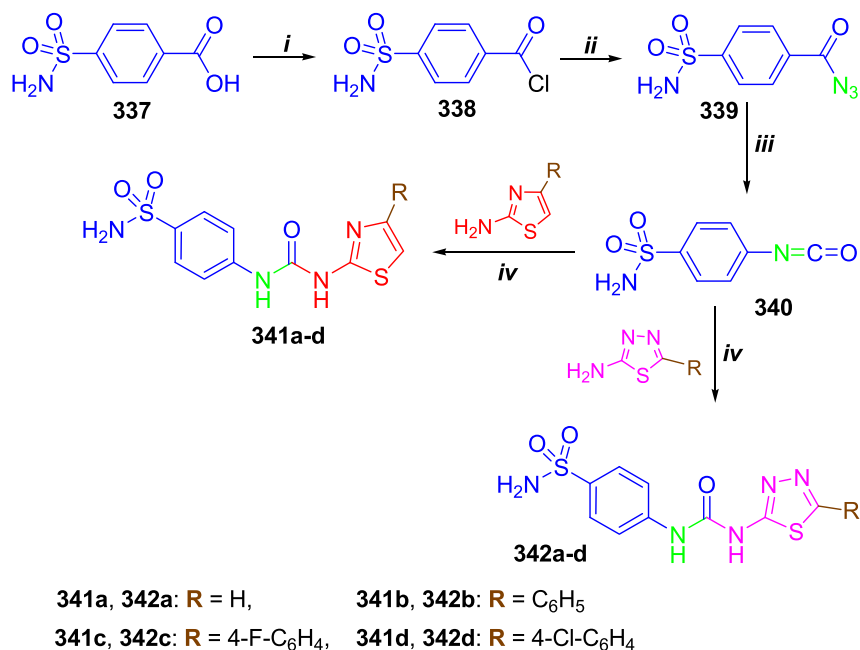


Figure 35. Representation of structures of molecules with strong PDGFR β affinity.

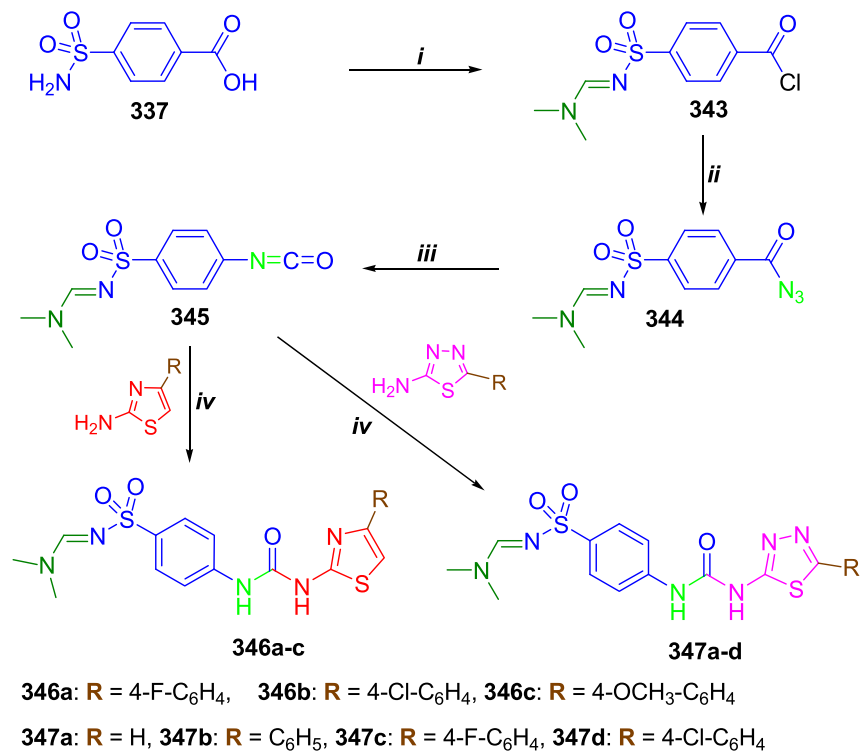


Scheme 74. Synthetic way for the preparation of the thiazolo-benzene sulfonamides [44]; **Reagents and conditions:** i) SOCl₂, reflux (12hr); ii) NaN₃/Ice bath/stirring (2hr); iii) Dry toluene/reflux (1hr); iv) Dry toluene/reflux (4hr).

5.5. Thiazolidine-2,4-dione-azole derivatives

Impairment of pancreas β -cells would lead to abnormal metabolism in carbohydrate and involved in diabetes development. In this situation, impairment of insulin secretion is also observed and clinically it results in diabetes. The enzymes α -glucosidase and α -amylase function in the digestion of starch, absorption of glucose. Alongside α -amylase is involved in the breakdown and absorption of insoluble starch molecules.

Hence inhibition of these enzymes might be an affordable and appreciable approach to control diabetes. In this regard, the thiazolidine-2,4-dione class of molecules has been in the limelight as they have blood glucose level normalizing effect. Derivatives of thiazolidine-2,4-dione and azole have not been subjected to α -amylase and α -glucosidase inhibitory properties; hence a series of thiazolidine-2,4-dione-azole derivatives are synthesized [48].



Scheme 75. Synthesis of the final compounds 346a-d and 347a-d [44]; **Reagents and conditions:** i) SOCl₂/DMF, reflux (5hr); ii) NaN₃/Ice bath/stirring (2hr); iii) Dry toluene/reflux (1hr); iv) Dry toluene/reflux (4hr).

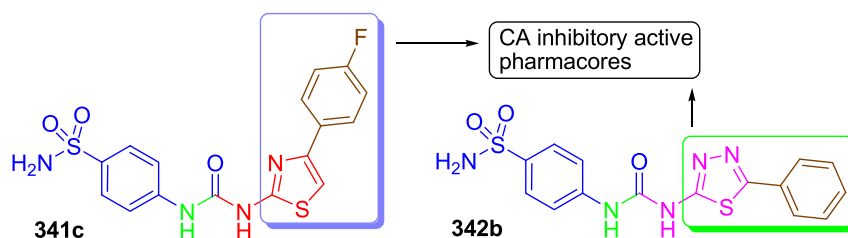


Figure 36. Representation of significant CA inhibitory molecules.

The synthetic route for the design of thiazolidine-2,4-dione derivatives involves the preparation of thiazolidine-2,4-dione **365** from chloroacetic acid **364** and thiourea. Substitution reaction of 4-fluorobenzaldehyde with compounds **366a-e** gave 4-substituted benzaldehyde derivatives **367a-e** which subsequently condensed with thiazolidine-2,4-dione **365** to produce 5-benzylidenethiazolidine-2,4-dione derivatives **368a-e** (Scheme 79).

Treatment of compound **368a** with bromo ethyl acetoacetate yielded *N*-ethylacetate substituted thiazolidine-2,4-dione analog **369** followed by hydrolysis rendered *N*-ethanoic acid derivative **370**. Again compound **368a** is utilized as intermediate wherein pyrrolopyridine moiety of compound **368a** coupled with aromatic amines **371a-c** at 4-position to form 4-aryl amino substituted pyrrolopyridine derivatives **372a-c** (Scheme 80).

The α -amylase and α -glucosidase inhibitory activities are conducted on all the synthesized molecules using **Acarbose** as a standard inhibitor. The inhibitory properties are depicted in terms of percentages. Compared to **Acarbose** (α -amylase: 43.0%, α -glucosidase: 40.91%), more than half of tested compounds have possessed potent inhibitory percentages. The compounds of the series **372a-c** (Figure 40) exhibited closest inhibitory percentages compared to **Acarbose** in the case of α -amylase activity

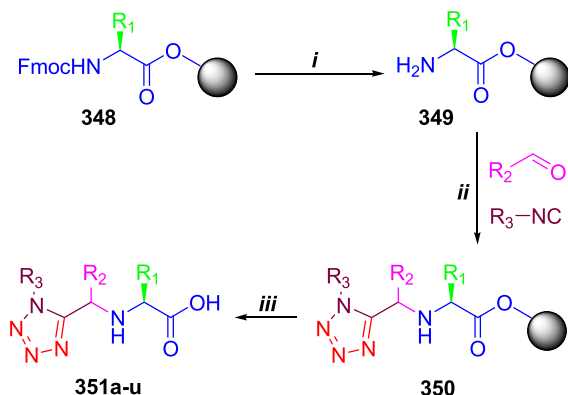
(Table 16). In those, compound **372c** having the strongest inhibitory percentage is only a little less potential compared to **Acarbose**. An almost similar inhibitory percentage is observed for compound **372b**; however diminished activity is shown by compound **372a** probably due to large OCF₃ moiety. Besides, compounds **368b-c** and compound **370** rendered moderate α -glucosidase inhibitory percentages.

The same course of inhibitory percentages is observed for designed compounds towards the α -glucosidase enzyme (Table 16). Inhibitory results reveal the importance of substitution of fluorinated aromatic amines at pyrrolopyridine 8-position of derivatives **372a-c**. In combination with a fluorinated aromatic amine at pyrrolopyridine 8-position, the presence of free thiazolidine-2,4-dione NH group allows the compounds of **372a-c** series to exhibit inhibitory properties at maximum level.

5.6. Thiazolylpyrazolyl coumarin derivatives

Angiogenesis is the physiological process through which essential nutrients and oxygen are supplied subsequently enhancing tumor progression and metastasis. VEGFR-2 kinase is one of the enzymes/factors responsible for angiogenesis. Overexpression of the VEGFR-2 kinase signaling pathway suppresses the tumor growth. The literature revealed coumarin derivatives have attracted great attention owing to their inhibition of VEGFR-2 kinase signaling pathway. Considering VEGFR-2 kinase inhibitory activity of coumarin scaffolds along with thiazolylpyrazolone motif, hybrid compounds of coumarin and thiazolylpyrazolone have been engineered [49].

In the synthesis of title compounds, coumarin-linked arylamines via chalcone fragment **373a, b** are cyclized with thiosemicarbazide in the intermolecular fashion to form intermediate compounds pyrazole-coumarin derivatives **374a, b**. The thioamide fragment of pyrrole is utilized in the design of thiazole-pyrrole derivatives **375a, b**, **376a, b** and **377a, b** with chloroacetone, phenacyl bromide and chloroethylacetoacetate respectively (Scheme 81). Intermolecular cyclization of pyrazole-thioamide derivatives **374a, b** with bromoethylacetate and bromoethylpropionate to yield coumarin tethered thiazolones through pyrazole ring **378a, b**, and **379a, b** respectively (Scheme 82). The intermediate compounds **374a, b** could also be transformed into



Scheme 76. Solid-phase synthesis of tetrazole-peptidomimetics by Ugi-azide reaction [45].

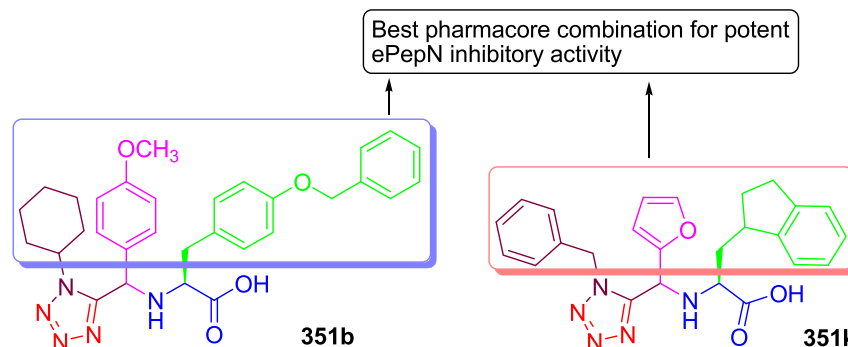
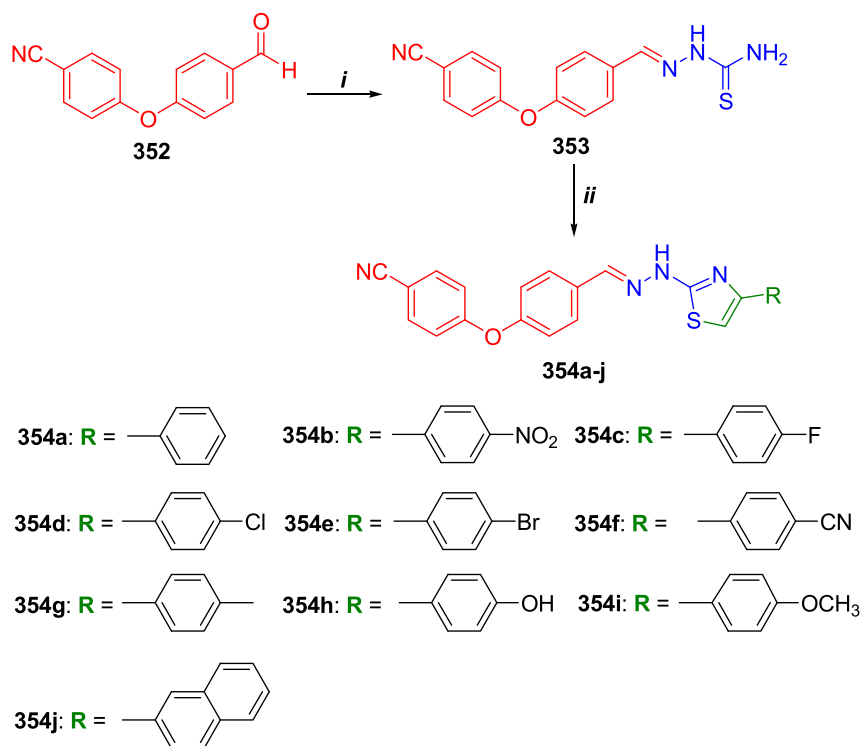


Figure 37. Demonstration of structures of significant ePepN inhibitors.



Scheme 77. Synthetic route for the preparation of the compounds 354a-j [46]; **Reagents and conditions:** i) $\text{NH}_2\text{CSNHNH}_2$, EtOH, reflux (12h); ii) RCOCH_2Br , EtOH, reflux (6h).

corresponding azo-thiazole-pyrazole derivative by reacting with $\text{CH}_3\text{CO}(\text{Cl})\text{C}=\text{NNHAr}$ (Scheme 83). The title compounds 376a, b are further derivatized with aryldiazo group to render compounds 381a, b (Scheme 84).

The synthesized molecules are subjected to anticancer activity using doxorubicin as a standard compound. Most of the title compounds have exhibited moderate anti-proliferative activity towards MCF-7 cell lines except few derivatives which shown poor inhibitory activity.

The pyrazolo-thioamide derivatives 374a, b have failed to render decent anti-proliferative activity revealing that simple pyrazoline ring with thioamide functionality is not enough for good MCF-7 anti-proliferation. A slight increment in the activity is observed for the 4-phenylthiazolo-pyrazole derivatives 376a, b; and 4-hydroxycoumarin analog 376b has comparatively higher activity than 376a. Further enhanced activity is reported for the compounds thiazole 5-ethyl carboxylate scaffolds 377a, b. Again the hydroxycoumarin analog 377b has exhibited threefold stronger activity compared to 377a. A diversified pyrazolo-thiazolones 378a, b have not qualified as good candidates for MCF-7 anti-proliferative activity indicating thiazolone motif is not apt

pharmacore for the activity. However, the 5-methylthiazolone derivatized pyrazoles 379a, b resulted in the finest inhibitory values. In that, compound 379a (Table 17) is the best between the two. Aryldiazo modified thiazolones 380a-d have shown improved MCF-7 anti-proliferation activity. In this series, compound 380c (Table 17 & Figure 41) elicited the closest inhibitory activity compared to the standard compound. It entails methyl and 4-chlorophenyldiazo structural units at thiazole 4- and 5-positions respectively and plane coumarin 3-yl moiety at pyrazole 3-position. The *p*-tolyldiazo analogs 380a and 380b have resulted in diminished activity which infers that the 4-chloro group has much impact on anti-proliferative activity. Twofold reduced activity is noticed for the compound 380d which is 4-hydroxycoumarin analog.

The most significant anti-proliferative activity has been exhibited by compounds of 381a-d series. Except for compound 381a (moderate inhibitor), the other three derivatives bestowed the most significant activity and comparatively greater activity than doxorubicin. In particular, 381d (Figure 41) has elicited excellent activity; structurally the compound possesses phenyl and 4-chlorophenyldiazo motif at 4- and 5-positions of thiazole ring respectively. An almost similar activity is rendered by compounds 381b and 381c. All the potent anti-proliferative molecules have been allowed to inhibit VEGFR-2 kinase using sorafenib as a standard VEGFR-2 kinase inhibitor. Out of these compounds, derivatives 379a, 380b and 380c could only show moderate inhibitory activity. The significant anti-proliferative molecule 381d has also shown the strongest activity. Alongside the significant activity is exhibited by the compound 380c.

5.7. Tropinone-thiazole derivatives

Melanoma is most common in skin malignancies. Statistics revealed that approximately 30000 new cases are reported worldwide. The dysregulation of melanin melanocytes is the main cause of melanoma; subsequently, the dysregulation leads to uncontrolled melanocyte proliferation followed by observation of high melanin content.

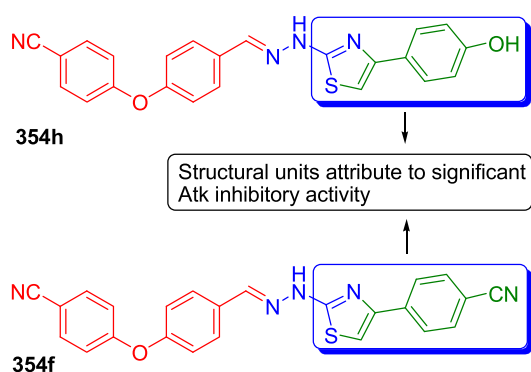
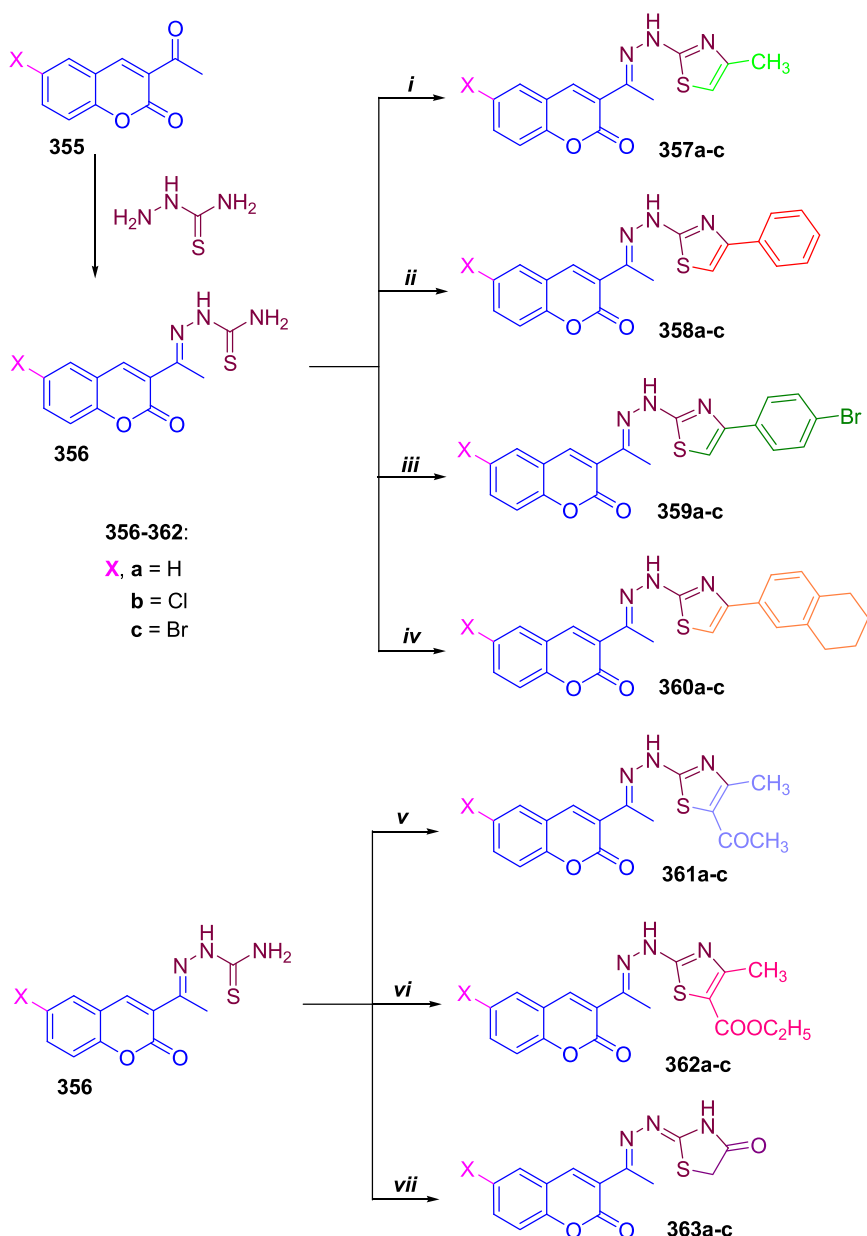


Figure 38. Illustration of structures of potent Akt inhibitors.



Scheme 78. Synthetic route for the preparation of thiazolo-hydrazolo-coumarin derivatives [47]; **Reagents and conditions:** *i*) EtOH, Anhyd. CH_3COONa , $\text{CH}_3\text{COCH}_2\text{Cl}$, reflux; *ii*) EtOH, Anhyd. CH_3COONa , Phenacyl bromide, reflux; *iii*) EtOH, Anhyd. CH_3COONa , 4-Bromo phenacyl bromide, reflux; *iv*) EtOH, Anhyd. CH_3COONa , 2-bromoacetyltetralin, reflux; *v*) EtOH, Anhyd. CH_3COONa , 3-chloroacetylacetone, reflux; *vi*) EtOH, Anhyd. CH_3COONa , ethyl-2-chloroacetoacetate, reflux; *vii*) EtOH, Anhyd. CH_3COONa , ethyl bromoacetate, reflux.

Tropinone derivatives are explored in the medicinal field and have been found to be pharmaceutically significant. Tropinone scaffolds **381** (Figure 42) and **382** are reported to possess strong activity towards HL-60 cell lines and HCT116 cell lines respectively. Recently designed hydrazinyl triazoles have exhibited decent activity towards MV4-11 cells. All these observations have led to the design of tropinone-thiazole derivatives [50].

Tropinone **384** on condensation with thiosemicarbazide gave thiosemicarbazone of tropinone **385**. The thioamide fragment of the derivative **385** is made use in intermolecular cyclization with *p*-substituted

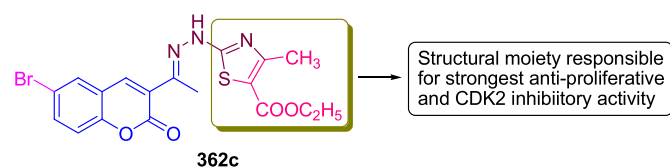


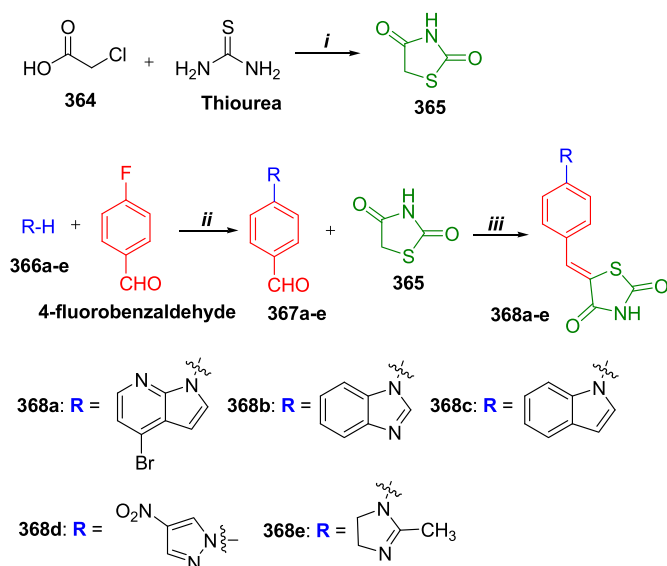
Figure 39. Demonstration of potent anti-proliferative (Hela) and anti-CDK2 inhibitory compound.

phenacyl bromides yielded tropinone compounds of thiazole linked via hydrazone spacer **386a-h** (Scheme 85).

The tropinone derivatives are tested for their anti-proliferative properties on cancer cell lines such as MV4-1, A549, MCF-7, B16-F10, and BALB/3T3 using chlorambucil as a positive control. In this activity, almost all the tested molecules have shown better anti-proliferative

Table 15. Anti-proliferative (Hela) activity and CDK2 inhibitory activity of designed molecules.

Compd	Anti-proliferative activity	CDK2 inhibitory activity
	IC ₅₀ (μM)	IC ₅₀ (nM)
361c	0.0654 ± 0.0038	1.546 ± 0.021
362a	0.0596 ± 0.0026	1.629 ± 0.012
362b	0.0236 ± 0.0011	0.216 ± 0.014
362c	0.0091 ± 0.0007	0.022 ± 0.002
Doxorubicin	1.1073 ± 0.0062	-
Staurosporine	-	0.044 ± 0.002



Scheme 79. Synthesis of a series of thiazolidine-2,4-dione-azole derivatives [48]; **Reagents and conditions:** *i*) H₂O, Conc. HCl, reflux (10h); *ii*) K₂CO₃, DMF, 100 °C (5h); *iii*) piperidine, PhCOOH, 100 °C (1h).

activity. However, compounds **386c**, **386g**, and **386h** are reported to possess stronger inhibitory activity compared to chlorambucil and among other derivatives of the series.

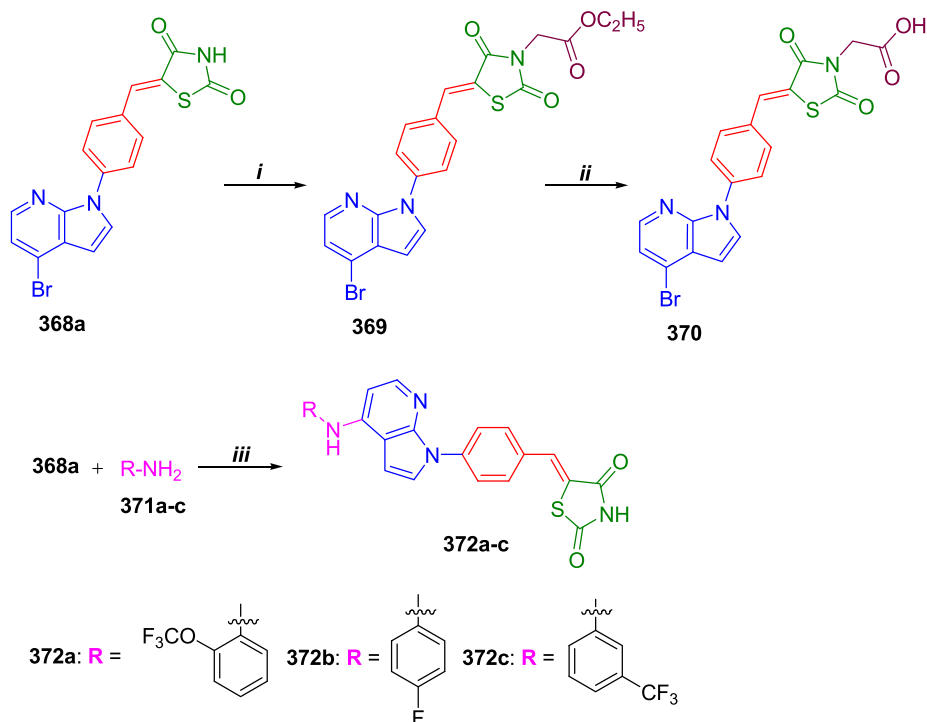
The designed molecules have also been subjected to tyrosinase inhibitory activity using ascorbic acid and kojic acid as reference compounds. Compared to ascorbic acid all evaluated derivatives have possessed higher activity. However, when inhibitory values are compared with kojic acid, half of the synthesized molecules have decent tyrosinase inhibitory activity (Table 18).

The compound **386f** has shown activity as potent as kojic acid and twofold higher inhibitory activity is shown by the compound **386e**.

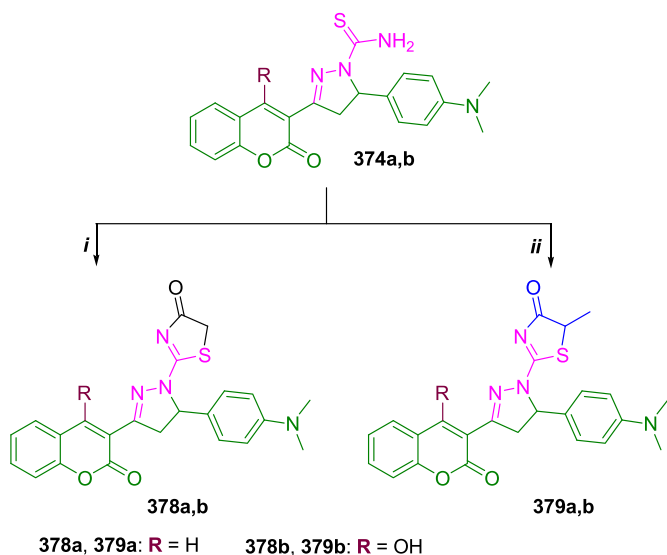
Whereas compounds **386g** and **386h** (Figure 43) with similar activities are approximately 21-fold greater potencies compared to kojic acid. Among the various substituted phenylthiazole derivatives, compound **386g** possessing 3,4-dichlorophenyl ring at thiazole 4-position has bestowed the most significant activity. The 2,4-dichlorophenyl analog bearing has exhibited slightly reduced activity. A very poor inhibitory activity is rendered by the compounds **386a** and **386b** possessing *p*-F/*p*-Cl phenyl moieties. These facts reveal two chloro atoms on the phenyl ring either at 2,4- or 3,4-positions have been attributed to remarkable inhibitory activity. However, the monosubstituted phenyl rings connected at thiazole 4-positions would not give expected inhibitory properties. The research team would have tried the dibromo and difluoro disubstituted phenyl analogs for further improvement in the tyrosinase inhibitory activity.

6. Discussion and conclusion

Whole classified content entails the schematic representation of the synthesis of enzyme inhibitors, followed by pharmacological evaluation of synthesized molecules. The relation between the structure of a remarkable enzyme inhibitor and the corresponding inhibitory property is discussed qualitatively highlighting responsible structural pharmacophores. [1,4] Dioxino [2,3-*f*] quinazoline derivatives have been synthesized and the compounds have shown exhibited c-Met and VEGFR-2 inhibitory activity even at a nanomolar concentration wherein compound **7k** is found to be as potent as cabozantinib. SAR revealed the presence of *p*-F-phenyl ring of cyclopropane-1,1-dicarboxamide moiety has a great impact on inhibitory activity. The compound **15y** has exhibited the most significant MTB PtpB inhibitory activity; which is one of the compounds of 1,2,3-*1H*-triazoles linked to 4*H*-pyrano [2,3-*d*] pyrimidine. The significant activity is attributed to -OMe, -OH, and -NO₂ at 3, 4 and 5-positions of phenyl ring respectively. Moderate carbonic anhydrase inhibitory activity is observed for the compound **18c** amongst the evaluated 1,2,4-triazole-5-one derivatives. Out of the 1,2,4-triazole-based benzothiazole/benzoxazole derivatives prepared, compound **27b** has elicited stronger p38 α MAB kinase inhibitory activity than that of



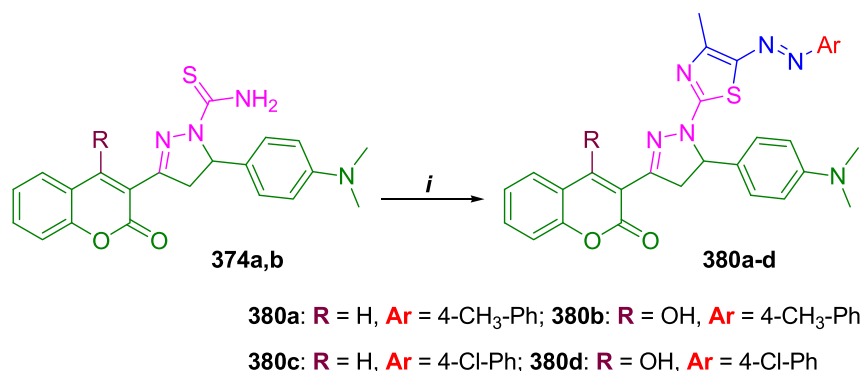
Scheme 80. Synthetic route for the design of pyrrolo-pyridine derivatives [48]; **Reagents and conditions:** *i*) Bromoethylacetoacetate, K₂CO₃, DMF, 100 °C (30 min); *ii*) HCl/CH₃COOH; *iii*) Pd(dba)₃ Xantphos, CsCO₃, dioxane, 100 °C (1h).



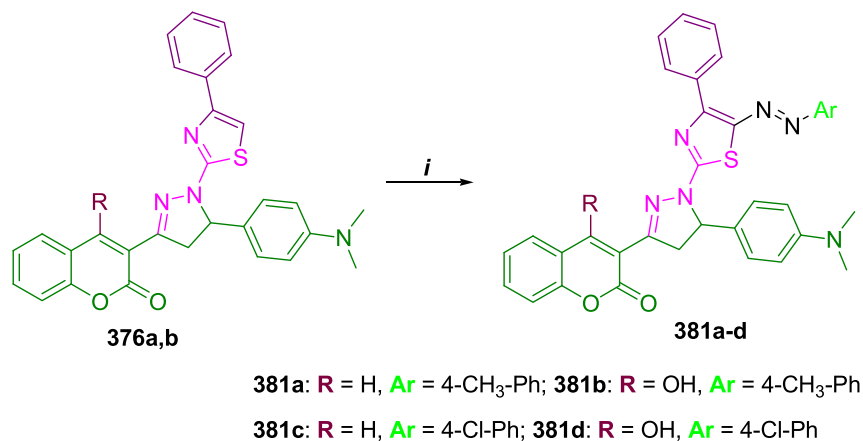
Scheme 82. Synthetic route for the design of the compounds 378a & b and 379a & b [49]; **Reagents and conditions:** i) $\text{BrCH}_2\text{COOC}_2\text{H}_5$, CH_3COONa , EtOH, reflux; ii) $\text{CH}_3\text{CH}(\text{Br})\text{COOC}_2\text{H}_5$, CH_3COONa , EtOH, reflux.

pyrazole rings and an intact saccharin ring in compound 111 have bestowed the strongest activity. In the synthesized benzenesulfonamides-linked quinazoline scaffolds, compound 120c has elicited 15-fold higher activity compared to AAZ. The tyrosinase inhibitory activity of carbazole and hydrazone derivatives revealed compound 121a as the most significant inhibitory compound; the potent activity is thought to be due *N*-ethyl carbazole appended to benzimidazole via thiopropanamide

linker. Carbazole-imidazole derivatives are synthesized to render α -glucosidase inhibitory effects and pharmacological evaluation infers simple phenyl ring at the 4-position of carbazole-imidazole moiety has attributed remarkable inhibitory activity for compound 127v. Synthesis and biological evaluation of coumarin-1,3,4-oxadiazole hybrids revealed compound 132b, a remarkable CA XII inhibitor. Coumarin appended with methylene oxadiazole thiol and in turn, benzoyl moiety attached to thiol functionality of oxadiazole has bestowed compound 132b with remarkable inhibitory activity. *C*- β -D-Glucopyranosyl azole derivatives designed to check glycogen phosphorylase inhibitory potential exhibited moderate activity; particularly compound 140 reported as a most potent inhibitor. While diaryl-1,5-diazoles have been synthesized and their COX-2 and 5-LOX inhibitory activities are performed; wherein compound 147h having benzenesulfonamide and 4-trifluoromethyl benzene at 1- and 5-positions of pyrazole in addition to propylcarboxamide flanked by pyrazole and morpholine moiety rendered decent activity. Dihydroquinazoline-2-amines revealed promising reverse transcriptase inhibitory activity in which compound 155b with *p*-cyanobenzeneamine ring shown to possess noteworthy activity. Compound 168j of dioxino [2,3-*f*] quinazoline derivatives has resulted in striking VEGFR-2 inhibitory activity. *N*-Propylmorpholine moiety connected to oxygen at 7-position of quinazoline and 2-fluoro-4-trifluoromethyl benzene appended to the NH end of urea fragment is thought to be responsible for its activity. In the multi-tyrosine kinase inhibitory activities of 1,2,3-triazole analogs, derivative 174d bearing 4-methylphenyl ring and 6-methoxypyridine motifs is found to be strong Tie-2 inhibitor. Meanwhile, aromatic ring-linked hydroxyazole scaffolds have been designed to prove *pf*DHODH inhibitory properties; wherein compound 190e bearing 3-trifluoromethylphenol connected to methyl group at 5-position of the pyrazole in addition to hydroxyl and carboxylic acid moieties at 3- and 4-positions of pyrazole ring respectively. Phenylthiazoles revealed weak



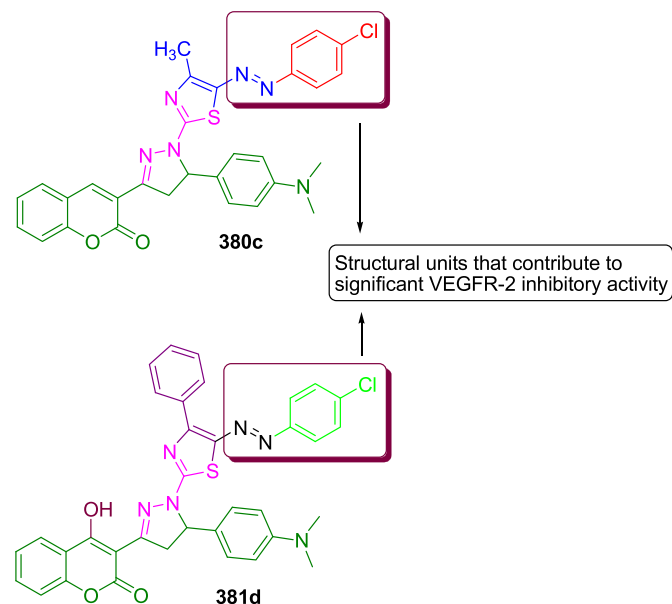
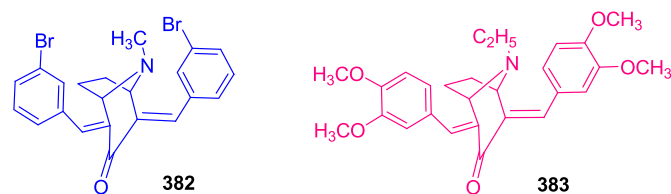
Scheme 83. Synthesis of the compounds 380a,b [49]; **Reagents and conditions:** i) $\text{CH}_3\text{CO}(\text{Cl})\text{C}=\text{NNHAr}$, Dioxane, Et₃N, reflux.



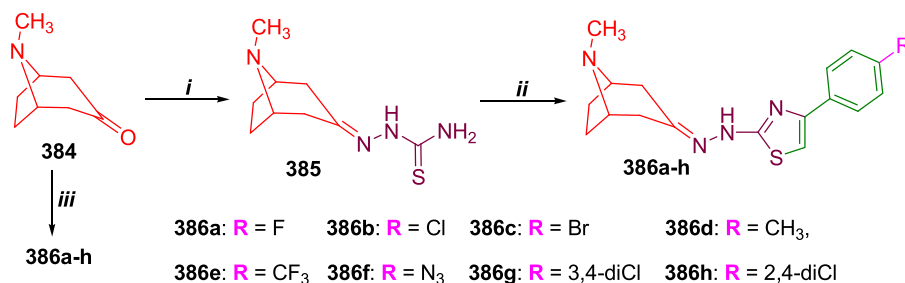
Scheme 84. Design and preparation of compounds 381a, b [49]; **Reagents and conditions:** i) ArN_2Cl , EtOH, $\text{CH}_3\text{COONa} \cdot 3\text{H}_2\text{O}$.

Table 17. Anticancer properties (MCF-2) and VEGFR-2 inhibitory properties of potent molecules.

Compd	Anticancer activity (MCF-7) IC ₅₀ μM (μg/ml)	VEGFR-2 activity
379a	10.75 (4.80 ± 0.47)	0.169 ± 0.010
380c	8.61 (4.90 ± 0.50)	0.081 ± 0.003
381b	6.56 (4.11 ± 0.60)	0.212 ± 0.014
381c	6.51 (4.11 ± 0.60)	0.582 ± 0.021
381d	5.41 (3.50 ± 0.50)	0.034 ± 0.002
Doxorubicin	6.73 (3.66 ± 0.42)	-
Sorafenib	-	0.019 ± 0.002

**Figure 41.** Demonstration of structures of potent molecules with anti-proliferation/VEGFR-2 activity.**Figure 42.** Structures of tropinone derivatives having anticancer properties.

to moderate UppPase inhibitory activity. Pyrazole derivatives witnessed significant COX inhibitory activity; wherein compound 203a stood atop in the list comprising benzene sulfonamide connected to pyrazole

**Scheme 85.** Design and synthesis of tropinone derivatives 386a-h [50]; **Reagents and conditions:** i) H₂NNHCSNH₂, AcOH, EtOH, reflux (20h); ii) *p*-substituted phenacyl bromide EtOH, reflux (20h); iii) H₂NNHCSNH₂, *p*-substituted phenacyl bromide EtOH, reflux.**Table 18.** Tyrosinase inhibitory values of tropinone derivatives.

Compd	Tyrosinase inhibitory activity IC ₅₀ ± SD (μM)
386e	33.74 ± 0.42
386f	72.30 ± 7.55
386g	3.22 ± 0.24
386h	3.51 ± 0.15
Ascorbic acid	386.5 ± 11.95
Kojic acid	72.27 ± 3.14

N₁-position and morpholine appended to pyrazole 5-position via methylene amide fragment. Further moderate tyrosinase inhibitory activity is exhibited among phthalimide-1,2,3-triazole hybrid compounds. Synthesis and evaluation of 15-LOX inhibitory properties of purine-pyrazole hybrids revealed the noteworthy inhibitory potential of the compound 217d possessing 4-methoxyphenyl ring at pyrazole 4-position. Promising anti-CDK2 effects are exhibited by the compound 221d of pyrazole and pyrazolo [1,5-*a*] pyrimidine scaffolds. COX-1 Inhibitory property investigation of dihydropyran fused pyrazole derivatives inferred moderate effects on the enzyme. Whereas, the strongest hCA I inhibitory activity is bestowed by the compound 235 of heterocycle fused pyrazole analogs; it is 25-fold stronger potent compared to the reference and possesses 3, 4-dimethyl benzene and phenyl ring at pyrazole N₁ and C₅ positions of pyrazole. Compounds 254k and 254l have been found to be decent topoisomerase I inhibitors; these are the part of pyrazole-linked benzothiazole-β-naphthol derivatives. The remarkable COX-2 inhibitory values are observed for compounds of pyrazoles and pyrazolo [3,4-*b*] pyridines in which compound 249j possessing 3-fluoroaniline, 4-bromophenylhydrazone moiety at 3, 4-positions respectively in addition to *N*-methylene 2,6-dimethylaniline at N₁-position has excelled in exhibiting most significant activity. In continuation, excellent COX inhibitory properties are shown by the pyrazoles containing thiophene, thienopyrimidine, and thienotriazolopyrimidine derivatives. hCA and AChE dual inhibitory properties have been elicited by derivatives of pyrazoline benzenesulfonamides. Compound 269d is reported to be the most significant hCA I inhibitor. Pyrazolopyrimidine scaffolds are synthesized and evaluated for COX-2 inhibitory properties and found to be only moderate inhibitors. The compound 284d has exhibited NPP1/NPP3 dual inhibitory activity and is part of the series of the pyrazolyl pyrimidinetriones and thioxypyrimidinediones. The GSK3β/p38α dual inhibitory potential of compound 305c among pyridinyl imidazoles might be due to pyridine-cyclopropyl amide and 2-alkyl substituted imidazole motifs. Quinazolin-4(3*H*)-one derivatives are reported to exhibit moderate urease inhibitory properties. In the pharmacological evaluation of quinoline based 4,5-dihydropyrazoles, compound 322b possessing 4-tolyl and 2-chloro-6-methoxyquinoline at dihydropyrazole 3- and 5-positions respectively in addition to substituted thiazole-2yl motif at N₁-position as a basic structure witnessed strongest EGFR inhibitory activity. Radioiodinated benzo [d] imidazole-quinoline derivatives have failed to exhibit improved PDGFRβ inhibitory potentials compared to their

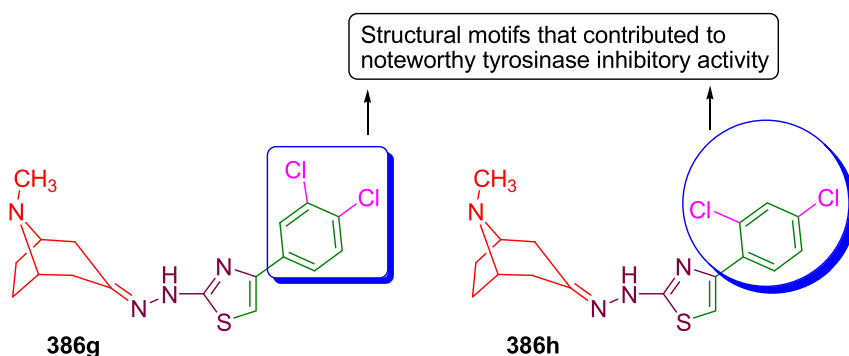


Figure 43. Illustration of tropinone-thiazole derivatives as potent tyrosinase inhibitors.

non-labeled analogs. SLC-0111 thiazole and thiazolidine analogs have proven to be better hCA inhibitory compounds in which compound **342b** comprising benzenesulfonamide on one end of the urea and 3-phenylthiazole-5-yl on the other end exhibited remarkable hCA I and hCA XII inhibitory activity. Most significant (27-fold) ePepN inhibitory activity is elicited by the compound **351k** entailing benzyl moiety at the tetrazole N_1 position, furan-2-yl appended to methine flanked by tetrazole & amino acid groups and indole-3-yl pharmacore attached to propionic acid 3-position. Thiazoles linked to diaryl ethers are designed to exhibit good Atk inhibitory properties wherein compound **354f** bearing 4-hydroxyphenyl moiety at thiazole 4-position bestowed with most significant Atk inhibitory potential. Furthermore, thiazol-hydrazono-coumarins have been synthesized in order to exhibit cyclin-dependent kinases inhibitory effects. The compound **362** with -Br atom at coumarin 6-position stood top of the potent anti-proliferative molecules possessing approximately 115-fold greater activity compared to doxorubicin. Thiazolidine-2,4-dione-azole derivatives are reported to possess promising α -glucosidase and α -amylase inhibitory properties. Compound **381d** structurally comprising phenyl and 4-chlorophenyldiazo motifs at 4- and 5-positions of thiazole ring respectively resulted in most VEGFR-2 kinase inhibitory property among thiazolylypyrazolyl coumarin derivatives. Finally, tropinone-thiazole derivatives have been synthesized and found to be potent towards tyrosinase inhibitory activity wherein the derivative **386g** possessed the strongest inhibitory activity with 21-fold higher potential compared to kojic acid.

Declarations

Author contribution statement

All authors listed have significantly contributed to the development and the writing of this article.

Funding statement

This research did not receive any specific grant from funding agencies in the public, commercial, or not-for-profit sectors.

Competing interest statement

The authors declare no conflict of interest.

Additional information

No additional information is available for this paper.

References

- [1] D. Wei, H. Fan, K. n Zheng, X. Qin, L. Yang, Y. Yang, Y. e Duan, Q. Zhang, C. Zeng, L. Hu, Synthesis and anti-tumor activity of [1,4] dioxino [2,3-f] quinazoline derivatives as dual inhibitors of c-met and VEGFR-2, *Bioorg. Inside Chem.* 88 (2019) 10291.
- [2] N.D. Thanh, D.S. Hai, N.T.T. Ha, D.T. Tung, C.T. Le, H.T.K. Van, V.N. Toan, D.N. Toan, L.H. Dang, Synthesis, biological evaluation and molecular docking study of 1,2,3-1Htriazoles having 4H-pyrano[2,3-d]pyrimidine as potential *Mycobacterium tuberculosis* protein tyrosine phosphatase B inhibitors, *Bioorg. Med. Chem. Lett.* 29 (2019) 164–171.
- [3] Safak Akin, Hasan Ayaloglu, Ergun Gultekin, Ahmet Colak, Olcay Bekircan, Melike Yildirim Akatin, Synthesis of 1,2,4-triazole-5-on derivatives and determination of carbonic anhydrase II isoenzyme inhibition effects, *Bioorg. Chem.* 83 (2019) 170–179.
- [4] S. Tariq, P. Kamboj, O. Alam, M. Amir, 1,2,4-Triazole-Based benzothiazole/benzoxazole derivatives: design, synthesis, p38 α MAP kinase inhibition, anti-inflammatory activity and molecular docking studies, *Bioorg. Chem.* 81 (2018) 630–641.
- [5] H.H. Georgey, F.M. Manhi, W.R. Mahmoud, N.A. Mohamed, E. Berrino, C.T. Supuran, 1,2,4-Trisubstituted imidazolinones with dual carbonic anhydrase and p38 mitogen-activated protein kinase inhibitory activity, *Bioorg. Chem.* 82 (2019) 109–116.
- [6] T. Umar, S. Shalini, M.K. Raza, S. Gusain, J. Kumar, P. Seth, M. Tiwari, N. Hoda, A multifunctional therapeutic approach: synthesis, biological evaluation, crystal structure and molecular docking of diversified 1H-pyrzolo[3,4-b]pyridine derivatives against Alzheimer's disease, *Eur. J. Med. Chem.* 175 (2019) 2–19.
- [7] S. Akin, E.A. Demir, A. Colak, Y. Kolcuoglu, N. Yildirim, O. Bekircan, Synthesis, biological activities and molecular docking studies of some novel 2,4,5-trisubstituted-1,2,4-triazole-3-one derivatives as potent tyrosinase inhibitors, *J. Mol. Struct.* 1175 (2019) 280–286.
- [8] B.G.M. Youssif, M.F.A. Mohamed, M.M. Al-Sanea, A.H. Moustafa, A.A. Abdelhamid, H.A.M. Gomaa, Novel aryl carboximidamides and 3-aryl-1,2,4-oxadiazoles analogs of naproxen as dual selective COX-2/15-LOX inhibitors: design, synthesis, and Docking studies, *Bioorg. Chem.* 85 (2019) 577–584.
- [9] B. Qi, Y. Yang, G. Gong, H. He, X. Yue, X. Xu, Y. Hu, J. Li, T. Chen, X. Wan, A. Zhang, G. Zhou, Discovery of N1-(4-((7-(3-(4-ethylpiperazin-1-yl)propoxy)-6-methoxyquinolin-4-yl)oxy)-3,5-difluorophenyl)-N3-(2-(2,6-difluorophenyl)-4-oxothiazolidin-3-yl)urea as a multi-tyrosine kinase inhibitor for drug-sensitive and drug-resistant cancers treatment, *Eur. J. Med. Chem.* 163 (2019) 10–27.
- [10] E. Mentese, M. Emirik, B.B. Sokmen, Design, molecular docking and synthesis of novel 5,6-dichloro-2-methyl-1Hbenzimidazole derivatives as potential urease enzyme inhibitors, *Bioorg. Chem.* 86 (2019) 151–158.
- [11] B. Cornelio, M. Laronze-Cochard, R. Miambo, M. De Grandis, R. Riccioni, B. Borisova, D. Dontchev, C. Machado, M. Ceruso, A. Fontana, C.T. Supuran, J. Sapi, 5-Arylisothiazol-3(2H)-one-1,(1)-(di)oxides: a new class of selective tumor-associated carbonic anhydrases (hCA IX and XII) inhibitors, *Eur. J. Med. Chem.* 175 (2019) 40–48.
- [12] D.E.P. Sumalapao, N.G. Gloriani, Hierarchically weighted principal component analysis evaluation of antifungal azoles inhibitory potency on lanosterol-14 α -demethylase in *Candida albicans*, *Curr. Res. Environ. Appl. Mycol.* 9 (2019) 44–52.
- [13] E.S. Taher, T.S. Ibrahim, M. Fares, A.M.M. AL-Mahmoudy, A.F. Radwan, K.Y. Orabi, O.I. El-Sabbagh, Novel benzenesulfonamide and 1,2-benzisothiazol-3(2H)-one-1,1-dioxide derivatives as potential selective COX-2 inhibitors, *Eur. J. Med. Chem.* 171 (2019) 372–382.
- [14] A.S. El-Azab, A.A. Abdel-Aziz, S. Bua, A. Nocentini, M.A. El-Gendy, M.A. Mohamed, T.Z. Shawer, N.A. AlSaif, C.T. Supuran, Synthesis of benzenesulfonamides linked to quinazoline scaffolds as novel carbonic anhydrase inhibitors, *Bioorg. Chem.* 87 (2019) 78–90.
- [15] Z.A. Kaplancikli, Synthesis of some novel Carbazole derivatives and evaluation of their antimicrobial activity, *Marmara Pharm. J.* 15 (2011) 105–109.
- [16] Z.A. Kaplancikli, et al., Synthesis, antimicrobial activity and cytotoxicity of some new carbazole derivatives, *J. Enzym. Inhib. Med. Chem.* 27 (2012) 868–874.
- [17] L. Yurttas, et al., Synthesis and antimicrobial activity of some new hydrazone bridged thiazole-pyrrole derivatives, *J. Enzym. Inhib. Med. Chem.* 28 (2013) 830–835.
- [18] U. Ghani, Carbazole and hydrazone derivatives as new competitive inhibitors of tyrosinase: experimental clues to binuclear copper active site binding, *Bioorg. Chem.* 83 (2019) 235–241.
- [19] M. Adib, F. Peytam, R. Shourgeshty, M.M.-. Khanaposhtani, M. Jahani, S. Imanparast, M.A. Faramarzi, B. Larjani, A.A. Moghadamnia, E.N. Esfahani,

- F. Bandarian, M. Mahdavi, Design and synthesis of new fused carbazole-imidazole derivatives as antidiabetic agents: in vitro α -glucosidase inhibition, kinetic, and in silico studies, *Bioorg. Med. Chem. Lett.* (2019).
- [20] N.S. Goud, S.M. Ghouse, M. Arifuddin, M. Alvala, A. Angeli, C.T. Supuran, Synthesis and biological evaluation of coumarin-1,3,4-oxadiazole hybrids as selective carbonic anhydrase IX and XII inhibitors, *Bioorg. Chem.* 87 (2019) 765–772.
- [21] D. Barr, E. Szennyes, E. Bokor, Z.H. Al-Oanzi, C. Moffatt, S. r Kun, T. Docsa, Á. Sipos, M.P. Davies, R.T. Mathomes, T.J. Snape, L. Agius, L. Somsak, J.M. Hayes, Identification of C- β -D-glucopyranosyl azole type inhibitors of glycogen phosphorylase that reduce glycogenolysis in hepatocytes: in silico design, synthesis, in vitro kinetics and ex-vivo studies, *ACS Chem. Biol.* 147 (2019) 1460–1470.
- [22] Z. Li, Z.-C. Wang, X. Li, M. Abbas, S.-Y. Wu, S.-Z. Ren, Q.-X. Liu, Y. Liu, P.-W. Chen, Y.-T. Duan, P.-C. Lv, H.-L. Zhu, Design, synthesis, and evaluation of novel diaryl-1,5-diazoles derivatives bearing morpholine as potent dual COX-2/5-LOX inhibitors and antitumor agents, *Eur. J. Med. Chem.* (2019), <https://doi.org/10.1016/j.ejmech.2019.03.008>.
- [23] K. Jin, Y. Sang, S. Han, E. De Clercq, C. Pannecouque, G. Meng, F. Chen, Synthesis and biological evaluation of dihydroquinazoline-2-amines as potent non-nucleoside reverse transcriptase inhibitors of wild-type and mutant HIV-1 strains, *Eur. J. Med. Chem.* 176 (2019) 11–20.
- [24] H. Fan, D. Wei, K. Zheng, X. Qin, L. Yang, Y. Yang, Y. Duan, Y. Xu, L. Hu, Discovery of Dioxino [2,3-*f*] quinazoline derivative VEGFR-2 inhibitors exerting significant antiproliferative activity in HUVECs and mice, *Eur. J. Med. Chem.* 175 (2019) 349–356.
- [25] X. Pan, L. Liang, R. Si, J. Wang, Q. Zhang, H. Zhou, L. Zhang, J. Zhang, Discovery of novel anti-angiogenesis agents. Part 10: multi-target inhibitors of VEGFR-2, Tie-2, and EphB4 incorporated with 1,2,3-triazole, *Eur. J. Med. Chem.* 163 (2019) 1–9.
- [26] A.C. Pippione, S. Sainas, P. Goyal, I. Fritzon, G.C. Cassiano, A. Giraudo, M. Giorgis, T.A. Tavella, R. Bagnati, B. Rolando, R. Caing-Carlsson, F.T.M. Costa, C.H. Andrade, S. Al-Karadaghi, D. Boschi, R. Friemann, M.L. Lolli, Hydroxyazole scaffold-based Plasmodium falciparum dihydroorotate dehydrogenase inhibitors: synthesis, biological evaluation, and X-ray structural studies, *Eur. J. Med. Chem.* 163 (2019) 266–280.
- [27] M.M. Elsebaei, H. Mohammad, A. Samir, N.S. Abutaleb, A.B. Norvil, A.R. Michie, M.M. Moustafa, H. Samy, H. Gowher, M.N. Seleem, A.S. Mayhoub, Lipophilic efficient phenylthiazoles with potent undecaprenyl pyrophosphatase inhibitory activity, *Eur. J. Med. Chem.* 175 (2019) 49–62.
- [28] G.S. Hassan, D.E. Abdel Rahman, E.A. Abdelmajeed, R.H. Refaey, M. Alaraby Salem, Y.M. Nissan, New pyrazole derivatives: synthesis, anti-inflammatory activity, cyclooxygenase inhibition assay and evaluation of mPGES, *Eur. J. Med. Chem.* 171 (2019) 332–342.
- [29] M.B. Tehrani, P. Emani, Z. Rezaei, M. Khoshneviszadeh, M. Ebrahimi, N. Edraki, M. Mahdavi, B. Larjani, S. Ranjbar, A. Foroumadi, M. Khoshneviszadeh, Phthalimide-1,2,3-triazole hybrid compounds as tyrosinase inhibitors; synthesis, biological evaluation, and molecular docking analysis, *J. Mol. Struct.* 1176 (2019) 86–93.
- [30] O.S. Afifi, O.G. Shaaban, H.A. Abd El Razik, S. El-Dine A Shams El-Dine, F.A. Ashour, A.A. El-Tombary, M.M. Abu-Serie, Synthesis and biological evaluation of purine-pyrazole hybrids incorporating thiazole, thiazolidinone or rhodanine moiety as 15-LOX inhibitors endowed with anticancer and antioxidant potential, *Bioorg. Chem.* 87 (2019) 821–837.
- [31] G.M.E. Ali, D.A. Ibrahim, A.M. Elmetswali, N.S.M. Ismail, Design, synthesis and biological evaluation of certain CDK2 inhibitors based on pyrazole and pyrazolo [1,5-*a*] pyrimidine scaffold with apoptotic activity, *Bioorg. Chem.* 86 (2019) 1–14.
- [32] M. Murahari, V. Mahajan, S. Neeladri, M.S. Kumar, Y.C. Mayur, Ligand-based design and synthesis of pyrazole based derivatives as selective COX-2 inhibitors, *Bioorg. Chem.* 86 (2019) 583–597.
- [33] F. Turkan, A. Cetin, P. Taslimi, M. Karaman, I. Gulcin, Synthesis, biological evaluation and molecular docking of novel pyrazole derivatives as potent carbonic anhydrase and acetylcholinesterase inhibitors, *Bioorg. Chem.* 86 (2019) 420–427.
- [34] B. Nagaraju, J. Kovvuri, C.G. Kumar, S.R. Routhu, D.A. Shareef, M. Kadagathur, P.R. Adiyala, S. Alavala, N. Nagesh, A. Kamal, Synthesis and biological evaluation of pyrazole linked benzothiazole- β -naphthol derivatives as topoisomerase I inhibitors with DNA binding ability, *Bioorg. Med. Chem.* 27 (2019) 708–720.
- [35] L.W. Mohamed, M.A. Shaaban, A.F. Zaher, S.M. Alhamaky, A.M. Elshahar, Synthesis of new pyrazoles and pyrazolo [3,4-*b*] pyridines as anti-inflammatory agents by inhibition of COX-2 enzyme, *Bioorg. Chem.* 83 (2019) 47–54.
- [36] M.S. El-Shoukrofy, H.A. Abd El Razik, O.M. AboulWafa, A.E. Bayad, I.M. El-Ashrawy, Pyrazoles containing thiophene, thienopyrimidine and thienotriazolopyrimidine as COX-2 selective inhibitors: design, synthesis, in vivo anti-inflammatory activity, docking and in silico chemo-informatic studies, *Bioorg. Chem.* 85 (2019) 541–557.
- [37] D.O. Ozgun, H.I. Gul, C. Yamali, H. Sakagami, I. Gulcin, M. Sukuroglu, C.T. Supuran, Synthesis and bioactivities of pyrazoline benzensulfonamides as carbonic anhydrase and acetylcholinesterase inhibitors with low cytotoxicity, *Bioorg. Chem.* 84 (2019) 511–517.
- [38] E.K.A. Abdelall, P.F. Lamie, A.K.M. Ahmed, E.-S. EL-Nahass, COX-1/COX-2 inhibition assays and histopathological study of the newly designed anti-inflammatory agent with a pyrazolopyrimidine core, *Bioorg. Chem.* 86 (2019) 235–253.
- [39] H. Andleeb, S. Hameed, S. Abida Ejaz, I. Khan, S. Zaib, J. Lecka, J. Sévigny, J. Iqbal, Probing the high potency of pyrazolyl pyrimidinetriones and thioxypyrimidinediones as selective and efficient nonnucleotide inhibitors of recombinant human ectonucleotidases, *Bioorg. Chem.* 88 (2019) 102893.
- [40] F. Heider, F. Ansideri, R. Tesch, T. Pansar, U. Haun, E. Döring, M. Kudolo, A. Poso, W. Albrecht, S.A. Laufer, P. Koch, Pyridinylimidazoles as dual glycogen synthase kinase 3 β /p38 α mitogen-activated protein kinase inhibitors, *Eur. J. Med. Chem.* 175 (2019) 309–329.
- [41] E. Mentese, G. Akyuz, M. Emirik, N. Baltas, Synthesis, in vitro urease inhibition and molecular docking studies of some novel quinazolin-4(3*H*)-one derivatives containing triazole, thiadiazole, and thiosemicarbazide functionalities, *Bioorg. Chem.* 83 (2019) 289–296.
- [42] R.F. George, E.M. Samir, M.N. Abdelhamed, H.A. Abdel-Aziz, S.E.-S. Abbas, Synthesis and anti-proliferative activity of some new quinoline based 4,5-dihydro-pyrazoles and their thiazole hybrids as EGFR inhibitors, *Bioorg. Chem.* 83 (2019) 186–197.
- [43] Nurmaya Effendi, Kenji Mishiro, Takeshi Takarada, Daisuke Yamada, Ryuichi Nishii, Kazuhiro Shiba, Seigo Kinuya, Akira Odani, Kazuma Ogawa Design, synthesis, and biological evaluation of radioiodinated benzo[d] imidazole-quinoline derivatives for platelet-derived growth factor receptor β (PDGFR β) imaging, *Bioorg. Med. Chem.* 27 (2019) 383–393.
- [44] M.F. Abo-Ashour, W.M. Eldehna, A. Nocentini, H.S. Ibrahim, S. Bua, H.A. Abdel-Aziz, S.M. Abou-Seri, C.T. Supuran, Novel synthesized SLC-0111 thiazole and thiadiazole analogs: determination of their carbonic anhydrase inhibitory activity and molecular modeling studies, *Bioorg. Chem.* 87 (2019) 794–802.
- [45] Y. Mendez, Ge. De Armas, I. Perez, T. Rojas, M.E. Valdes-Tresanco, M. Izquierdo, M.A.d. Rivero, Y.M. Alvarez-Ginarte, P.A. Valiente, C. Soto, L. de Leon, A.V. Vasco, W.L. Scott, B. Westermann, J. Gonzalez-Bacero, D.G. Rivera, Discovery of potent and selective inhibitors of the Escherichia coli M1-aminopeptidase via multicomponent solid-phase synthesis of tetrazole-peptidomimetics, *Eur. J. Med. Chem.* 163 (2019) 481–499.
- [46] M.D. Altintop, B. Sever, G.A. Ciftci, A. Ozdemir, Design, synthesis, and evaluation of a new series of thiazole-based anticancer agents as potent Akt inhibitors, *Molecules* 23 (2018) 1318.
- [47] S.S.A. El-Karim, Y.M. Syam, A.M. El Kerdawy, T.M. Abdelghany, New thiazol-hydrazono-coumarin hybrids targeting human cervical cancer cells: synthesis, CDK2 inhibition, QSAR, and molecular docking studies, *Bioorg. Chem.* 86 (2019) 80–96.
- [48] N. Senthilkumar, V. Vijayakumar, S. Sarveswari, G.A. Gayathri, M. Gayathri, Synthesis of new thiazolidine-2-,4-dione-azole derivatives and evaluation of their α -amylase and α -glucosidase inhibitory activity, *Iran J. Sci. Technol. Trans. Sci.* 43 (2019) 735–745.
- [49] T.K. Mohamed, R.Z. Batran, S.A. Elseginy, M.M. Alic, A.E. Mahmoud, Synthesis, anticancer effect and molecular modeling of new thiazolylpyrazolyl coumarin derivatives targeting VEGFR-2 kinase and inducing cell cycle arrest and apoptosis, *Bioorg. Chem.* 85 (2019) 253–273.
- [50] K. Piechowska, M. Switalska, J. Cytrarska, K. Jaroch, K. Luczykowski, J. Chalupka, J. Wietrzyk, K. Misiura, B. Bojko, S. Kruszewski, K.Z. Laczkowski, Discovery of tropinonethiazole derivatives as potent caspase 3/7 activators, and noncompetitive tyrosinase inhibitors with high antiproliferative activity: rational design, one-pot tricomponent synthesis, and lipophilicity determination, *Eur. J. Med. Chem.* 175 (2019) 162–171.